UNIVERSITAT DE BARCELONA

# Role of p38α in lung tumor progression

Jessica Vitos Faleato

Barcelona, 2017

# ROLE OF p38α IN LUNG TUMOR PROGRESSION

Memòria presentada per **Jessica Vitos Faleato** per optar al grau de doctor per la Universitat de Barcelona


Director
Ángel Rodríguez Nebreda, PhD

Tutor
Antonio Zorzano Olarte, PhD

INSTITUT DE REÇERCA BIOMÈDICA
(IRB) BARCELONA
Laboratori de Senyalització i Cicle Cel·lular

UNIVERSITAT DE BARCELONA
Facultat de Biologia
Doctorat en Biomedicina

*A mis abuelos Ramiro y Felisa,*
*y a Jordi*

# ACKNOWLEDGEMENTS

*Cuando emprendas tu viaje a Ítaca, pide que el camino sea largo, lleno de aventuras, lleno de experiencias.*

Mi 'viaje a Ítaca' particular comienza en otoño de 2011, en la oficina de Ángel Nebreda hablando sobre una beca para estudiar una tal p38 MAPK. A él quiero agradecer haber depositado su confianza en mí aquél día y todos los siguientes hasta hoy, apoyándome y dándome libertad para avanzar por cada isla hasta llegar a puerto.

En este viaje he tenido la suerte de compartir un barco llamado IRB Barcelona con grandes científicos y mejores personas que, sin duda, han hecho la travesía mucho más interesante. Gracias a todos. Aquí van algunos de mis Eolos en esta tesis: gracias a Roger Gomis, Francesc Ventura, y Marco Milán, por vuestros seguimientos anuales del proyecto; a Antonio Zorzano, por hacer de tutor; a Raquel, por estar disponible siempre que necesité sugerencias, correcciones o discutir resultados; a Petra, Sami, y Elisa, por vuestro cariño y buenos consejos; a Núria, por ser la sonrisa del laboratorio; a Laura, Marc, Kostya, y Anna Bellmunt, por contagiarme vuestra alegría a diario; a Sebas y Marc Guiu, por vuestro buen rollo y vuestra ayuda con los animales; a Elisabet, por todas tus horas invertidas en mis immunohistoquímicas; a Lorena Pereira y Michi, por los buenos ratos en la poyata pasadas las diez de la noche; y gracias a la larga lista de miembros del Nebreda's lab que habéis compartido conmigo este viaje: Catrin, Mónica, Lorena González, Nati, Natalia Dave, Jalaj, Sandra, Begoña, Emma, Marianna, Mercè... He de mencionar también mi deuda con las vidas de muchos ratones, y que muchos experimentos no habrían sido posibles sin la

ayuda de nuestros colaboradores, de las unidades de microscopía, genómica, citometría, immunohistopatología, bioestadística, y del estabulario. ¡Gracias!

*Pide que el camino sea largo. Que muchas sean las mañanas de verano en que llegues -¡con qué placer y alegría!- a puertos nunca vistos antes.*

Un tesoro que me llevo de mi paso por el IRB Barcelona es la amistad con Carlos, Miquel, Simone, Francisco, y Joan, sois extraordinarios, no imagináis cuánto me habéis hecho crecer, y lo mucho más divertido que ha sido mi viaje gracias a vosotros. También me siento afortunada de haber encontrado en el camino a Raffaella, Lorenzo, Franky, Sara, e Ilda, gracias por ser siempre tan alentadores; a Gemma, gracias por las horas que hemos pasado colgadas; a Ágata, y Sílvia Pairet, gracias por inculcarme vuestro amor por los animales; y a Sílvia Vilaprinyó, gracias por tu energía infinita.

*Ten siempre a Itaca en tu mente. Llegar allí es tu destino. Mas no apresures nunca el viaje. Mejor que dure muchos años y atracar, viejo ya, en la isla, enriquecido de cuanto ganaste en el camino.*

No quiero olvidar nombrar a los que están desde mucho antes de zarpar: gracias a Andre y a Síl, simplemente os adoro; gracias a mis amigos de la facultad de Oviedo (Carmen, Pravos, Cris, Ele, Carla, Astrid, Lara, Ali, y Eva), porque, entre risa y risa, siempre me dais fuerza; y gracias a los amigos que conocí en Barcelona (Bea, Amaia, Esther, Elena, Patri y Alba), porque hicisteis que llegar nuevo a una ciudad grande fuese la experiencia más fácil y alocada del mundo.

Finalmente, quiero dar las gracias a Jordi, gràcies per que fas que tot valgui la pena, ets el meu millor company de viatge!, gràcies per que sempre has estat lo que l'Hermes per a l'Ulises, i per això que aquesta tesi et deu molt. Gracias a mis padres. Gracias a mis abuelos Dámaso y Honesta. Gracias a mi nueva familia alcoiana. Y gracias a mis abuelos Ramiro y Felisa, por ser mi Atenea, siempre atentos a mi hoja de ruta, por ser mis confidentes y mis maestros, por

cuidarme incondicionalmente, y por darme más amor y apoyo del que cabe imaginar. Nunca os lo podré agradecer bastante.

*... con tanta experiencia, entenderás ya qué significan las Itacas.*

# CONTENTS

# ABBREVIATIONS

## A

| | |
|---|---|
| AAH | Atypic adenomatous hyperplasia |
| AD | Adenoma |
| ADC | Adenocarcinoma |
| AE2 | Alveolar epithelial cell type II |
| AMPK | AMP-activated protein kinase |
| APC | Allophycocyanin |
| ARE | AU-rich element |
| ATF | Activating transcription factor |
| ATP | Adenosine triphosphate |
| AUF1 | AU-rich element RNA-binding protein 1 (HNRNPD) |
| a.u. | Arbitrary units |

## B

| | |
|---|---|
| BADJ | Bronchioalveolar duct junction |
| BASC | Bronchioalveolar stem cell |
| bFGF | Basic fibroblast growth factor |
| bp | Base pairs |
| BrdU | Bromodeoxyuridine |
| BSA | Bovine serum albumin |

## C

| | |
|---|---|
| CAF | Cancer-associated fibroblasts |
| CCSP | Club cell specific protein |
| CD | Cluster of differentiation |
| CDDP | Cisplatin |
| cDNA | Complementary deoxyribonucleic acid |
| CDKN | Cyclin-dependent kinase inhibitor |
| C/EBPα | CCAAT/enhancer-binding protein α |
| COX-2 | Cyclooxygenase 2 |
| CRE | Cyclic recombinase |
| CXCL | C-X-C motif chemokine ligand |

## D

| | |
|---|---|
| DAB | 3,3′-Diaminobenzidine |
| DAPI | 4′,6-diamidino-2-phenylindole |
| DMEM | Dulbecco's modified Eagle medium |
| DMSO | Dimethyl sulfoxide |
| dNTP | Deoxyribonucleotides triphosphate |
| DTT | Dithiothreitol |

## E

| | |
|---|---|
| EDTA | Ethylenediamine tetra-acetic acid |
| eGFP | Enhanced green fluorescent protein |
| EGFR | Epithelial growth factor receptor |
| EGTA | Ethylene glycol tetra-acetic acid |
| ERK | Extracellular signal-regulated kinase |

## F

| | |
|---|---|
| FACS | Fluorescence-activated cell sorting |
| FBS | Fetal bovine serum |
| FITC | Fluorescein isothiocyanate |
| FlpO | Flippase O recombinase |
| FGFR | Fibroblast growth factor receptor |
| FRT | Flippase recognition target |
| FSP1 | Fibroblast specific protein 1 |

## G

| | |
|---|---|
| GAPDH | Glyceraldehyde 3-phosphate dehydrogenase |
| GEMM | Genetically engineered mouse models |
| GEO | Gene expression omnibus |
| GTP | Guanosine triphosphate |

## H

| | |
|---|---|
| HPRT | Hypoxanthine-guanine phosphoribosyltransferase |
| HRP | Horseradish peroxidase |
| Hsp27 | Heat shock protein 27 |
| H&E | Hematoxylin & Eosin |

## I

| | |
|---|---|
| IHC | Immunohistochemistry |
| IKKα | Inhibitor of nuclear factor κ-B kinase subunit α |
| IL | Interleukin |
| iNOS | Inducible nitric oxide synthase |

## J

| | |
|---|---|
| JNK | c-Jun N-terminal kinase |

## K

| | |
|---|---|
| KO | Knock-out |
| K-Ras | Kirsten rat sarcoma viral oncogene homolog |

## L

| | |
|---|---|
| LGR6 | Leucine rich repeat containing G protein-coupled receptor 6 |
| LoxP | Locus of X-over P1 |

## M

| | |
|---|---|
| MAPK | Mitogen-activated protein kinase |
| MAP2K | Mitogen-activated protein kinase kinase |
| MAP3K | Mitogen-activated protein kinase kinase kinase |
| MCP | Monocyte chemotactic protein |
| MEF | Mouse embryonic fibroblasts |
| MEK | Mapk/Erk kinase |
| miRNA | Micro-ribonucleic acid |
| MKK | Mitogen-activated protein kinase kinase |
| mKLC | Murine K-Ras$^{G12V}$ lung cancer |
| MK2 | MAPK-activated protein kinase -2 |
| MMP | Matrix metalloproteinase |
| mRNA | Messenger ribonucleic acid |
| MTT | 3-(4,5-Dimethylthiazol-2-yl)-2,5-diphenyltetrazolium bromide |

## N

| | |
|---|---|
| NFκB | Nuclear factor κ-light-chain-enhancer of activated B cells |
| NSCLC | Non-small cell lung cancer |

## O

| | |
|---|---|
| o.n. | Overnight |

## P

| | |
|---|---|
| PBS | Phosphate buffered saline |

| | |
|---|---|
| PCR | Polymerase chain reaction |
| PDGF | Platelet-derived growth factor |
| PDL1 | Programmed death-ligand 1 |
| PE | Phycoerythrin |
| PFA | Paraformaldehyde |
| Pfu | Plaque formation units |
| PGC1α | Peroxisome proliferator-activated receptor gamma coactivator 1-α |
| PI | Propidium iodide |
| PI3K | Phosphatidylinositol-4,5-bisphosphate 3-kinase |
| PKCα | Protein kinase C α |
| PP2A | Protein phosphatase 2 |
| PRAK | p38-regulated/activated protein kinase |
| Pro | Proline |

## Q

| | |
|---|---|
| qPCR | Quantitative real time PCR |

## R

| | |
|---|---|
| RB1 | Retinoblastoma |
| ROS | Reagent oxygen species |
| RT | Room temperature |

## S

| | |
|---|---|
| SCLC | Small cell lung cancer |
| SDF1 | Stromal cell-derived factor 1 (CXCL12) |
| SDS | Sodium dodecyl sulfate |
| Ser | Serine |
| SMA | Smooth muscle actin |
| SPC | Surfactant protein C |
| SPF | Specific pathogen free |
| STAT | Signal transducer and activator of transcription |
| STK11 | Serine/threonine kinase 11 (Lkb1) |

## T

| | |
|---|---|
| TAK1 | TGF-β activated kinase 1 (MAP3K7) |
| TBS | Tris-buffered saline |
| TGF-β | Transforming growth factor β |
| Thr | Threonine |
| TIMP-1 | Tissue inhibitor of metalloproteases 1 |
| TME | Tumor microenvironment |
| TMX | Tamoxifen |
| TNFα | Tumor necrosis factor α |
| TTF1 | Thyroid transcription factor 1 (Nkx2.1) |
| TUNEL | Terminal deoxynucleotidyl transferase dUTP nick-end labeling |
| Tyr | Tyrosine |

## U

| | |
|---|---|
| UV | Ultraviolet radiation |

## V

| | |
|---|---|
| VEGF | Vascular endothelial growth factor |
| vWF | von Willebrand factor |

## W

| | |
|---|---|
| Wip1 | WT P53-induced phosphatase 1 |
| WT | Wild type |

# SUMMARY

Tumors evolve by sequentially acquiring genetic abnormalities, like K-Ras activation and Tp53 loss of function, which enable transformed cells to survive, proliferate, invade, and reprogram their microenvironment. Simultaneously, transformed cells need to cope with a stressful scenario, including an accelerated metabolism, genome instability, or immune surveillance. Therefore, cancer cells must rely on some non-oncogenic signaling pathways to tolerate homeostatic control deficiencies, adapt to the new demands, and monitor continuous changes in the microenvironment to respond accordingly.

The p38 MAPK signaling pathway is a stress-related pathway that cells use to transduce extracellular cues and orchestrate appropriate responses. p38α, the most widely expressed p38 MAPK family member, has been classically attributed tumor suppressor functions due to its ability to arrest the cell cycle, induce cell differentiation, and trigger apoptosis. Nevertheless, in several human tumor types, p38 MAPK activity levels have been found increased and sometimes correlated to poor survival, suggesting a pro-tumorigenic role.

In this study, we observed a negative correlation between p38α mRNA expression levels and the overall survival of lung adenocarcinoma patients. Using a K-Ras$^{G12V}$ driven mouse model of lung cancer, we show that indeed p38α signaling plays a dual role during lung tumorigenesis. On one hand, p38α avoids malignant transformation in lung epithelial cells by promoting their differentiation. However, in the transformed lung epithelial cells, p38α enhances proliferation as well as the secretion of inflammatory cytokines to form a favorable niche for cancer progression. p38α also plays a pro-tumorigenic role by promoting tumor vascularization and immunotolerance of tumor-infiltrated myeloid cells. Altogether, our data suggest that targeting this pathway might be therapeutically useful for lung adenocarcinoma.

# RESUMEN

Los tumores evolucionan al adquirir anormalidades genéticas de manera secuencial, como la activación de K-Ras y la pérdida de funcionalidad de Tp53, que permiten a las células transformadas sobrevivir, proliferar, e invadir, así como acondicionar su microambiente. Simultáneamente, las células transformadas también han de lidiar con situaciones de estrés, incluyendo un metabolismo acelerado, un genoma altamente inestable, o el sistema de vigilancia de las células inmunes. Por lo tanto, las células cancerosas han de apoyarse en vías de señalización no-oncogénicas que les permiten tolerar las deficiencias en los sistemas de control de homeostasis, adaptarse a los nuevos requerimientos funcionales, y monitorizar los cambios en el microambiente para responder de manera apropiada.

La vía de las p38 MAPK está íntimamente relacionada con la respuesta al estrés y es utilizada por las células para transducir señales extracelulares y orquestrar las respuestas correspondientes. p38α es el miembro de la familia de p38 MAPK más ampliamente expresado, y se le han atribuido clásicamente funciones supresoras tumorales gracias a su habilidad para detener el ciclo celular, inducir diferenciación, y desencadenar procesos apoptóticos. No obstante, hay evidencia de que el nivel de actividad de p38 MAPK podría estar incrementado en varios tipos de tumor humanos y, en algunos casos, se ha correlacionado con una baja supervivencia, lo que sugiere un papel pro-tumoral.

En este estudio, hemos observado una correlación negativa entre los niveles de expresión de p38α y la supervivencia en pacientes de adenocarcinoma pulmonar. Hemos usado un modelo murino de cáncer de pulmón inducido por la expresión del oncogen K-Ras para demostrar que, efectivamente, p38α juega un papel dual durante el desarrollo de la carcinogénesis de pulmón. Por una

parte, p38α evita la transformación maligna de las células pulmonares epiteliales sanas mediante la inducción de diferenciación celular. Sin embargo, en las células epiteliales pulmonares transformadas, p38α estimula la proliferación y la secreción de citocinas inflamatorias que preparan un nicho favorable para la progresión tumoral. p38α también juega un rol pro-tumorigénico al promover la vascularización del tumor y la immunotolerancia por parte de las células mieloides infiltradas. En conjunto, nuestros datos sugieren que la inhibición de esta vía de señalización podría ser útil en términos terapéuticos para los casos de adenocarcinoma de pulmón.

# *Preface*

# BRIEF HISTORY OF ONCOLOGY

Our knowledge of the nature of cancer is quite recent, although humanity has known about this illness since ancient times. The very first testimonies about cancer date back to 1600 BC when ancient Egyptians wrote the Edwin Smith Papyrus describing how to remove breast tumors by cauterization. The study of cancer in antiquity was, however, established by Greek physicians between the 420 BC and 200 AD, most notably by Hippocrates and Galen. They coined the term cancer *(Mukherjee 2010)* and the suffix *-oma*, to name cancerous lesions, which they could only describe outwardly *(Karpozilos and Pavlidis 2004)*. It was not until the 17th century, when autopsies were no longer considered profane acts, that physicians could better comprehend the anatomy and functions of the human body, and actually study the cause of cancer.

The initial clues about carcinogenesis emerged from the first epidemiological studies and the use of microscopes. In 1713, Bernardino Ramazzini reported a relatively high incidence of breast cancer in nuns speculating about a possible relationship to their celibate lifestyle. These associations suggested for the first time the influence of hormones on carcinogenesis *(Bode and Dong 2009)*. The first link between cancer and an external agent was established in 1761, when John Hill related cancer with the use of tobacco, which today is known as one of the most harmful oncogenic agents *(Doll and Hill 1956)*.

The 19th century certainly brought progress to the oncology field. Johannes Muller showed that tumors are actually made of cells and not of extravasated lymph. Rudolf Ludwig Karl Virchow, described leukemia for the first time, and suggested that cancer cells come from the "activation" of otherwise normal cells, which are dormant *(Huntly and Gilliland 2005)*. He also was the first to observe white blood cells infiltrating tumors, and to suggest that many cancers

develop after sustained inflammation, pointing for the first time towards a recently identified hallmark of cancer: tumor-promoting inflammation *(Balkwill and Mantovani 2001; Coussens and Werb 2002)*.

Regarding the metastatic process, in 1889 Stephen Paget concluded that cancer cells spread through the bloodstream to the entire body but are able to grow only in a few organs *(Paget 1889)*. His thoughts inspired the recent concept of tumor microenvironment and would encourage doctors later on to develop systemic adjuvant drug treatments to be used after surgery, to destroy remaining metastatic cells.

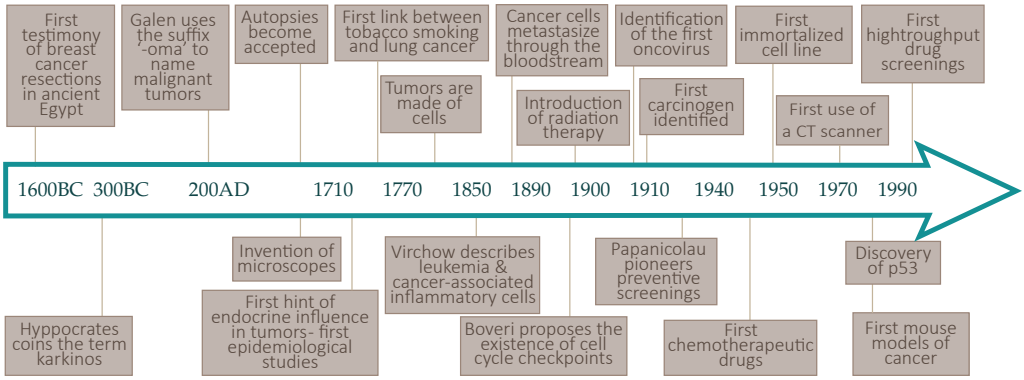


**FIGURE 1. Timeline**. Depiction of some of the most relevant events in the history of oncology.

The genetic basis of cancer remained hidden till the 20th century. In 1902 Theodor Boveri suggested that tumors arise from aberrant mitoses and uncontrolled cell growth caused by radiation, physical or chemical insults or by microscopic pathogens. Furthermore, he proposed the existence of cell cycle checkpoints and, hence, the existence of genes with oncogenic and tumor suppressor roles *(Boveri 2008)*, which were not identified till the late 1970s.

In addition, during this century, the first oncovirus and many new carcinogens were identified. In sight of the cancer-related risks to which we are daily exposed, a need for cancer preventive screenings among the population arose. George Papanicolaou proposed the first screening test in 1923, which is still in

use today for the detection of cervical cancer *(Bode and Dong 2009)*.

Now, in 2017, we can see that the body of knowledge that we have acquired along the centuries **(FIGURE 1)** has remarkably improved prevention, early detection and treatment of cancer. We have developed mouse models that mimic human cancers and immortalized cell lines to study the disease at the cellular and molecular levels. We have developed imaging tests, such as computed tomography scans, which have replaced many exploratory surgeries. We have developed radiotherapy and many different chemotherapeutic treatments. However, despite the current advances, many cancer patients die every year so both researchers and clinicians nowadays keep focusing their efforts on a more precise characterization of the individual tumors *(Doroshow and Kummar 2014)*, and in performing high-throughput screenings and clinical trials to find better therapeutic drugs. The future is promising, but definitely, we still have a long path in front of us.

# *Introduction*

# CANCER

Tumors are complex tissues, composed of different cell types, with an uncontrolled proliferation potential and the ability to highjack the control mechanisms of the organism to fight for their survival. Tumors develop in a multistep process where cells sequentially acquire genetic abnormalities, which provide them with new biological capabilities, and a growth advantage under otherwise deleterious circumstances *(Hanahan and Weinberg 2000)*.

The carcinogenesis process can be divided into three major steps: the initiation involves an irreversibly alteration in a cell, the promotion step is defined as the expansion of the initiated cell clone leading to a benign lesion, and progression is the last stage where the cancerous clone expands rapidly generating a malignant cancer *(Barrett 1993)*. In humans, at least four to six mutations are required to reach the malignant state *(Hahn and Weinberg 2002)*. These mutations may be a combination of inherited alterations, modifications induced by environmental factors or the result from cell replication errors. Two thirds of the cancer cases are estimated to be caused by errors during stem cell divisions, hence tissues that host the greatest number of stem cell divisions are usually those most vulnerable to cancer *(Tomasetti and Vogelstein 2015)*.

During the process of malignant transformation, cells rely on genome instability *(Tomlinson et al. 2002)* to acquire features of limitless replicative potential, insensitivity to antigrowth cues, evasion of apoptosis, self-sufficiency in growth signals, and avoidance of immunosurveillance *(Hanahan and Weinberg 2000)*. Furthermore, tumors evolve by gathering support from surrounding stromal cells for niche remodeling, and by attracting new blood vessels for the supply of nutrients and oxygen. This evolution goes hand in hand with tumor-promoting inflammation, which will foster the progression of the tumor till it can invade and metastasize

**(FIGURE 2)** *(Lu et al. 2006; Hanahan and Weinberg 2011)*.
Many of the aforementioned features can be brought about by genetic alterations in key oncogenes (gain of-function mutations, amplification, and overexpression) and tumor suppressors (loss-of-function mutations, deletion, and epigenetic silencing) *(Hahn and Weinberg 2002)*. Aside, there are non-oncogenic signaling pathways that must also be rewired to adapt to these new biological capacities and to tolerate the new cellular stresses. For instance, once transformed cells enter an uncontrolled proliferation state, they express more telomerase to overcome the shortening of telomeres, and they weaken their spindle checkpoint to survive aberrant mitosis *(Luo et al. 2009b)*. Another consequence of enhanced proliferation is the need for an increase in biosynthesis; hence tumor cells need to adapt their metabolism to fulfill

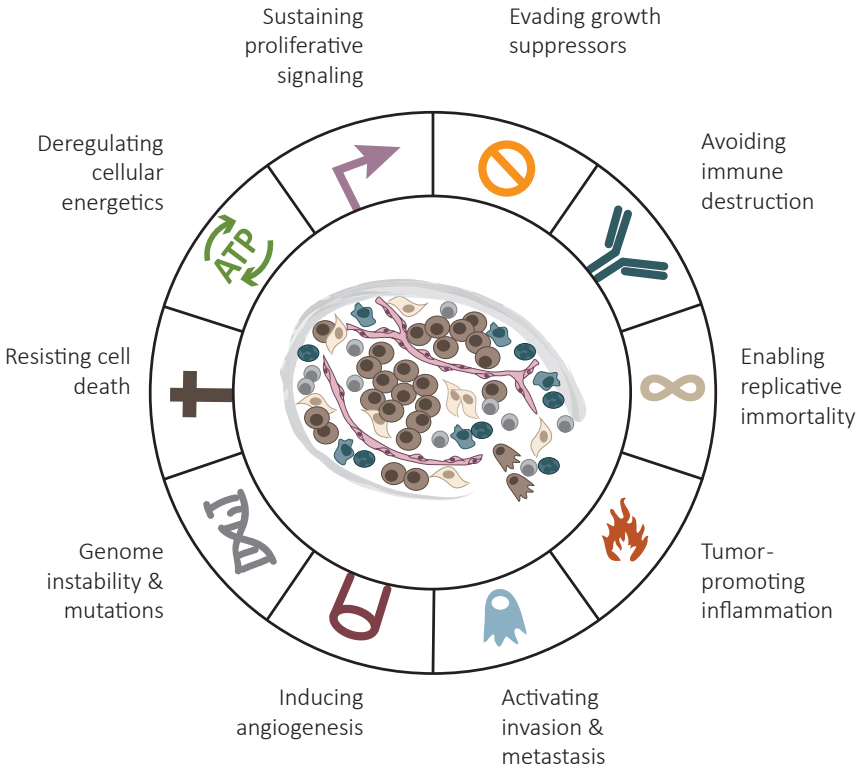


**FIGURE 2. The hallmarks of cancer.** Illustration of the classical and emerging hallmark capabilities of cancer cells. Modified from *(Hanahan and Weinberg 2011)*.

the new demands. As a side-effect, the cell will experience an accumulation of unfolded proteins and will need to constitutively activate the heat-shock response and the proteasome. The newly accelerated metabolism will eventually exhaust the available nutrients and the delivery capabilities of the local vasculature, forcing the tumor cells to monitor these changes in their microenvironment and develop a strategy to survive this metabolic stress, for example by inducing neo-angiogenesis *(Jones and Thompson 2009)*. Therefore, there are two key mechanisms: changes in stress-support pathways within the neoplastic cells, and changes in the environment that alter the selective pressure on those neoplastic cells *(Barcellos-Hoff et al. 2013)*.

There are more than 100 distinct types of cancer and several subtypes of tumors can be found within specific organs. Although the mentioned biological features are common to almost every tumor, their acquisition appears in variable sequences, both among tumors of the same type and certainly between tumors of distinct types. This huge complexity makes it instrumental to understand the cellular circuitries involved, which ones are common to several or all tumor types, and whether they act in a cell-autonomous way or in collaboration with the other cells of the microenvironment *[reviewed in (Hanahan and Weinberg 2000)]*.

# NON-SMALL CELL LUNG CANCER

Each year 1.8 million new cases of lung cancer are diagnosed (13% of the total cancer incidence). In the year 2012, it accounted for 1.5 million deaths (19.4% of the total cancer-related deaths), affecting populations all around the world. Lung cancer is one of the most aggressive human cancers, with a 5-year overall survival of only 10–15% *(Brambilia and Travis 2014)*. The most important risk factor for lung cancer is smoking. In populations with prolonged cigarette use, the proportion of lung cancer cases attributable to cigarette smoking has reached 90% *(Doll 2000; IARC Working Group on the Evaluation of Carcinogenic Risks to Humans 2004)*. However, other factors such as asbestos or environmental smog also influence the risk of suffering lung cancer.

Due to its complexity and abundant subtypes, pathologists have long been challenged to accurately classify lung cancer, and this becomes of essential importance at the time of deciding a therapeutic treatment. According to histopathological criteria, lung cancer is classified into small-cell lung cancer (SCLC) and non-small cell lung cancer (NSCLC). NSCLC accounts for 82% of lung cancer cases and can be further divided into three major histologic subtypes: adenocarcinoma, squamous cell carcinoma and large cell carcinoma *(Travis et al. 1999; Tuveson and Jacks 1999)*. Adenocarcinomas are the most frequent type of NSCLC. They account for 40% of all lung cancer cases, are epithelial tumors, and can be distinguished by positive staining for surfactant proteins and thyroid transcription factor (TTF1) *(Tuveson and Jacks 1999; Travis et al. 2015)*.

## Common genetic alterations

Lung cancer is one of the most genomically altered cancers *(Kan et al. 2010)*. Arguably, the most common mutated or deleted genes in both NSCLC and SCLC are the tumor suppressor genes *TP53* and retinoblastoma *(RB1)*. *TP53* is altered in more than 75% of SCLC, and in 50% of NSCLC. The *TP53* mutations, mostly G–T transversions, carry the hallmark of smoking *(Lewis and Parry 2004)*. *RB1*, on the other hand, is inactivated in more than 90% of SCLC while being less frequent in NSCLC (~15%)*(Reissmann et al. 1993; Dosaka-Akita et al. 1997)*. In contrast, mutations or promoter hypermethylation of cyclin dependent kinase inhibitor 2A (*CDKN2A*), mutations of *RAS* genes, or aberrant expression of *HER2* occur frequently in NSCLC but rarely in SCLC *(Zochbauer-Muller et al. 2002; Fong et al. 2003)*.

Specifically in lung adenocarcinoma, exome and genome sequencing has identified a wide variety of genetic abnormalities as drivers of this cancer subtype **(TABLE 1)**. Activating mutations of *EGFR* and the Kirsten Ras (*K-RAS*) oncogene are the most common genetic lesions, and are mutually exclusive. We can also find amplifications of *TTF1*, activating mutations on *BRAF*, and inactivation of tumor suppressor genes like *STK11*. Moreover, fusion genes bounding a tyrosine kinase domain and a dimerization domain can also act as driver mutations. They usually involve the anaplastic lymphoma receptor tyrosine kinase (*ALK*), or the proto-oncogenes *ROS1* or *RET (Sanchez-Cespedes et al. 2002; Wood et al. 2015; Campbell et al. 2016)*. Noteworthy, *ALK* or *EGFR* mutations are more frequent in patients who have never smoked, while *K-RAS* mutations are predominant in those patients with a smoking history *(Pao et al. 2004; Heist and Engelman 2012)*.

### Mutations in *K-RAS*

The work reported in this thesis is focused on the so far intractable K-RAS mutant adenocarcinoma, which accounts for 25% of lung adenocarcinomas and 20% of all NSCLCs *(Slebos et al. 1990; Rodenhuis and Slebos 1992)*. K-RAS is one of the four members of the Ras family of small GTPases. It has two isoforms, *KRAS4A* and *KRAS4B*, the latter one being the most abundant splicing variant *(Wang and You 2001)*. This 21kDa protein serves as a transducer

that couples surface receptor tyrosine kinases to intracellular effector pathways, transducing growth-promoting and survival cues. In homeostatic conditions, it cycles between 'on' (GTP-bound) and 'off' (GDP-bound) conformations. This cycle requires catalyzers to stimulate the exchange of GDP for GTP (guanine nucleotide exchange factors) or to accelerate the hydrolysis of GTP (GTPase-activating proteins).

The most frequent mutations of *K-RAS* occur in codon 12 (85%) and 13 (14%) and prevent the formation of van der Waals bonds between RAS and GTPase-

**TABLE 1.** Frequent genetic alterations and targeted therapies for NSCLC

| Gene | Status* | Available GEMM | Available targeted therapy | References |
|---|---|---|---|---|
| ALK | F | ALK fusion, L1196M, F1174L | Crizotinib, ceritinib | *(Soda et al. 2007; Chen et al. 2010)* |
| EGFR | M | L858, Del19, T790M, Ins20 | Erlotinib, gefitinib, afatinib, osimertinib | *(Paez et al. 2004; Ji et al. 2006)* |
| MET | F | OE | Crizotinib | *(Engelman et al. 2007; Xu et al. 2012a)* |
| ROS1 | F | N/A | Crizotinib | *(Rikova et al. 2007; Davies et al. 2012)* |
| BRAF | M | V600E | N/A | *(Paik et al. 2011)* |
| CDKN2A | M | Null | N/A | *(Wang et al. 2003; Lou-Qian et al. 2013)* |
| HER2 | M/C | HER2-YVMA insertion | N/A | *(Stephens et al. 2004; Wang et al. 2006b)* |
| K-RAS | M | G12D, G12V, G12C | N/A | *(Jackson et al. 2001; Mascaux et al. 2005)* |
| MEK1 | M | N/A | N/A | *(Marks et al. 2008)* |
| PIK3CA | M | p110α | N/A | *(Kawano et al. 2006; Engelman et al. 2008)* |
| TP53 | M | Conditional null, R172H | N/A | *(Mitsudomi et al. 2000; Chen et al. 2012)* |

Abbreviations are explained in the main text except for: Del19, EGFR exon 19 deletion; Ins20, EGFR exon 20 insertion; N/A, not available; OE, overexpression. *Status refers to the mechanisms by which each gene is altered in tumors: mutation (M), copy number gain (C) or fusion (F). Modified from *(Chen et al. 2014)*.

activating proteins *(Pylayeva-Gupta et al. 2011)*. In consequence, the GTPase function of K-RAS is disrupted, rendering the protein and the downstream effector pathways constitutively active. The most frequent missense mutations in KRAS codon 12 are *K-RAS*$^{G12V}$ and *K-RAS*$^{G12D}$. The Glycine to Valine substitution has been associated with a worse prognosis than the substitution to Glutamate, raising the possibility that specific amino acid substitutions might dictate particular transforming features *(Keohavong et al. 1996)*.

K-RAS shows pleiotropic activity; for instance, it leads to cell cycle progression through the RAF/MEK/ERK cascade, to epithelial-to-mesenchymal transition via RHO B or to apoptosis inhibition through PI3K/PDK1/AKT, to name a few *(Marshall 1999; Zondag et al. 2000; Malumbres and Barbacid 2003)*. K-RAS overactivation can also induce senescence but this might even favour the selection of clones with defective checkpoints, e.g. mutated *TP53 (Collado et al. 2005; Halazonetis et al. 2008)*. In view of the pro-growth and pro-survival functions that K-RAS can mediate, the pro-tumorigenic activity of the constitutively active mutant K-RAS might not be surprising.

## The cell of origin

Lung adenocarcinoma is predominantly diagnosed in the distal airways, namely the bronchioles and alveoli. In humans, the basal epithelium of the bronchioles contains basal cells; while the luminal epithelium contains ciliated, neuroendocrine, goblet and club cells. Differently, mouse bronchioles are composed just by a monolayer epithelium of club, neuroendocrine and ciliated cells *(Cheung and Nguyen 2015)*. The epithelium of the alveoli is made up of alveolar epithelial type 1 cells (AE1), which provide the interface for gas exchange; and alveolar epithelial type 2 cells (AE2), which are characterized by surfactant protein C expression (SPC$^+$) and secrete pulmonary surfactant to reduce surface tension so the alveoli do not collapse upon exhalation. Immature AE2 cells (SPC$^+$, Integrin $\alpha6\beta4^+$) have been proposed as progenitors of the adult alveolar epithelium, together with multipotent bronchioalveolar stem cells (BASC). Situated in the junction between the bronchiole and the alveolus (BADJ), BASC co-express CCSP and SPC markers, can self-renew, and

can give rise to both AE2 and club cells (CCSP+) *(Rock and Hogan 2011; Kotton and Morrisey 2014)*.

It is possible that the biology of the different cells is what drives the different phenotypes of lung cancer with distinct genotypes **(FIGURE 3)**. It has been proposed that stem and progenitor cells are the cells of origin of carcinoma because they are the only ones with enough lifespan to accumulate the many genetic alterations required for tumor progression. Furthermore, given their self-renewing capacity they would not need to be subjected to extensive epigenetic reprogramming *(Visvader 2011)*. However, it is also plausible that a more mature, differentiated cell with acquired self-renewal capabilities might give rise to malignancy.

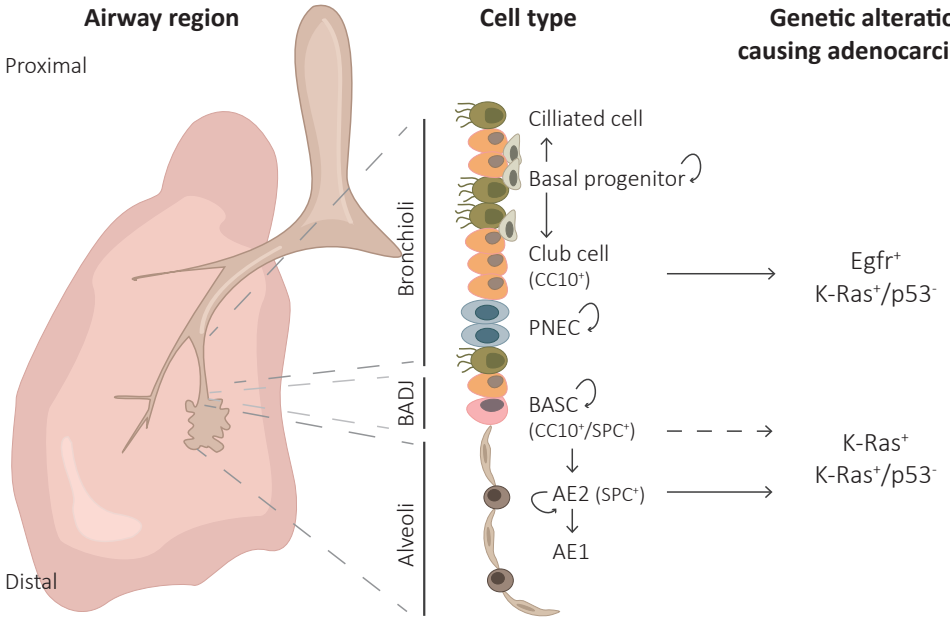


**FIGURE 3. Cells of origin of lung cancer.** Known (arrows) and predicted (dashed arrow) influence of the cell of origin and the oncogenic mutation in the formation of lung adenocarcinoma. Abbreviations: PNEC, pulmonary neuroendocrine cell. Circled arrows show cells with self-renewing capacity. Adapted from *(Cheung and Nguyen 2015)*.

The cell of origin of lung adenocarcinoma is still under discussion because the distal airway epithelium is very plastic and several cell types can be induced to transform under different conditions. AE2 progenitors have historically been seen as the tumor initiating cells, consistent with the staining of human adenocarcinoma samples with the SPC marker *(Cheung and Nguyen 2015)*. However, in 2001 the BASC population was identified *(Jackson et al. 2001)* and soon proposed as the putative cell of origin of K-Ras-driven adenocarcinomas *(Kim et al. 2005)*. Nevertheless, recent studies in genetically engineered mouse models (GEMM) targeted the expression of oncogenic K-Ras only in $CCSP^{+}$ cells (club cells and BASC) or only in $SPC^{+}$ cells (AE2 and BASC), and AE2 cells seemed to be the only cells capable to give rise to advanced adenocarcinomas, while club and BASC seemed limited to low grade lesions *(Xu et al. 2012b; Mainardi et al. 2014)*.

## Progression of NSCLC

### Stages of lung tumor progression

The histologic progression of NSCLC was poorly understood until the beginning of the 21st century. In 2001, the laboratory of Tyler Jacks used a $K\text{-}Ras^{G12D}$-driven lung cancer mouse model to propose atypical adenomatous hyperplasias (AAH) as the precursor lesions of lung adenomas. AAH are formed by the proliferation of atypical epithelial cells growing along alveolar septa without disrupting the alveolar architecture, while adenomas are neoplasms indeed distinguished by the distortion of this architecture **(FIGURE 4)**. Adenomas, in turn, might be the previous stage to malignant lung adenocarcinoma formation *(Jackson et al. 2001; Kerr 2001)*. As adenomas progress they show features of malignancy, including nuclear hyperchromatism and increased mitotic rate. Nuclear pleomorphisms are found already in the adenocarcinoma stage, e.g. enlarged nuclei.

Aside of this histologic classification, clonal evolution inside lung tumors can make lesions derive into a different cancer subtype. For instance, lineage-tracing experiments in GEMM have shown that K-Ras-transformed club cells can form hyperplasias in the terminal bronchioles that eventually switch to

SPC-expressing adenocarcinomas. Inflammation at the moment of *K-Ras* activation or the loss of *Tp53* might be the driving force behind this switch *(Mainardi et al. 2014; Sutherland et al. 2014)*. Also K-Ras-driven adenocarcinomas arising from AE2 progenitors can transdifferentiate into lung squamous cell carcinomas when mutating *Stk11 (Ji et al. 2007; Han et al. 2014)*. In consequence, this non-linear evolution is an added difficulty to the already arduous tasks of accurately classifying and treating lung tumors.

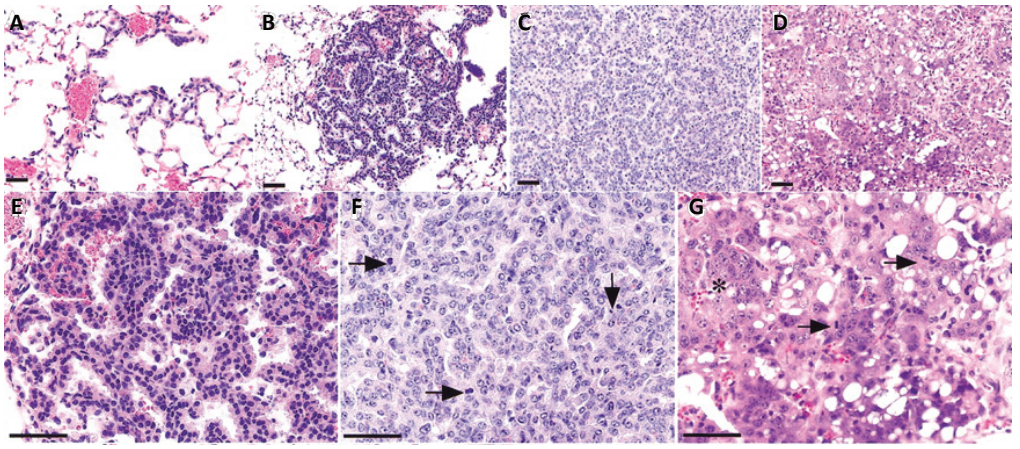


**FIGURE 4. Stages of tumor progression in K-Ras$^{G12D}$ mice.** (A) AAH 2 weeks post-induction. (B) Papillary adenoma 6 weeks post-induction. (C) Large adenoma 12 weeks post-induction. (D) Adenocarcinoma 16 weeks post-induction. (E) Higher magnification of the adenoma in B. (F) Higher magnification of the lesion in C (arrows indicate mitosis). (G) Higher magnification of the lesion in D. The tumor shows increased mitotic rate (arrows), nuclear enlargement, and prominent nucleoli (asterisk). Taken from *(Jackson et al. 2001)*.

## Lung cancer metastasis

More than 70% of patients with advanced stage NSCLC, die within 18 months of diagnosis due to metastasis *(Wood et al. 2014)*. Metastatic spread starts with cancer cells invading and migrating toward surrounding tissues by rearranging their cytoskeleton to gain motility and secreting extracellular matrix remodelers that will ultimately degrade the basal lamina and permeabilize the nearby vessels *(Kessenbrock et al. 2010)*. Cancer cells also need to lose their epithelial features,

like adhesion or polarization, in a process named epithelial-to-mesenchymal transition so they can intravasate and disseminate in the circulation. In this regard, loss of E-cadherin is a well-established prognostic marker which is observed in local lung cancer invasion and correlates with poor prognosis *(Kalogeraki et al. 2003)*.

Tens of thousands of cancer cells can be shed into the circulation, yet less than 0.01% will survive to produce metastasis because once in the circulation, cancer cells need to survive the attack of innate immune natural killer cells and the hemodynamic shear stress in small blood vessels. Thus, for enhancing their survival, tumor cells associate with blood platelets, that will also help them to slow down the velocity in the bloodstream and adhere to the endothelium at their destination *(Joyce and Pollard 2009)*. In the case of lung cancer cells, the most frequent metastatic sites are brain, adrenal gland, liver, bone and the lung itself *(Valastyan and Weinberg 2011)*. Once metastatic cells extravasate and settle in a secondary site, they must adapt to the new microenvironment of the host organ, and revert their mesenchymal phenotype through mesenchymal-to-epithelial transition to finally reinitiate the tumor growth *(Brabletz 2012)*.

**The lung cancer microenvironment**

Nowadays the reductionist view of tumors as groups of homogenous cancer cells is outdated and cancer is considered an ecological disease where malignant cells interplay with non-malignant stromal cells, conforming the tumor microenvironment (TME). Signals from cancer cells can act both systemically and locally, recruiting and reprogramming normal stromal cells. These stromal cells signal back to both the cancer cells and themselves, building up a network to construct, stabilize and expand the tumor niche, thus enabling proper tumor survival, growth and progression *(Polyak et al. 2009)*. In NSCLC, as in other cancers, the main stromal players are the activated fibroblasts (local and bone-marrow derived), the immune cells, the endothelial cells, and the pericytes **(FIGURE 5)**.

Cancer-associated fibroblasts (CAF) are marked by α-smooth muscle actin, and promote tumor progression. They can interplay with cancer cells and

other stromal cells through direct cell contact and by secreted factors. CAF are responsible for the aberrant production of mitogens, matrix metalloproteinases (MMP), and inflammatory mediators, that can stimulate tumor cell proliferation, induce remodeling of the niche, and recruit immune cells, respectively *(Levental et al. 2009; Erez et al. 2010)*. CAF have been shown to induce drug resistance in lung tumor cells by secreting hepatocyte growth factor *(Wang et al. 2009)*. Additionally, CAF are the main producers of extracellular matrix proteins, mainly fibronectin in lung adenocarcinomas, which supports tumor growth *(Kaplan et al. 2005)*.

The immune cells that usually infiltrate NSCLC include myeloid derived suppressor cells, regulatory T cells, tumor-associated macrophages, and tumor-associated neutrophils. Myeloid derived suppressor cells and regulatory T cells are the main responsible for the blockade of antitumor immunity, by downregulating the proliferation and induction of effector T cells *(Mantovani et al. 2008)*. In parallel, tumor cells can evade immunosurveillance on their own by expressing molecules that maintain tolerance to normal peripheral tissues, namely the tumor-associated programmed cell death 1 ligand (PDL1), which inhibits $CD8^+$ cytotoxic response *(Juneja et al. 2017)*.

Tumor-associated macrophages and tumor-associated neutrophils can show different phenotypes according to their role in impeding (type I immune response) or promoting (type II) tumor progression. In lung cancer, tumor-promoting macrophages and neutrophils secrete pro-angiogenic factors such as platelet-derived growth factor (PDGF) and vascular endothelial growth factor (VEGF), thus they are associated with increased microvessel formation. Moreover, they also produce inflammatory cytokines, reactive oxygen species (ROS), and proteases that will induce mitogenic signals in the neighboring cells and restructure the extracellular matrix *(Vignaud et al. 1994; Mantovani et al. 2011)*.

Finally, endothelial cells and pericytes are responsible for constructing new blood vessels and producing blood-borne factors to nourish the tumor as it grows *(Lu et al. 2006; Hanahan and Coussens 2012)*. The angiogenic switch is arguably the inflection point in the growth and malignization of tumors.

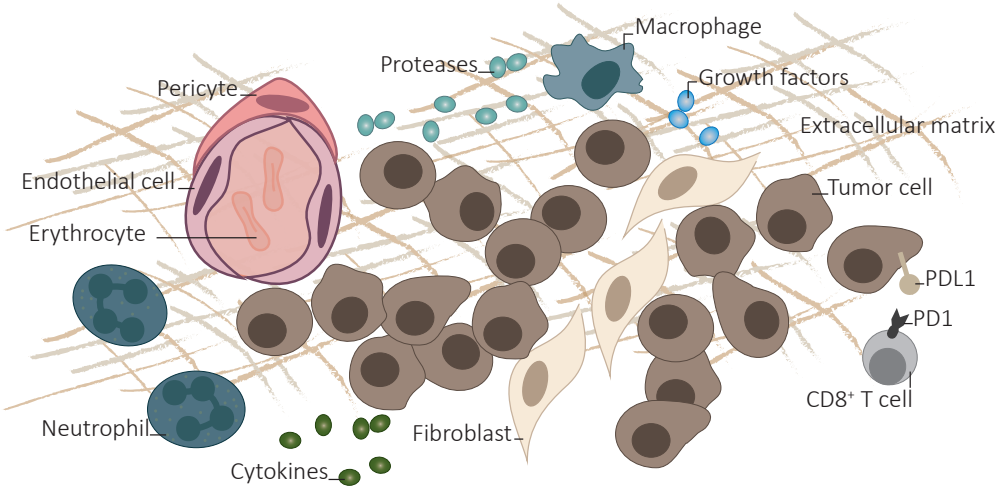


**FIGURE 5. Lung cancer microenvironment.** The TME includes, among others, recruited endothelial cells, fibroblasts, myeloid cells (macrophages, neutrophils), and lymphoid cells. Extracellular matrix gives structural support to tumor cells. Tumor cells, moreover, often express immune checkpoint molecules, such as PDL1, to attenuate a cytotoxic response from T cells. Modified from *(Chen et al. 2014)*.

Although the lungs is a highly vascularized organ, eventually local blood vessels cannot keep up anymore with the rate of tumor growth. Thus, tumor cells and their surrounding stromal cells enter a hypoxia state that leads to secretion of VEGF and PDGF, which increase intratumoral microvascular density. The expression of these factors is frequently reported in NSCLC and correlates with poor prognosis *(Masuya et al. 2001)*.

Elucidating the nature of co-evolution of tumor cells with their microenvironment is not only crucial for a better understanding of the primary tumor, as the TME is involved in the metastatic process as well. To name a few aspects, immune cells secrete proteases that facilitate cell motility, CAF produce transforming growth factor β (TGF-β) that induces epithelial-to-mesenchymal transition in cancer cells *(Pietras and Ostman 2010)*, and the tortuous vasculature of tumors has deficient intercellular junctions, which makes them permeable, facilitating cancer cell intravasation *(Xian et al. 2006)*. Moreover, the primary tumor releases factors to distant organs to recruit immune cells that will prepare a favorable niche prior to the arrival of the metastatic cell *(Kaplan et al. 2006; Peinado et al. 2011)*.

Therefore, considering the TME as a potential target offers new therapeutic opportunities, with the advantage that the genetically stable cells composing the microenvironment are less plastic and thus less likely to acquire drug resistance *(Hu and Polyak 2008)*.

## Mouse models for the study of NSCLC

Mouse models have been an essential tool for learning the pathogenesis of lung cancer. The murine tumors share a great similarity in their histopathological features and genomic alterations with those found in human cancers. Therefore, they have enabled numerous experiments which would not be possible using patient samples or cancer cell lines, like studies of metastasis, preclinical trials for targeted therapies or lineage-tracings for the identification of tumor initiating cells *(Heist and Engelman 2012)*.

The first mouse models for lung cancer were based on the susceptibility of certain inbred strains to spontaneous tumor-development, like A/J mice, and their enhanced sensitivity to carcinogens such as polycyclic aromatic hydrocarbons and nitrosamines derived from tobacco, or ethyl carbamate (urethane) *(Shimkin and Stoner 1975)*. The molecular characterization of these mice revealed genetic alterations nowadays known to be important in the development of lung cancer, like activating mutations in *K-Ras (Chen et al. 1994)*, overexpression of c-Myc *(Re et al. 1992)* or inactivation of *Cdkn2a (Malkinson 2001)*. Nevertheless, the random mutagenesis process made it difficult to control the experimental conditions; thus, more specific and sophisticated models were needed, like transgenic mice that express an oncogene or knock-out (KO) mice which can inactivate a tumor suppressor. Today, GEMM for most of the common NSCLC driver mutations have been generated, including for *K-Ras*, *Egfr* and *Eml4-Alk* fusion *(Kwon and Berns 2013)*. Some examples are displayed in **TABLE 1**.

In the first generation of GEMM, the expression of genetic alterations was constitutive and ubiquitous, and many times driven by strong viral

promoters *(Tuveson and Jacks 1999)*. The main problem was that mutated cancer genes in the germ line often led to embryonic lethality, impeding the study of their effects in adult mice. Moreover, a constitutive and ubiquitous model is far from resembling the physiological situation where few transformed cells with a stochastic-occurring mutation try to thrive surrounded by ostensibly normal cells in a specific organ.

This was partially solved by the use of conditional alleles, which better mimic the sporadic tumorigenesis process and which also allow for a spatio-temporal control of the expression of the mutated gene *(Jonkers and Berns 2002)*. The K-Ras$^{G12D}$ inducible model is the most widely used nowadays for the study of NSCLC. It develops adenocarcinomas after 9 to 12 weeks after oncogenic K-Ras induction, but no metastasis is detected *(Meuwissen et al. 2001)*. Moreover, it allows the control of tumor initiation and multiplicity by the dose of Cre recombinase that is inoculated into the animal using an adenovirus, facilitating the analysis of tumor progression. The model also mimics sporadic tumor development as activation of K-Ras$^{G12D}$ occurs in some tumor cells while the surrounding cells are normal.

## Development of targeted therapies

Diagnosis and treatment of NSCLC has greatly improved in the last decade thanks to the implementation of personalized medicine. Nowadays, stratification and treatment selection for patients not only relies in radiography and pathological evaluation but also in the genetic characteristics of the tumor.

On one hand, patients of advanced NSCLC with *EGFR* mutations or *ALK* fusions can benefit from targeted therapy with tyrosine kinase inhibitors. Unfortunately, almost every treated tumor will become resistant in less than a year and continue to progress *(Travis et al. 2015)*. Therefore, the use of targeted therapy in NSCLC is restricted to non-resectable and late stage tumors *(Timmerman et al. 2010; Heist and Engelman 2012)*. On the other hand, patients of advanced stage NSCLC without targetable genomic alterations, like mutant

A

| GENETIC VALIDATION IN GEMM MODEL | PHARMACOLOGIC INHIBITION IN GEMM MODEL | REFERENCE |
|---|---|---|
| Tumor initiation in *K-Ras*-driven NSCLC | | |
| 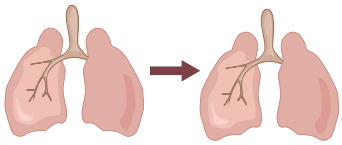 | | |
| **C-RAF** | | |
| **MEK1/2 or ERK1/2** | | *(Blasco et al., 2011)* |
| **p110α** | | *(Gupta et al., 2007)* |
| **p85** | *PI3K inh + MEK inh* | *(Engelman et al., 2008)* |
| Tumor initiation & progression in *K-Ras*-driven NSCLC | | |
| 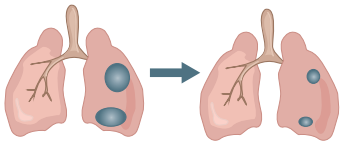 | | |
| **CDK4** | *CDK4 inhibitor* | *(Puyol et al., 2010)* |
| **GATA2** | *Proteasome inhibitor + ROCK inhibitor* | *(Kumar et al. 2012)* |
| **MYC** | | *(Soucek et al., 2008)* |
| Tumor initiation & progression in *K-Ras* + *Tp53*-driven NSCLC | | |
| 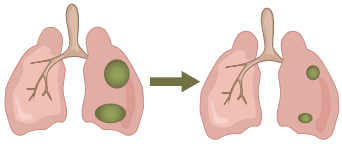 | | |
| **NFκB (IκB-SR)** | | *(Meylan et al., 2009)* |
| **NFκB (IKKβ)** | | *(Xia et al. 2012)* |

B

| SYNTHETIC LETHALITY | |
|---|---|
| Mutant *K-RAS* human NSCLC cell lines (RNAi screens) | |
| 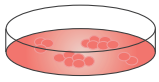 | |
| **TKB1** | *(Barbie et al., 2009)* |
| **PLK1** | *(Luo et al., 2009)* |
| **GATA2** | *(Kumar et al. 2012)* |

**FIGURE 6. Preclinical studies to validate therapeutic targets in K-RAS-driven NSCLC.** (A) GEMM driven by conditional mutant K-Ras alleles (in blue) and GEMM that also carry mutated, KO or null Tp53, which develop more aggressive metastatic adenocarcinomas (in green), are indicated together with the pharmacologic approaches, which use selective targeted inhibitors. (B) RNAi screenings aimed at identifying human genes that induce synthetic lethality in combination with K-RAS oncogenes. Modified from *(Barbacid 2012)*.

*K-RAS* or *CDKN2A*, are limited to the general platinum-based combination therapy *(Hirsch et al. 2017)*.

Therefore, there is an urgent need for new therapeutic approaches. As K-RAS has largely remain undruggable, many strategies targeting RAS downstream kinases and synthetic lethal partners have been developed. Validated targets that induce tumor regression include components of the ERK and PI3K/AKT cascades *(Engelman et al. 2008)*, or other pathways not directly linked to K-RAS like CDK4 *(Puyol et al. 2010)* or GATA2 *(Kumar et al. 2012)*. **FIGURE 6** summarizes some of the most relevant preclinical studies in the last few years using GEMM of K-Ras-driven NSCLC. Nevertheless, these studies report some targets that have shown only partial tumor regression or have only been studied during tumor initiation. Aside, some of the inhibitors, like those for MEK, show undesirable toxicities. As well, some strategies have been tested only in Tp53-proficient tumors, and the development of drug resistance has not yet been evaluated in many cases. Hence, we still need to continue studying and searching for better therapies against this aggressive cancer.

# p38 MAPK SIGNALING

Cells need to be aware of the constant changes in their environment to respond accordingly. Transmembrane receptors integrate the extracellular stimuli and trigger signaling cascades which eventually lead to the activation of intracellular programs. Protein phosphorylation is one of the main mechanisms of signal transduction, indeed almost every known signaling pathway eventually impinges on a protein kinase or phosphatase *(Graves and Krebs 1999)*.

## The mitogen-activated protein kinase family

Mitogen-activated protein kinases (MAPKs) are a superfamily of proline-directed serine/threonine protein kinases. Their activation may be induced by a broad variety of stimuli (hormones, growth factors, cytokines, and environmental stresses) deriving in the regulation of many cellular processes such as proliferation, differentiation, and survival *(Roux and Blenis 2004)*.

Four major MAPK pathways have been identified in mammals: the extracellular signal regulated kinase (ERK) 1/2 (Boulton and Cobb 1991), the c-Jun N-terminal kinase (JNK) 1/2/3 *(Derijard et al. 1994; Kyriakis et al. 1994)*, the p38 MAPK α, β, γ, ∂ *(Freshney et al. 1994; Han et al. 1994; Lee et al. 1994; Rouse et al. 1994)* and the ERK5 pathway *(Lee et al. 1995; Zhou et al. 1995)*. Four additional MAPK–like components have been also identified (ERK3/4 and ERK7/8) but they do not seem to follow the canonical mechanism of activation of classical MAPKs *(Coulombe and Meloche 2007)*.

Canonical transmission of signals occurs through three evolutionarily conserved, sequentially acting kinases: a MAP kinase kinase kinase (MAP3K)

receives the upstream signal and activates a MAP kinase kinase (MAP2K), which in turn will activate the MAPK. MAPKs are catalytically inactive until dually phosphorylated by MAP2Ks on their activation loop, containing a Thr-Xaa-Tyr motif *(Kyriakis and Avruch 2001)*. In general, the ERK1/2 cascade is activated by mitogens, whereas the JNK and p38 MAPK cascades are activated mainly by stresses and pro-inflammatory cytokines **(FIGURE 7)**. Once activated, MAPKs can phosphorylate downstream targets like transcription factors, other protein kinases or RNA binding proteins *(Dhillon et al. 2007; Trempolec et al. 2013a)*.

Specificity of MAPKs is provided in part by conserved docking domains to bind substrates, which are mainly phosphorylated on serines or threonines followed by a proline. Additionally, scaffold proteins link components of the pathway together to ensure effective signal transmission. The level of MAPKs usually does not change throughout the course of stimulation, and the magnitude and duration of signaling is typically regulated through dephosphorylation

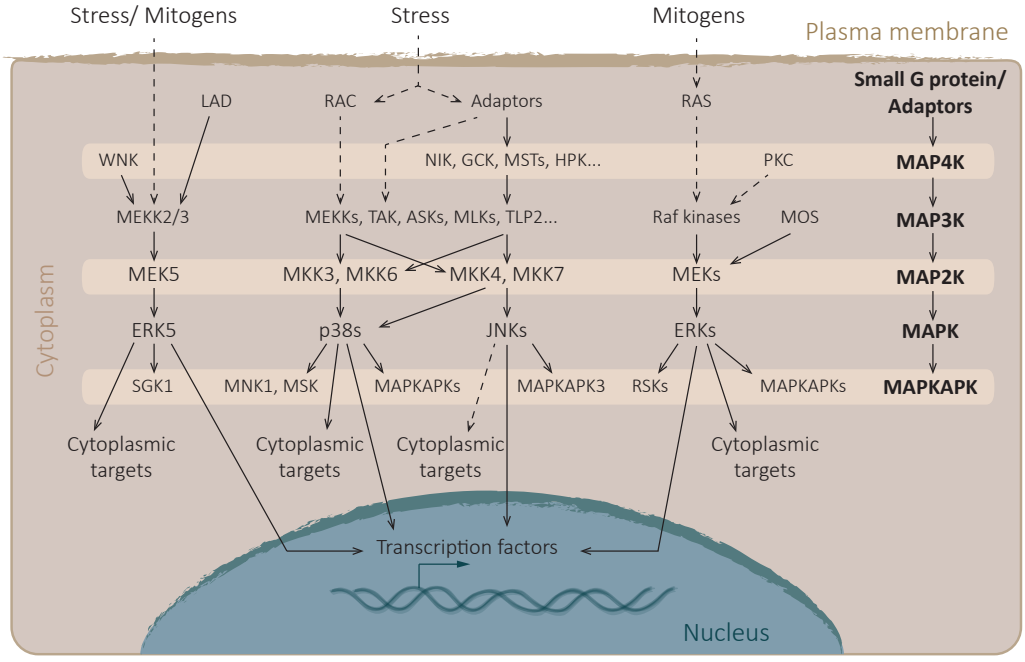


**FIGURE 7. Scheme of the canonical mammalian MAPK signaling cascades.** MAPK signaling shows a cascade organization, in which activation of upstream kinases leads to sequential activation of the MAPK modules. Adapted from *(Keshet and Seger 2010)*.

by generic phosphatases or dual-specificity phosphatases that downregulate MAPK activity *(Krishna and Narang 2008; Pan et al. 2012)*.

Despite the complexity of the MAPK system, consisting of more than 200 distinct components, tight mechanisms of regulation define which MAPKs will be activated and, consequently, what will be the cellular response to a particular stimulus. Likewise, since a given stimulus can activate different MAPKs, it is possible that crosstalk among them contributes to the final response. For example, p38 MAPKs can inhibit the JNK pathway at the level of MAP3Ks, or inhibit the ERK1/2 pathway through the phosphatase PP2A *(Stalheim and Johnson 2008; Cuadrado and Nebreda 2010; Keshet and Seger 2010)*.

## The p38 MAPK pathway

Four genes encode for the four p38 MAPKs: *MAPK14* for p38α, *MAPK11* for p38β, *MAPK12* for p38γ, and *MAPK13* for p38δ. p38α was the first member identified, and is the homologue of Saccharomyces cerevisiae Hog1. Moreover, three alternatively spliced isoforms of the *MAPK14* gene have been reported: Mxi2, Exip and CSBP1 *(Lee et al. 1994; Faccio et al. 2000; Yagasaki et al. 2004)*.

Despite the ~60% homology in their amino acid sequences, p38α, p38β, p38γ and p38δ show different target preferences, different sensitivity to chemical inhibitors and also different tissue expression patterns. p38α and p38β, but not p38γ or p38δ, can phosphorylate MAPKAPK2 (MK2) and MAPKAPK3 (MK3), and can be inhibited by low concentrations of pyridinylimidazole drugs, such as SB203580 or SB202190. These inhibitors bind competitively to the ATP-binding pocket in p38α and p38β, but p38γ and p38δ have a bulky methionine in position 106 that impedes inhibitor binding *(Coulthard et al. 2009; Cuadrado and Nebreda 2010)*.

p38α is highly abundant in most cell types, and p38α KO mice are embryonic lethal due to placental defects *(Adams et al. 2000; Allen et al. 2000; Mudgett et al. 2000; Tamura et al. 2000)*. Conditional deletion of p38α in the mouse embryo bypasses the lethality, but pups die soon due to lung dysfunction *(Hui et al. 2007)*. Conversely, expression of p38β, p38γ and p38δ is more restricted to

specific tissues: p38β is generally expressed at low levels, except for brain where it shows significantly higher levels; p38γ is highly expressed in skeletal muscle, and p38δ is mainly found in pancreas, kidney and small intestine. Single deficiency of p38β, p38γ or p38δ does not affect normal development in mice, suggesting putative compensatory functions among the p38 MAPKs *(Beardmore et al. 2005; Cuenda and Rousseau 2007; Ruiz-Bonilla et al. 2008)*.

Three MAP2Ks can phosphorylate p38 MAPKs: MKK3 can activate p38α, p38γ and p38∂; MKK4, which is also an activator of JNKs, can activate p38α; and MKK6 is a potent activator of the four p38 MAPKs. The contribution of each MAP2K depends on the stimulus *(Remy et al. 2010)* and the expression level of each MAP2K in the given cell type. For instance, T cell-receptor-mediated p38 MAPK activation is selectively disrupted in MKK6 KO immature thymocytes but not in the MKK3 KO *(Enslen et al. 1998; Brancho et al. 2003)*. Of note, MAP2K-independent activation mechanisms have been reported as well, like p38α autophosphorylation induced by the interaction with TAK1-binding protein (TAB1) *(Ge et al. 2002; Tanno et al. 2003)*.

In mammals, twenty MAP3Ks have been identified so far and about ten of them can phosphorylate MKK3/4/6 to elicit p38 MAPK activation. Some examples are: apoptosis signal-regulating kinase (ASK) 1, which can activate p38α in response to oxidative stress *(Dolado et al. 2007)*; TGF-β-activated kinase (TAK) 1, which preferentially responds to inflammatory cytokines activating p38, JNK and nuclear factor kappa B (NFκB) pathways *(Wang et al. 2001)*; and MAPK/ERK kinase kinase (MEKK) 3, which impinges on the MKK3-p38 axis during hyperosmotic shock *(Uhlik et al. 2003)*. Upstream of the cascade, the regulation of MAP3Ks is complex, involving phosphorylation by STE20 family kinases, binding of small GTP-binding proteins of the Rho family or ubiquitination-based mechanisms. The diversity of MAP3Ks and their regulatory mechanisms allows cells to respond to a wide variety of stimuli through the p38 MAPK cascade, and also to activate other signaling pathways in parallel *(Cuevas et al. 2007; Stalheim and Johnson 2008)*.

p38 MAPKs act like a funnel for the different upstream stimuli but also allow for a downstream diversification of the signal **(FIGURE 8)** so that multiple functions can be simultaneously controlled; for example, protein degradation,

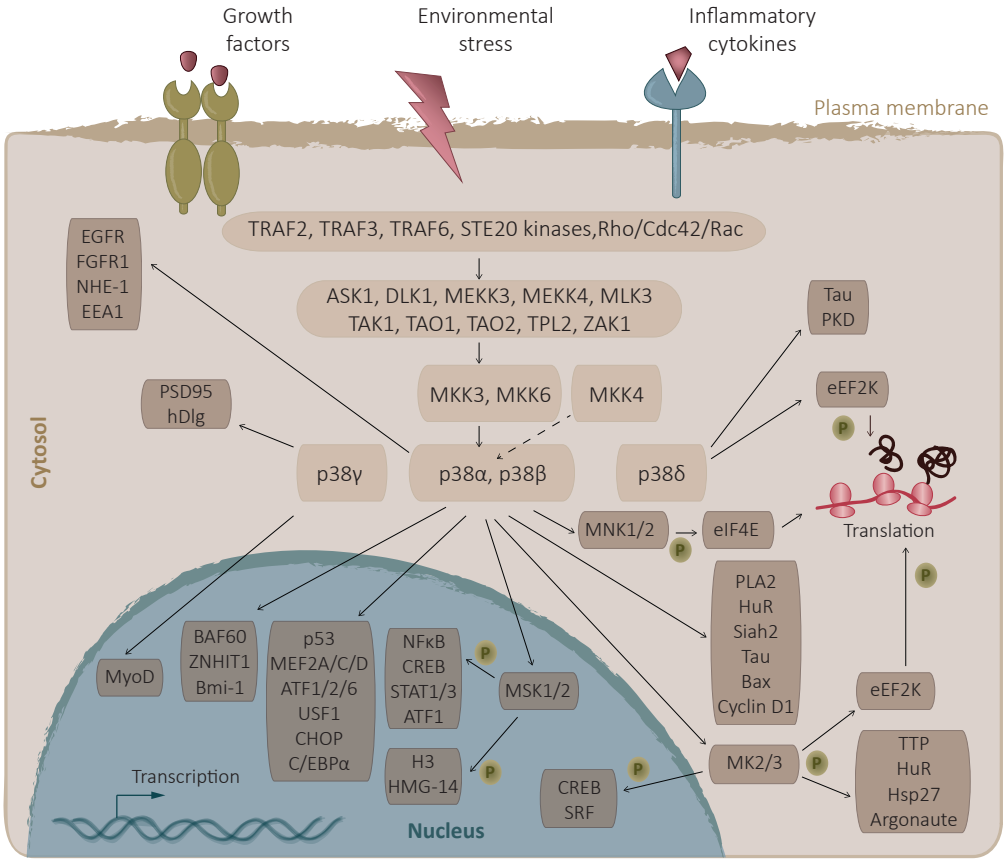


**FIGURE 8. The p38 MAPK pathway.** Different stimuli such as growth factors, inflammatory cytokines or environmental stresses can activate p38 MAPKs, which in turn target protein kinases, cytosolic substrates, transcription factors or chromatin remodelers. Abbreviations are explained in the main text except for: ASK1, apoptosis signal-regulating kinase 1; CHOP, C/EBP-homologous protein; DLK1, dual-leucine-zipper-bearing kinase 1; EEA1, early-endosome antigen 1; NHE-1, Na+/H+ exchanger 1; PSD95, postsynaptic density 95; TAO, thousand-and-one amino acid; TPL2, tumor progression loci 2; TTP, tristetraprolin; ZAK1, leucine zipper and sterile-α motif kinase 1; ZNHIT1, zinc finger HIT-type 1. Adapted from *(Cuadrado and Nebreda 2010)*.

mRNA stability, endocytosis, cytoskeleton dynamics or cell migration *(Shi and Gaestel 2002)*. p38 MAPKs have been reported to induce the expression of immediate-early response genes via the mitogen- and stress-activated kinases (MSK) 1 and 2 which, in turn, phosphorylate the nucleosomal proteins histone

H3 and high-mobility group (HMG) 14 *(Soloaga et al. 2003)*; or transcription factors, such as activating transcription factor (ATF) 1 and NFκB p65 *(Wiggin et al. 2002; Vermeulen et al. 2003)*. p38 MAPKs can also directly phosphorylate a number of transcription factors that will mediate differentiation or stress responses, like C/EBPα, myocyte enhancer factor 2C (MEF2C), ATF2/6 or Tp53 *(Perdiguero and Muñoz-Cánoves 2008; Geest et al. 2009)*.

Gene expression is also regulated by p38 MAPKs at the post-transcriptional level, for example by inhibiting the miRNA biogenesis mediator Drosha *(Yang et al. 2015)* or by inducing MK2-mediated phosphorylation of both AU-rich element (ARE)-binding proteins, that mediate mRNA stability *(Winzen et al. 1999; Mahtani et al. 2001)*, and argonaute2 (Ago2) that silences miRNAs *(Zeng et al. 2008)*. MK2 is also known to phosphorylate the heat-shock protein (Hsp) 27, which remodels actin cytoskeleton, on serines 15, 78 and 82 in response to growth factors and stress *(Stokoe et al. 1992; Rouse et al. 1994; Guay et al. 1997)*.

p38 MAPK can regulate protein synthesis too, via MK2/3-mediated phosphorylation of the eukaryotic elongation factor 2 kinase (eEF2K) *(Knebel et al. 2002)* and via MAPK interacting serine/threonine kinase (MNK) 1/2-mediated phosphorylation of the eukaryotic initiation factor 4E (eIF4E) *(Knauf et al. 2001)*. Moreover, many cytosolic proteins can be phosphorylated by p38 MAPKs, including phospholipase A2 (PLA2), glycogen synthase, the microtubule associated protein tau, cyclin D1, cyclin-dependent kinase inhibitors like CDKN1C, the ubiquitin ligase Siah2, Bcl-2 family proteins, EGFR, fibroblast growth factor receptor (FGFR)1 or keratins *(Khurana et al. 2006; Cuenda and Rousseau 2007; Swat et al. 2009; Trempolec et al. 2013b)*.

An additional layer of complexity is provided by the ability of p38 MAPKs to phosphorylate some substrates on non-proline directed sites instead of the Ser/Thr-Pro consensus motif *(Reynolds et al. 2000; Cheung et al. 2003)*. Moreover, kinase independent functions have been described for the yeast homolog Hog1 involving the recruitment of transcription machinery *(de Nadal and Posas 2010)*, although in mammalian cells there is yet little evidence.

p38 MAPKs are important regulators of inflammation, stress response, proliferation, apoptosis and cell survival *(Wagner and Nebreda 2009)*. Since the

**TABLE 2.** Studies on the roles of p38α in cancer using GEMM

| Organ | Mouse line | Cancer model | Phenotype// p38α role | References |
|---|---|---|---|---|
| Breast | WT treated with CDDP + p38i | MMTV-PyMT | Reduced tumor growth and malignancy, increased apoptosis // TP | *(Pereira et al. 2013)* |
| Colon | p38α (F/F) × Villin-Cre or Villin-CreERT2 | Deletion previous to AOM/DSS | Increased tumor load, impaired differentiation and barrier function // TS | *(Wakeman et al. 2012; Gupta et al. 2014)* |
| | p38α (F/F) x Villin-CreERT2 | Deletion previous to AOM/DSS- tumors | Reduced tumor load, enhanced apoptosis // TP | *(Gupta et al. 2014)* |
| | WT treated with p38i | $APC^{min}$ /AOM | Reduced tumors, highly infiltrated // TP | *(Chiacchiera et al. 2009)* |
| | WT treated with p38i + MEKi | AOM/DSS | Reduced tumor load, differentiated lesions, increased apoptosis // TP | *(Chiacchiera et al. 2012)* |
| Liver | p38α (F/F) × Alb-Cre or Mx-Cre | DEN and phenobarbital | Increased tumor load, erythroid proliferation defect // TS | *(Hui et al. 2007)* |
| | p38α (F/F) × Alb-Cre or Mx-Cre | DEN | Increased tumor burden, increased damage, and increased ROS levels // TS | *(Sakurai et al. 2008)* |
| Lung | p38α (F/F) x RERTn-Cre | $K\text{-}Ras^{LSLG12V}$ x Ad-Cre | AE2 hyperplasia and sensitivity to oncogenic insults // TS | *(Ventura et al. 2007)* |
| | $p38^{Y182F}$ x FSP1-Cre | $K\text{-}Ras^{G12D}$ | Reduced tumor burden, impaired reprogramming of the stroma // TP | *(Brichkina et al. 2016a)* |
| | $p38^{P224I}$ | $K\text{-}Ras^{G12D}$ | Reduced tumor load, increased apoptosis upon CDDP // TP | *(Brichkina et al. 2016b)* |
| Pancreas | p38α/β $^{Y323F}$ | $Trp53^{LSLR172H}$; $K\text{-}Ras^{LSLG12D}$ x Pdx1-Cre | Reduced tumors and secreted inflammatory cytokines // TP | *(Alam et al. 2015)* |
| Skin | K14-p38α DN | UV light | Reduced tumor burden, and reduced inflammation // TP | *(Dickinson et al. 2011; Liu et al. 2013;* |

Abbreviations: AOM, azoxymethane; CDDP, cisplatin; DEN, N-diethylnitrosamine; DN, dominant negative; DSS, dextran sodium sulfate; (F/F), floxed p38α; MEKi, MEK inhibitor; PyMT, polyoma middle T oncoprotein; p38i, p38 MAPK inhibitor; TP, tumor promoter; TS, tumor suppressor.

year 2000, gene-targeting experiments in mice have evidenced the contribution of p38 MAPKs to tissue homeostasis and pathological conditions, such as neurodegeneration, autoimmunity, and cancer *(Wagner and Nebreda 2009)*. See **TABLE 2** for an overview of the functions of p38α in cancer, which have been studied using different mouse models.

## The dual role of p38α in cancer

The pleiotropic activity of p38 MAPKs covers a compendium of the different hallmarks of cancer **(TABLE 3)**. Furthermore, p38 MAPK signaling can impact on many stresses affecting the cancer cells, including hypoxia, detachment from matrix, inflammation, or oxidative, metabolic, and chemotherapy-induced genotoxic stresses.

### Tumor suppressing functions

The activation of p38 MAPKs, and specifically of p38α, has been classically associated with tumor suppression due to its capacity to induce cell cycle arrest. For example, in response to stress, p38α can stop the G1/S transition by downregulating the expression of cyclin D1 *(Lavoie et al. 1996)*, by stabilizing the cyclin-dependent kinase inhibitor p21 *(Lafarga et al. 2009)*, or by phosphorylating RB1 *(Gubern et al. 2016)*. As well, p38α has been reported to negatively feedback on growth-promoting signals, such as oncogenic Ras, thus avoiding cell transformation *(Chen et al. 2000; Li et al. 2003)*. Accordingly, several proteins that can potentially downregulate the activity of p38α have been found overexpressed in human tumors and cancer cell lines, like the phosphatase Wip1 in breast cancer *(Bulavin et al. 2002; Li et al. 2002)*. p38α has been also associated with the G2/M checkpoint by activating Tp53 upon UV-induced damage *(Bulavin et al. 2001)*, or in response to replication stress *(Llopis et al. 2012)*. The irreversible cell cycle arrest that accompanies senescence requires p38α activity as well *(Iwasa et al. 2003; Zheng et al. 2013)*. However, senescence comes hand in hand with the senescence-associated secretory phenotype, a network of inflammatory cytokines controlled by p38α *(Freund*

*et al. 2011)* which has been shown to promote mammary tumor progression *in vivo (Alspach et al. 2014)*.

The ability of p38α to induce cell differentiation has also been connected to tumor suppression. p38α can stop cell proliferation to initiate differentiation-specific gene programs; like in the myogenesis process *(Perdiguero et al. 2007)* in which the absence of p38α impairs muscle differentiation and leads to rhabdomyosarcoma *(Puri et al. 2000)*. Likewise, other studies have showed the differentiation-mediated protective role of p38α against transformation in lung epithelial cells *(Ventura et al. 2007)*, intestinal epithelium *(Otsuka et al. 2010; Chiacchiera et al. 2012; Gupta et al. 2014)* and CD4- CD8- thymocytes *(Pedraza-Alva et al. 2006)*.

Another anti-tumoral role of p38α involves the induction of apoptosis. For instance, p38α can induce the expression of pro-apoptotic proteins in mammary epithelial cells to trigger anoikis *(Owens et al. 2009)*, or in mouse embryonic fibroblasts (MEFs) upon UV radiation *(Porras et al. 2004)*, and can inactivate anti-apoptotic Bcl-2 proteins by phosphorylation after serum withdrawal *(De Chiara et al. 2006)*. Also, p38α can induce apoptosis via the PP2A-mediated inactivation of AKT signaling, as long as cardiomyocytes are attached to their substrate *(Zuluaga et al. 2007)*. p38α is also able to activate Tp53 in response to genotoxic damage, which induces apoptosis both in normal and cancer cell lines *(Sanchez-Prieto et al. 2000; Cuadrado et al. 2007)*, halting situations of genomic instability. In addition, ROS accumulation, which can highly increase the rate of mutagenesis, activates p38α signaling, inducing apoptosis and preventing Ras-mediated transformation *(Dolado et al. 2007)*.

**Tumor promoting functions**

Nonetheless, some studies support pro-survival roles for p38α too. This is not surprising since p38α can mediate stress signaling, and several stress-related mechanisms can help to sort out mishaps before commiting the cell to death. Thereby, activation of DNA damage checkpoint by p38α has been reported to counteract tumor suppression, since it can favor resistance to cytotoxic agents or γ-radiation by facilitating DNA repair prior to mitosis entry, thus escaping

**TABLE 3.** Impact of p38α MAPK signaling on different hallmarks of cancer

| Trait | Mechanism// p38α role | Cell type | Stimulus | References |
|---|---|---|---|---|
|  | p38α induces senescence // TS | Fibroblastos | MKK3/6$^{EE}$; Ras$^{G12V}$; Wip1$^{-/-}$; late passage; low [$H_2O_2$] | *(Wang et al. 2002; Iwasa et al. 2003; Bulavin et al. 2004; Zheng et al. 2013)* |
|  | p38α reprograms the TME to produce growth signals // TP | CAF, mouse K-Ras-driven lung cancer cells | Bleomycin, hyaluronic acid | *(Alspach et al. 2014; Brichkina et al. 2016a)* |
| | GF and hormones stimulate proliferation via p38α // TP | Fibroblasts, PC12, MCF7 | Serum; FGF; estradiol; spermine | *(Maher 1999; Lewis et al. 2005; Faust et al. 2012)* |
| | p38α arrests G1/S transition of the cell cycle // TS | Fibroblasts, RIE1, U2OS, CRC cells, HEK293, MCF7 | MKK3/6$^{EE}$; NaCl; overconfluence, γ-radiation; $H_2O_2$ | *(Lavoie et al. 1996; Faust et al. 2005; Lafarga et al. 2009; Swat et al. 2009; Gubern et al. 2016)* |
|  | p38α promotes cell differentiation // TS | mESC, myofibroblasts, AE2 | Retinoic acid; low serum | *(Aoudi et al. 2006; Perdiguero et al. 2007; Ventura et al. 2007)* |
| | High p38 MAPK supports cancer cell dormancy // TS | Epidermal, glioma & lymphocytic cancer cell lines | uPAR OE; fibronectin; γ-secretase inhibitor | *(Aguirre-Ghiso et al. 2001; Masiero et al. 2011; Soeda et al. 2017)* |
|  | p38α activates proapoptotic proteins // TS | Cardiomyocytes, fibroblasts, keratinocytes | UV; nutrient deprivation | *(Porras et al. 2004; Van Laethem et al. 2004)* |
| | p38α-mediated G2/M arrest enhances survival // TP | Thymocytes, Jurkat, Daudi, U1810 | Phototherapy; etoposide; γ-radiation | *(Capellini et al. 2005; Kurosu et al. 2005; Cosaceanu et al. 2007)* |
|  | p38α activation regulates autophagy// TS or TP | Fibroblasts, HEK293 | Nutrient deprivation | *(Webber and Tooze 2010; Keil et al. 2013; Sui et al. 2014)* |
| | p38α modulates glucose metabolism // TP | Neutrophils, HeLa, OC316, H1299, MCF7, fibroblasts | LPS; nutrient deprivation | *(Schuster er al. 2007; Desideri et al. 2014; Chaube et al. 2015)* |

**TABLE 3 Continued.** Impact of p38α MAPK signaling on different hallmarks of cancer

| Trait | Mechanism// p38α role | Cell type | Stimulus | References |
|---|---|---|---|---|
|  | p38α stabilizes HIF1α and promotes angiogeniesis // TP | DU145, fibroblasts, glioma cells | Cr(VI); hypoxia; IL1β; γ-radiation | *(Gao et al. 2002; Emerling et al. 2005; Yoshino et al. 2006; Kim et al. 2014)* |
|  | Inflammatory molecules production depends of p38 // TP | Monocytes, HeLa, DC, cardiomyocytes | Endotoxin; LPS; active MEKK1; cortiescoesterone | *(Lee et al. 1994; Winzen et al. 1999; Saccani et al. 2002; Sun et al. 2008)* |
| | p38 promotes matrix remodeling // TP | Keratinocytes, fibroblasts, SCC cells, PC3 | TNFα; TGF-β | *(Johansson et al. 2000; Reunanen et al. 2002; Xu et al. 2006)* |
| | p38 activation triggers anoikis // TS | Intestine and breast EC, MDA-MB231 | Non-adherent conditions | *(Rosen et al. 2002; Owens et al. 2009; Zhang et al. 2009)* |
|  | p38α controls cytoeskeleton dynamics // TP | HUVEC, MSS31, fibroblasts | VEGF-A | *(Kobayashi et al. 2006; Rousseau et al. 2006)* |
| | p38α promotes EMT, invasion and migration // TP | NMuMG, PANC1, MCF10A, A549, PC9, PC14 | TGF-β; $Ras^{G12V}$; IL8/VEGF; CTGF | *(Bhowmick et al. 2001; Dreissigacker et al. 2006; Hang et al. 2011; Desai et al. 2013; Kato et al. 2016)* |
|  | p38α favors immunotolerance // TP | DC, macrophages, T cells | SN of myeloma cells; LPS; TGF-β | *(Wang et al. 2006a; Yao et al. 2006; Huber et al. 2008; Lu et al. 2014)* |
|  | p38α activates DNA damage response // TS | Fibroblasts, HeLa, HCT116, RPE, U2OS | CDDP; UV; monastrol; gemcitabine | *(Sanchez- Prieto et al. 2000; Bulavin et al. 2001; Thompson and Compton 2010; Kopper et al. 2013)* |
| | p38α controls ROS levels // TS or TP | Fibroblasts, colon and breast cancer cells | $Ras^{G12V}$; $H_2O_2$; CDDP | *(Dolado et al. 2007; Gutierrez-Uzquiza et al. 2012; Pereira et al. 2013)* |

Abbreviations: CDDP, cisplatin; CTGF, connective tissue growth factor; CRC, colorectal cancer; DC, dendritic cells; EC, epithelial cells; GF, growth factors; LPS, lipopolysaccharide; mAb, monoclonal antibody; mESC, mouse embryonic stem cells; OE, overexpression; SCC, squamous cell carcinoma; SN, supernatant; TP, tumor promotion; TS, tumor suppression.

mitotic catastrophe *(Kurosu et al. 2005; Cosaceanu et al. 2007)*. p38α has been also associated with resistance to cisplatin in breast cancer by reducing ROS accumulation *(Pereira et al. 2013)*, to sorafenib in hepatocellular carcinoma by supporting MEK-ERK signaling *(Rudalska et al. 2014)*, or to irinotecan in colon cancer by inducing pro-survival autophagy *(Paillas et al. 2012)*. Cancer cells can also survive metabolic stress via activation of the AMPK-p38α-PGC-1α axis *(Chaube et al. 2015)* or by a rearrangement of glucose metabolism to avoid autophagy-mediated cell death *(Desideri et al. 2014)*.

p38α can influence the maturation of immune cells, favoring immunotolerance. In response to inflammatory mediators like interferon-γ, p38α blocks the maturation of dendritic cells so that their antigen presentation capacity is impaired as well as their cytotoxic activity against the tumor cells *(Yao et al. 2006; Lu et al. 2014)*.

There is also evidence that p38α activity can promote cell cycle progression, like in estradiol-treated breast adenocarcinoma cells *(Lewis et al. 2005)*, in hepatocyte growth factor-stimulated melanoma cells *(Recio and Merlino 2002)*, or in cytokine-sensitive acute myeloid leukemia *(Srinivasa and Doshi 2002)*.

Interestingly, p38α not only mediates the signaling induced by cytokines but also controls the expression of some of them, including TNFα, IL-6 or monocyte-chemoattractant protein (MCP) 1, both at the transcriptional and posttranscriptional levels. Therefore, several p38α inhibitors have been developed and are now undergoing clinical trials for inflammatory diseases *(Goldstein et al. 2010; MacNee et al. 2013)*. Besides cytokines, p38α regulates cyclooxygenase (COX) 2 and inducible nitric oxide synthase (iNOS) production, further supporting chronic inflammation and tumor promotion *(Chen et al. 1999; Saklatvala 2004)*.

p38α can also favor tumor progression by promoting cell invasion and migration in several ways. It can induce expression of matrix remodeling proteases, such as MMP2 that has been reported to mediate invasion of TGF-β-stimulated prostate cancer cells *(Xu et al. 2006)*; and it can phosphorylate and stabilize Twist1, which in turn triggers epithelial-to-mesenchymal transition enhancing invasiveness of Ras-transformed breast cancer cells *(Hong et al.*

*2011)*. Migration requires changes in the cell cytoskeleton and p38α can control actin-fiber polymerization via MK2-Hsp27 *(Rousseau et al. 2006)* or directly via focal adhesion kinase (FAK) *(Yoshizuka et al. 2012)*.

The metastatic potential of breast cancer has been positively correlated with p38α *(Wu et al. 2014)*. However, high p38 MAPK activity has also been described to restrict colon cancer cells from metastasizing the lung after a previously established liver lesion *(Urosevic et al. 2014)*, and to induce cancer cell dormancy *(Aguirre-Ghiso et al. 2001; Masiero et al. 2011)*.

The induction of angiogenesis is an essential step for tumor progression and metastatic dissemination. p38α can contribute to this process positively by promoting the secretion of pro-angiogenic factors, like VEGF *(Gao et al. 2002; Yoshino et al. 2006; Kim et al. 2016)* or negatively by blocking neovasculature formation *(Matsumoto et al. 2002)*. This is important when considering p38 MAPK inhibitors as adjuvants for cancer treatment as inhibition of p38 MAPK can potentially downregulate VEGF production, stopping angiogenesis, and making blood vessels more organized, enhancing drug delivery and avoiding leaky walls that predispose to metastasis.

**Understanding the duality**

Taken together, the aforementioned studies suggest that cancer cells use p38α signaling to their advantage during tumor progression, whereas it acts as a caretaker in normal cells of the healthy tissue. For example, p38α can stimulate cell cycle progression in chondrosarcoma cells but not in primary normal chondrocytes *(Yosimichi et al. 2001; Halawani et al. 2004)*. Likewise, p38α is essential in colon tumor maintenance whereas in normal colon preserves the epithelial barrier and avoids colitis-associated tumor initiation *(Gupta et al. 2014)*. Accordingly, high levels of phosphorylated p38 MAPK have been correlated with malignancy in follicular lymphoma, non-small-cell lung cancer, thyroid cancer and lymph node-positive breast carcinomas *(Dolado and Nebreda 2008)*.

The outcome upon p38α activation is determined not only by the malignant

stage of the cell, but also by the cell type. In skin carcinogenesis, for instance, p38α induces senescence via p38-regulated/activated kinase (PRAK) in primary fibroblasts, thus p38α dominant negative mice cannot avoid the formation of papillomas *(Sun et al. 2007; Zheng et al. 2013)*. On the contrary, animals with p38α KO keratinocytes develop fewer and smaller skin papillomas *(Dickinson et al. 2011; Liu et al. 2013)*. Indeed, in Prak KO animals papillomas do not progress to carcinomas due to impaired angiogenesis capacity of the Prak KO endothelial cells *(Yoshizuka et al. 2012)*. Although both fibroblasts and endothelial cells are normal, the activation of p38α in each cell type leads to distinct functions, which have different consequences on tumor suppression.

It is also important to consider the nature of the stimulus and how it activates p38α signaling. It has been shown that the treatment of NIH3T3 fibroblasts with mitogens, like bFGF, weakly and transiently activates p38 MAPK favoring G1/S cell cycle transition, whereas the same cells exposed to stress, like anisomycin or sorbitol treatments, induce high and persistent phosphorylation of p38 MAPK that leads to cell cycle arrest *(Faust et al. 2012)*.

In addition, the cell fate depends on the functional compensation by other p38 MAPK isoforms and other pathways, which is dependent as well on the abundance of the other proteins in each cell type. For example, embryonic hepatocytes deficient in p38α or p38β can phosphorylate Tp53 on Ser 389, whereas double KO hepatocytes lose this phosphorylation ability and undergo apoptosis *(Saba-El-Leil et al. 2016)*.

Also, JNKs, ERK1/2 and p38 MAPKs can crosstalk and exert antagonistic effects on cell proliferation and survival. In some cases, p38α negatively regulates cell proliferation by antagonizing JNK1/2 signaling at different levels *(Wagner and Nebreda 2009)*. Accordingly, in liver and hematopoietic cells, p38α KO leads to enhanced proliferation and tumor development that correlates with upregulation of the JNK–c-Jun pathway *(Hui et al. 2007)*. Likewise, p38α can inactivate the ERK1/2 pathway to induce apoptosis, via dephosphorylation of MEK1/2 upon arsenite treatment *(Chen et al. 2000; Li et al. 2003)*. Furthermore, p38α has been reported to crosstalk with other pathways such as Wnt *(Thornton et al. 2008; Guinot et al. 2016)*, Notch *(Kondoh et al. 2007; Masiero et al. 2011)*, NFκB

*(Saccani et al. 2002; Vermeulen et al. 2003)* or AKT *(Wu et al. 2007; Zuluaga et al. 2007)*, leading to very different outcomes.

In conclusion, p38α can control tumor-related functions in very different ways, both in the cancer cell and in the TME, acting as a tumor suppressor in certain contexts and, in others, as a tumor promoter. Hence, further studies, including the use of specific mouse tumor models, are a must to identify the tumor types that can benefit from p38α inhibition.

## p38α in non-small cell lung cancer

In the lung, p38α ablation causes enhanced proliferation of the alveolar progenitors and differentiation defects leading to a disrupted alveolar architecture, with thickened alveolar septa both in young and adult mice *(Hui et al. 2007; Ventura et al. 2007)*. Moreover, the systemic absence of p38α predisposes lung tissue to K-Ras$^{V12}$-driven lung tumor development *(Ventura et al. 2007)*, pointing towards a tumor suppressor role of p38α in the healthy tissue. Accordingly, a recent report correlated decreased levels of p38α to increased Wnt signaling in stem cells from advanced human lung adenocarcinomas *(Guinot et al. 2016)*. However, whether depletion of epithelial p38α is sufficient for tumor formation, or whether it needs the collaboration between different cell types, remains to be confirmed.

Conversely, human lung adenocarcinomas show increased levels of phospho-p38 MAPK *(Greenberg et al. 2002)* and the NSCLC cell line U1810 can resist radiotherapy in a p38α dependent manner *(Cosaceanu et al. 2007)*. These facts therefore suggest that tumors may get advantage of the activity of p38α. In fact, a recent study claimed that kinase inactivation of p38α reduces K-Ras$^{G12D}$-driven tumors through abrogation of fibroblast-derived hyaluronan synthesis *(Brichkina et al. 2016a)*. It has been also reported that downregulation of the downstream p38α effector MK2 together with Tp53, or the inactivation of p38α sensitizes lung tumors to cisplatin treatment *(Morandell et al. 2013; Brichkina et al. 2016b)*. Nevertheless, in NSCLC, the role of p38α in progression to malignant stages, the effects of pharmacological inhibition, and the individual

contribution of p38α within the epithelial and the immune cell compartments have not been studied.

Regarding the interplay between epithelial cells and the stroma, p38α has been reported to maintain the crosstalk between human lung stem cells (defined as $LGR6^+$ cells) and activated fibroblasts, leading to cytokine secretion, which eventually attracts endothelial cells and establishes a functional niche for the pulmonary stem cell *(Ruiz et al. 2014)*. Accordingly, stromal p38α has been shown to help pre-metastatic niche formation within the lungs *(Hiratsuka et al. 2006; Hiratsuka et al. 2011)* and lung cancer cell extravasation *(Matsuo et al. 2006)*. None of these reports, however, have addressed the influence of p38α in the metastatic abilities of the lung cancer cell itself.

Therefore, taking into account all the possible functions that p38α can exert, before claiming its use as a therapeutic target, we need to study the role of p38α along the development of NSCLC, and among the different cell compartments of the TME, using both genetic tools and available chemical inhibitors of p38α.

# *Objectives*

The main goal of this thesis is to gain a deeper understanding on the role of p38α MAPK during K-Ras$^{G12V}$-driven lung tumorigenesis.

The specific goals that we have pursued are:

1. Characterization of the loss of function of p38α in the tumor initiating cells of K-Ras$^{G12V}$-driven non-small cell lung cancer.

2. Characterization of the function of p38α in established K-Ras$^{G12V}$-driven lung tumors and its influence on their metastatic potential.

3. Definition of the contribution of p38α signaling within different cell compartments of the lung tumor microenvironment.

4. Investigation of the potential impact of these findings on the understanding and treatment of human lung adenocarcinoma.

# *Materials & Methods*

## Mouse housing

Animals were housed in the specific pathogen free (SPF) mouse facilities of PRBB and PCB (Barcelona). Animals were maintained under a standard 12h light-dark cycle, at 21°C, with free access to regular chow diet and autoclaved sterile water. Breeding pairs were set at a minimum age of 6 weeks. Litters were weaned at 21 days of age and marked with an eartag. All experiments were performed according to the European Union, national and institutional guidelines. Experimental protocols were approved by the Animal Ethics Committee at the University of Barcelona.

## Generation of conditional mice

K-Ras$^{+/FSFG12V}$ mice carry a mutant codon 12 encoding a Valine, and a transcriptional inhibitory sequence flanked by Frt sites within the first intron of the K-Ras locus *(Francoz et al, submitted)*. K-Ras$^{+/FSFG12V}$ mice were crossed with p38α lox/lox and p38α lox/- mice *(Adams et al. 2000; Ventura et al. 2007; Heinrichsdorff et al. 2008)* and Ubiquitin-CreERT2 mice *(Wang et al. 2009)* to obtain the genotypes K-Ras$^{+/FSFG12V}$; p38α lox/lox; Ubiquitin-CreERT2 and K-Ras$^{+/FSFG12V}$; p38α lox/-; Ubiquitin-CreERT2. Both genotypes, named from now on as p38α–Δ$^{Ub}$, were on a mixed C57BL/6J-FVB background and showed indistinguishable lung phenotypes, as determined by histology studies *(Ventura et al. 2007)*. Additionally, p38α–Δ$^{Ub}$ mice were crossed to constitutive p38β$^{-/-}$ mice *(del Barco Barrantes et al. 2011)*. K-Ras$^{+/FSFG12V}$; p38αlox/lox were alternatively crossed to Sftpc-CreER mice *(Xu et al. 2012b)* to obtain lung-specific p38α KO mice (p38α–Δ$^{Spc}$), and were also combined to a Cre reporter line bearing the double fluorescent tdTomato/eGFP allele *(Muzumdar et al. 2007)*. Myeloid-specific p38α KO mice (p38α-Δ$^{Lys}$) and fibroblast-specific p38α KO mice (p38α-Δ$^{Fsp}$) were generated by crossing p38α lox/lox mice with constitutive LysM-Cre

*(Clausen et al. 1999)* or Fsp1-Cre *(Trimboli et al. 2008)*, respectively. p38α-$\Delta^{Fsp}$ mice were also crossed to the tdTomato/eGFP reporter line. Offsprings were maintained in a C57BL/6J background. The K-Ras$^{G12V}$ KI, the tdTomato/eGFP reporter and the Cre transgenes were always kept in heterozygosis. Littermate controls were used in all experiments.

## Isolation of genomic DNA and mouse genotyping

Mouse tails were digested in 750µl of Tail buffer (100mM NaCl, 50mM Tris-HCl pH8, 10mM EDTA pH8, 1% SDS in sterile dd$H_2O$) with proteinase K (0.5µg/µl) at 56°C. After overnight digestion, 250µl of saturated NaCl was added, mixed for 5min and centrifuged at 1600*xg* 10min at room temperature (RT). The supernatant was poured into a new tube containing 500 µl of isopropanol. Tubes were inverted several times and centrifuged again at full speed for 10 min at RT. The supernatant was carefully discarded without disturbing the DNA pellet. Pellet was washed with 70% ethanol and, after drying, resuspended in 150 µl of autoclaved dd$H_2O$.

The polymerase chain reaction (PCR) mixture was prepared with 50 ng of gDNA, 2 µl of 10x Taq buffer, 1.5 µl of each primer (10 µM), 0.5 µl of dNTP mix (10 mM), 0.3 µl Taq polymerase (BioTaq, Ecogen #21060) and dd$H_2O$ to a final volume of 20 µl. Primers were purchased from Sigma and sequences are shown in **TABLE 4**. The mix was subjected to the following PCR program in a BioRad thermocycler: 94°C for 5 min; 35 cycles of 94°C for 30 s, 57°C for 30 s, 72°C for 45 s; and 72°C for 10 min, then cool down to 4°C. PCR products were resolved by electrophoresis in a 2% agarose gel.

## Tumor induction

The K-Ras$^{+/FSFG12V}$ mouse strain *(Francoz et al, submitted)* can generate lung tumors upon activation with adeno-FlpO viral particles as previously described *(Jackson et al. 2001; Puyol et al. 2010)*. Concisely, 8 to 12 week old mice were anesthesized (75 mg/kg ketamine plus 1 mg/kg medetomidine, intraperitoneally) and

**TABLE 4.** Primer sequences for mouse genotyping

| Gene | Forward primer 5'-3' | Reverse primer 5'-3' | Product |
|---|---|---|---|
| Cre Tg | ACGAGTGATGAGGTTCGCAAG | CCCACCGTCAGTACGTGAGAT | 520 bp |
| K-Ras WT | CCACAGGGTATAGCGTACTATGCAG | CTCAGTCATTTTCAGCAGGC | 350 bp |
| K-Ras$^{G12V}$ KI | TAGTGCCTTGACTAGAGATCA | CTCAGTCATTTTCAGCAGGC | 507 bp |
| p38α WT | CTACAGAATGCACCTCGGATG | AGAAGGCTGGATTTGCACAAG | 121 bp |
| p38α lox | CTACAGAATGCACCTCGGATG | AGAAGGCTGGATTTGCACAAG | 188 bp |
| p38α del | CCAGCACTTGGAAGGCTATTC | AGAAGGCTGGATTTGCACAAG | 411 bp |
| p38α null | ATGCTACTGTCTGCGCCTCTCT | TACTTTCGGTTCCTCTTCCCATGA | 190 bp |
| Tm-GFP WT | CTCTGCTGCCTCCTGGCTTCT | CGAGGCGGATCACAAGCAATA | 330 bp |
| Tm-GFP Tg | CTCTGCTGCCTCCTGGCTTCT | TCAATGGGCGGGGGTCGTT | 250 bp |

Abbreviations: del, deletion; KI, knock-in; Tg, transgene; Tm, Tomato; WT, wild type.

placed on a platform by their front teeth so that their chest hangs vertically beneath them. A cold light was directed on the chest of the mouse to allow visibility of the trachea, the tongue was gently pulled out with flat forceps. A 0.5 mL syringe with a rubber catheter covering the needle was introduced through the vocal cords and a single dose of 100 µL of adenoviral solution ($10^9$ pfu) per mouse was intratracheally inoculated. 2 mg/kg atipamezol were subcutaneously injected to recover mice from anesthesia. Standard mismatch PCR was used for checking oncogenic K-Ras$^{G12V}$ activation in mice inoculated with adeno-FlpO (see **TABLE 7** below), as it allows identification of the G12V point mutation by amplification of cDNA from whole lung lysates.

## Genetic and chemical inhibition of p38α in mice

To activate the tamoxifen-inducible CreER and CreERT2, mice were injected intraperitoneally with tamoxifen (12.5 mg/ml, Sigma #T5648) dissolved in a mix 1:9 of ethanol (Panreac): corn oil (Sigma). Doses of 0.125 mg/g body weight were injected for five consecutive days. p38α downregulation was confirmed by western-blotting 15 days after last tamoxifen injection.

The inhibitor of p38α and p38β MAPKs, PH797804 (Selleckchem #S2726), was dissolved to a concentration of 1.75 mg/ml in PBS containing 0.5% methylcellulose (Sigma) and 0.025% Tween20 (Sigma). Mice were weighed and a daily dose of 17.5 mg/kg body weight was administered by oral gavage for 15 consecutive days. Control mice were administered the vehicle solution. The inhibition of p38α was confirmed by western-blotting 6 h after the last dose, using lysates of lungs treated with 300 mM of NaCl for 15 min.

## Generation of murine lung cancer cell lines and orthotopical implantation in mice

Primary tumors from p38α lox/lox; K-Ras$^{+/FSFG12V}$ mice were implanted in Crl:NU-Foxn1nu mice as previously described *(Ambrogio et al. 2014)*. A fragment of each engraftment was derived *in vitro* by mincing with sterile scalpels and plating the resulting single cells in cell culture plates with Dulbecco's modified Eagle medium (DMEM) supplemented with 20% fetal bovine serum (FBS) plus 1% penicillin/streptomycin under standard culture conditions. Medium was renewed once a week till cell colonies with epithelial cell morphology were observed. Then cells were trypsinized and expanded.

For orthotopical implantation of the murine K-Ras$^{G12V}$-driven lung cancer (mKLC) cells into immunocompetent mice, anesthetized animals were intratracheally inoculated 100 µl of a 2x10$^6$ cells/ml solution and tumors were left to grow for 25 days. For intratracheal administration, cells were cultured to 70% confluence in DMEM 10% FBS, diluted with PBS, kept on ice, and thoroughly mixed prior to each inoculation. The vocal cords were viewed directly with the help of a cold light source, and a blunted catheter coupled to a syringe was passed beyond them to inoculate the cells.

## Metastasis studies

4.5x10$^5$ mKLC cells were subcutaneously injected into the rear flanks of 8-week old female athymic nude mice (Envigo, Harlan). Allograft growth was followed

*in vivo* till reaching a maximum volume of 1 $cm^3$. Follow-up was performed using a caliper. Thereafter tumors were removed, incisions were closed and the mice were kept for 15 more days to monitor metastatic foci formation.

For colonization ability assays, $5x10^5$ mKLC cells were injected through the tail vein of 8-week old female athymic nude mice. Tumor burden was analyzed 18 days after the injection, by measuring the percentage of tumor area in hematoxylin and eosin (H&E) stained sections using computerized imaging software (Image J).

## TUNEL assay

To detect apoptosis in paraffin-embedded samples, the Fluorescein *in situ* cell death detection kit (Roche #11684795910) was used according to manufacturer's instructions. Fluorescent images were scanned with a Nanozoomer digital slide scanner (Hamamatsu) and analyzed by computerized image software (Image J).

## Immunohistochemistry

Lungs were fixed by insufflating 10% neutral buffered formalin (Sigma) through the trachea with a syringe, and incubated overnight at 4°C in 10 ml 10% neutral buffered formalin. Samples were then washed with PBS, dehydrated in a tissue processor (Sakura), and embedded in paraffin blocks using a paraffin embedding module (Leica). Blocks were cut with a microtome (Leica) into 4 μm thick sections. After a de-wax step in xylene for 10 min, samples were rehydrated in a descending series of ethanol solutions (100%, 95%, 75%, 50% and dd$H_2O$). Lung sections were then either stained with H&E following the standard protocol, or used for immunohistochemical staining (IHC). For IHC, rehydrated lung sections were treated with peroxidase blocking buffer for 15 min at RT to block endogenous peroxidase activity. Thereafter slides were washed in tap water and antigen retrieval was performed as noted in **TABLE 5**, according to the primary antibody to be used. Slides were then washed with PBS and incubated in blocking buffer (10% normal goat serum and 0.3% Triton

X-100 in PBS). Diluted primary antibodies were added as indicated in **TABLE 5**. After washing the primary antibody, HRP-conjugated secondary antibodies were added and incubated for the specified times. Signal was visualized with 3,3-diaminobenzidine (DAB), and counterstained with hematoxylin. Tissue was again dehydrated, washed in xylene, and mounted with a coverslip using DPX mounting medium.

**TABLE 5.** Antibodies for IHC of mouse lung tissue

| Antigen | Dilution/ Incubation | Vendor (Reference) | Antigen retrieval |
|---|---|---|---|
| **Primary antibodies** | | | |
| CCSP | 1:100/ o.n. 4˚C | Santa Cruz (sc-9772) | Citrate pH6 |
| CD3 | 1:10/ 2 h RT | Dako (IS50330) | EDTA pH9 |
| CD45 | 1:100/ o.n. 4˚C | BD biosciences (550539) | EDTA pH9 |
| CD68 | 1:750/ o.n. 4˚C | Biorbyt (orb47985) | Citrate pH6 |
| Cleaved caspase 3 | 1:500/ 2 h RT | Cell Signaling (9661) | Citrate pH6 |
| Ki67 | 1:500/ 1 h RT | Novocastra (NCL-Ki67-P) | Citrate pH6 |
| P-MK2 (T334) | 1:100/ o.n. 4˚C | Cell Signaling (3007) | Citrate pH6 |
| P-p38 (T180/Y182) | 1:500/ 2 h RT | Cell Signaling (4631) | Citrate pH6 |
| PDGFRβ | 1:300/ 2 h RT | Thermo (MA5-14851) | Citrate pH6 |
| Pro-SPC | 1:3000 /o.n. 4˚C | Millipore (AB3786) | Citrate pH6 |
| von Willebrand factor | 1:3/ 30 min RT | Dako (IS527) | EDTA pH9 |
| **Secondary antibodies** | | | |
| anti-goat IgG-HRP | 1:80/ 45 min RT | Dako (P0449) | |
| anti-mouse IgG-HRP | 1:100/ 30 min RT | Dako (P0447) | |
| anti- rabbit IgG-HRP | RTU/ 45 min RT | Immunologic (DPVR110HRP) | |
| anti-rat IgG-HRP | 1:80/ 45 min RT | Dako (P0450) | |

Abbreviations: o.n., overnight; RT, room temperature; RTU, ready to use.

## Histopathological analysis

Lungs were photographed and weighed. Tumors in freshly harvested lungs, and lung sections stained with H&E were counted, sized, and analyzed for tumor grade and inflammation by two independent observers in a blinded fashion. Evaluation of tumor grade followed the classification established by Tyler Jacks' laboratory *(Jackson et al. 2001)*.

IHC and X-Gal stained sections were visualized with a Nanozoomer digital slide scanner (Hamamatsu). Individual images were acquired for each tumor from each of the tissue sections. DAB or X-Gal staining were quantified in a completely automated manner corresponding to either the relative percentage of stained surface or the relative percentage of positive cells, using computerized imaging software (Image J).

## Lung single cells preparation and fluorescence activated cell sorting (FACS)

Lung lobules, with or without tumors, were isolated from upper respiratory airways and finely minced with a scalpel in 5 ml serum-free DMEM. Each lung was then added 5 ml of serum-free DMEM containing 2 mg/ml Collagenase A (Roche), 0.4 mg/ml Dispase II (Sigma) and 0.2 mg/ml DNAse I (Roche), and enzymatically digested at 37°C while rotating for 30 min. 30 ml of ice-cold DMEM 10% FBS was used for quenching the reaction, samples were put on ice, cell suspension was filtered through a 70 µm pore cell strainer (BD), and the filter was washed with 10 ml more of ice-cold DMEM 10% FBS. Cells were pelleted at 250*xg* for 5 min at 4°C, and supernatant was discarded. Erythrocytes were lysed in 4 ml Red cell lysis buffer (150 mM $NH_4Cl$, 1 mM $KHCO_3$, 0.1 mM EDTA in distilled water; pH 7.3) during 4min at RT and immediately washed with ice-cold DMEM 10% FBS. After a second filtration through a 70 µm pore cell strainer and centrifugation at 250*xg*, cells were resuspended in ice-cold fluorescence activated cell sorting (FACS) buffer (Dulbecco's Phosphate-Buffered Saline supplemented with 2% FBS). For the analysis of stem cell markers in immortalized lung tumors cells, we additionally permeabilized cell membranes with 0.5% w/v saponin for 15 min at RT in the dark.

Alive cells were counted using trypan blue in the TC10 cell counter from BioRad, then 2 million cells were blocked with anti-CD16/CD32 (clone 93, eBioscience; 1:200) for 5 min at RT plus 5 min at 4°C. Fluorophore conjugated antibodies were incubated for 30 min on ice in the dark. The list of antibodies is specified in **TABLE 6**. The excess of antibody was washed out once and resuspended in 300 µl of cold FACS buffer. Samples were run in a FACS Aria Fusion II cytometer (Beckton Dickinson). DAPI (1:100) was used for exclusion of dead cells and debris and doublets were excluded by plotting forward-scattered (FSC) versus side-scattered (SSC) channels. Data was analyzed using FlowJo software. For RNA or DNA extraction, a 70 µm sorter tip was used and sorted samples were harvested in a 1.5 ml tube containing 40 µL of lysis buffer (10mM Tris pH 7.4, 20 mM DTT, 0.5% SDS, 0.5 µg/µl proteinase K) to be subsequently processed as previously described *(Gonzalez-Roca et al. 2010)*.

## Isolation of peritoneal macrophages

Mice were sacrificed and skin was cut to expose the peritoneum. 5 ml of cold PBS were injected into the peritoneal cavity and recovered using a syringe. Process was repeated once. Cell suspension was centrifuged at 150*xg* for 5 min, resuspended in 3 ml DMEM 10% FBS and plated in a 6 cm tissue culture plate. Next day, cells were washed 3 times with cold PBS to remove dead cells. Adhered cells, mostly macrophages, were trypsinized and used for protein extraction.

## Cell culture

mKLC cell lines were maintained in DMEM (Sigma, #D5796). Both media were supplemented with 10% heat inactivated FBS (Thermo Fisher Scientific), 1% L-glutamine (Thermo Fisher Scientific) and 1% penicillin/streptomycin (Gibco) at 37°C and 5% $CO_2$, unless otherwise specified. All cell lines were tested for mycoplasma before performing experiments, using the colorimetric kit from Lonza (#LT07-710).

**TABLE 6.** Antibodies for FACS staining of mouse lung single cell preparations

| Antigen | Fluorophore | Dilution | Vendor (Reference) |
|---|---|---|---|
| CCSP | + 2ry ab Alexa 647 | 1:200 | Santa Cruz (sc-9772) |
| CD11b | FITC | 1:150 | BD Bioscience (553310) |
| CD11c | Brilliant Violet 711 | 1:150 | Biolegend (117349) |
| CD31 | PE | 1:100 | BD Bioscience (553373) |
| CD31 | PE-Cy7 | 1:100 | Biolegend (102417) |
| CD45 | APC | 1:200 | BD Bioscience (559864) |
| CD45 | APC-eFluor 780 | 1:300 | eBioscience (47-0451-80) |
| CD90.2 | Aleza 488 | 1:200 | Biolegend (105316) |
| EpCAM | FITC | 1:50 | Santa Cruz (sc-53532) |
| EpCAM | APC-Cy7 | 1:50 | Biolegend (118217) |
| F4/80 | PE | 1:150 | Biolegend (123109) |
| Gr-1 | APC | 1:150 | Biolegend (108412) |
| ItgB2 (CD18) | PE | 1:100 | Biolegend (101407) |
| PDGFRα | Brilliant Violet 786 | 1:100 | Biolegend (740930) |
| PDGFRβ | APC | 1:100 | eBioscience (17-1402-82) |
| SPC | + 2ry ab Alexa 488 | 1:100 | Chemicon (ab3786) |

## Generation of retrovirus and stable cell lines

For retroviral production, $CaCl_2$-mediated transfection method was used. Briefly, a 500 µl mixture of 5.5 µg retroviral plasmid (pWZL-blasticidin-CreERT2, which was a kind gift from Mariano Barbacid's lab in CNIO Madrid), 5 µg packaging vector (pcL-Eco; Addgene #12371), and 2.5 M $CaCl_2$ was bubbled up by air injection while adding 500 µl of 2X HBS buffer pH 7 drop-wise. After 20 min, HEK293T cells that had been cultured at 50% confluence in DMEM 10% FBS in 10 cm plates and seeded 24 h beforehand, were transfected with this mixture. 16 h later, cell medium was refreshed. After 48 h the viral supernatant was removed, cleared with a centrifugal filter device (Amicon Ultra-15 #910024;

Merck) at 3000*xg*, for 1 h at 4°C, and recovered in 1 ml DMEM 10% FBS.

Target cells were incubated with 300 µl of the obtained virus solution plus polybrene 8 mg/ml for 24 h. Medium was replaced with DMEM 10% FBS and 24 h later cells were selected with 2 µg/ml Blasticidin (Thermo Fisher Scientific #A1113903) for 7 days and maintained subsequently in the normal growth medium.

## p38α downregulation in cells in culture

To induce p38α deletion, mKLC cells carrying p38α floxed alleles were treated with 150 µg/ml of Tat-Cre protein *(Peitz et al. 2002)* for 10 h in serum-free DMEM with 1% penicillin/streptomycin. Thereafter medium was changed to DMEM 10% FBS and cells were checked by western-blot.

For mKLC cells carrying both p38α floxed alleles and inducible CreERT2, p38α deletion was induced in vitro with 3 daily doses of 10 µM 4-hydroxytamoxifen (Sigma #H6278) or *in vivo* with 5 intraperitoneal injections of tamoxifen (12.5 mg/ml, Sigma #T5648).

For chemical inhibition of p38α, mKLC cells were seeded, let to attach overnight, and then treated for 4 days with PH797804 (1 µM; Selleckchem #S2726) every 24 h, or SB203580 (10 µM every 48 h; Axon MedChem #1363). Control cells were treated with the DMSO vehicle every 48 h.

## RNA processing and analysis

Total RNA was extracted from tumors, lung tissue, or isolated cells using the Purelink RNA minikit (Ambion #12183018A) following the manufacturer's instructions. The obtained total RNA was then treated with DNase I. RNA concentration and purity was determined using NanoDrop 2000 spectrophotometer.

cDNA was obtained from 1 µg of the purified RNA using random primers

(Invitrogen #48190-011) following exactly the SuperScript II reverse transcriptase protocol from Invitrogen (#18064-014) in a final volume of 20 μl.

For quantitative real-time PCR, 20 ng of cDNA were used in triplicate, in 20 μl of total volume, on a BioRad CFX96™ thermal cycler machine using SYBR green (BioRad #1708886). Each primer **(TABLE 7)** was used at a final concentration of 0.25 μM. PCR program was run as follows: 50°C for 2 min, 95°C for 10 min, 40 cycles of denaturation at 95°C for 15 s, plus annealing at 56°C for 15 s, plus elongation at 72°C for 60 s, and three final steps of 95°C for 15 s, 60°C for 2 min and 95°C for 15 s. Relative levels of gene expression were measured by the ΔΔC(t) method and normalized against the endogenous control p38α exon 12.

**TABLE 7.** Primer sequences for quantitative RT-PCR

| Gene | Forward primer 5'-3' | Reverse primer 5'-3' |
|---|---|---|
| *K-Ras WT* | CTTGTGGTGGTTGGAGCTGGT | CTCCCCAGTTCTCATGTACTGG |
| *K-Ras$^{G12V}$* | CTTGTGGTGGTTGGAGCTGTA | CTCCCCAGTTCTCATGTACTGG |
| *Mdm2* | CAAGAGACTCTGGTTAGACC | GGATCCTTCAGATCACTCCC |
| *p21waf1/cip* | ATGTCCAATCCTGGTGATGTCC | TCAGGGTTTTCTCTTG CAGAAG |
| *p38α exon 2* | GCATCGTGTGGCAGTTAAGA | GTCCTTTTGGCGTGAATGAT |
| *p38α exon 12* | GCCCTCCCTCACTTCAGGAG | TGTGCTCGGCACTGGAGACC |

## Cytokine array analysis of tumor lysates and cell culture supernatants

Four different plates of wild type (WT) and Tat-Cre treated cells (passage 3) were grown at same confluence for 48 h in 4.5 ml DMEM 10% FBS. Supernatants were then harvested, centrifuged, pooled and 1 ml of total volume was assayed immediately on the array membranes. For tumor lysates, five dissected tumors from four different mice of each genotype were pooled together and lysed in 80 μl of buffer (10 μg/ml aprotinin, 10 μg/ml leupeptin, and 10 μg/ml pepstatin in PBS) using Precellys cell disruptor (Bertin Technologies). Triton X-100 was added to a final concentration of 1%, and lysates were frozen at -80°C overnight. Protein content was quantified for each pool with the DC

Protein assay kit (BioRad) and 1600 µg of protein were used for loading onto the array membranes. Cytokine profiler array instructions (R&D Systems, #ARY006) were followed exactly. Concisely, array membranes were blocked for 1 h, samples were incubated with antibody cocktail for 1 h at RT, and altogether were incubated overnight at 4°C while rocking. Next day, membranes were washed three times and incubated with Streptavidin-HRP for 30 min. ECL-reagent and X-ray film (Fujifilm, #47410-19236) were then used to detect signal. Pixel densities on developed X-ray film were collected and analyzed using a transmission mode scanner and image analysis software (Image J).

## Flow cytometry-based assays for the analysis of cell proliferation

For the analysis of cell cycle profiles, trypsinized cells and their supernatant were centrifuged at 250*xg* for 5 min, washed with PBS and diluted to $10^6$ cells/ml. 330 µl of cell suspension were thoroughly mixed with 660 µl ice cold absolute ethanol added drop-wise. After overnight incubation at 4°C, ethanol was removed by centrifugation (250*xg*, 5 min). Pellet was washed with PBS and resuspended in 500 µl DNA staining solution (0.2 mg/ml RNAse A from Roche [#109-169], 20 µg/ml propidium iodide [PI] from Sigma [#P4864]). Cells were incubated for 30 min at 30°C in a water bath in the dark, and then run in a Gallios flow cytometer (Beckman Coulter).

To measure cellular BrdU incorporation, cells were pulsed for 90 min with 10 µM BrdU, harvested, and resuspended in 500 µl PBS. 5 ml of cold 70% ethanol were added drop-wise while agitating the tube, and cells were stored overnight in the freezer. Cells were then pelleted, washed and their DNA was denatured with 0.5 ml of 0.1 M HCl/ 0.5% Tween 20 for 10min on ice and then washed and boiled. Cells were next washed twice with 0.5% Tween/ 1% BSA in PBS and then incubated with anti-BrdU-FITC antibody. After incubation for 30 min at RT in the dark, excess of antibody was washed out and cells were resuspended ($10^6$ cells in 400 µl) in PBS containing 2 mg/ml PI plus 5 mg/ml RNase A. Cell suspensions were run in a Gallios flow cytometer and analyzed using FlowJo software.

## Proliferation curves

To analyze the proliferation of cells in culture, 8000 cells per well were plated in 12-well plates in quadruplicate for each of the time points of interest. At every point, cells in each of the four wells were trypsinized and counted using a Neubauer chamber and trypan blue to differentiate dead cells.

Complementary, the number of metabolically active cells was measured by MTT [3-(4,5-Dimethylthiazol-2-yl)-2,5-diphenyltetrazolium bromide] assays. Concisely, 800 cells in a 100 µl volume were plated in quadruplicate for every indicated time point and condition in 96-well plates with a repetition pipette. The metabolic activity was measured using the MTT kit from Sigma (#11465007001), adding 10 µl of the MTT labeling reagent were added to each well and 4 h later 100 µl of the solubilization solution were used to quench reaction. Color intensity was measured on the next day in a spectrophotometer using a 595 nm filter.

## Clonogenic assay

For colony formation assays, cells were seeded at a density of 2000 cells per well in 6-well plates. After 15 days, cells were fixed for 30 min in 4% paraformaldehyde (PFA) and subsequently stained with 0.05% crystal violet for 15 min. After washing with $ddH_2O$, draining, and photographing the plates, the number of colonies was counted in an automatized manner using ImageJ software.

## Soft agar assay

To measure cell proliferation in anchorage-independent conditions, semisolid proliferation media were prepared with 0.35% and 0.5% agarose in DMEM 10% FBS. 0.5% agarose was used to homogeneously cover the bottom of the 6-well plate. When solidified, 2000 mKLC cells were mixed with an equal volume of the 0.35% agarose in DMEM and plated on top of the previous layer. After solidification of the second layer, 1 ml of DMEM 10% FBS was added, and

renewed once a week. After 25 days, colonies per well were manually counted under a microscope and photographed for size analysis with Image J software. One well without any cells was used as background control for image analysis.

## Anoikis assay

The bottom of a 24-well plate was coated with 120 µl of 0.03 g/ml poly-HEMA (Sigma-Aldrich) in 95% ethanol and left dry-out overnight. $5x10^4$ cells per well are seeded and counted after 48 h under the microscope with a Neubauer chamber using trypan blue.

## Cell attachment assay

Assays were done in 24-well plates either empty or coated with 10 µg/ml fibronectin, or 10 µg/ml collagen I overnight at 4°C. Cells were labeled with Cell Tracker Green (Invitrogen #C7025) on the previous day (30 min at 37°C) and kept in low serum overnight (DMEM 0.5% FBS). $5x10^4$ cells in serum free media were added to each well for 2 h. Thereafter, wells were washed once and adhered cells were fixed in formalin for 30 min at RT. Three different fields (10X magnification) of each well were photographed under a microscope and green cells were counted manually.

## Migration assay

To assay cell migration ability, Boyden chambers (Falcon #353097) were inserted into the wells of 24-multiwell plate containing 700 µl DMEM 10% FBS. $4x10^4$ cells, which had been grown overnight in DMEM 0.5% FBS, were seeded in duplicates in the upper part of the chamber in 500 µl DMEM 0.5% FBS. Chambers with 0.5% FBS in the upper and bottom parts were used as controls. Cells were incubated for 14 h and then fixed with 4% PFA in PBS, stained with 0.1% crystal violet, and washed with $ddH_2O$. Migrated cells were quantified by taking pictures of each well at 20X magnification and counting manually.

## Preparation of protein extracts

Single cells were homogenized in lysis buffer (50 mM Tris–HCl pH 7.5, 150 mM NaCl, 1% NP-40, 5 mM EDTA, 5 mM EGTA, 20 mM NaF, 0.1 mM sodium orthovanadate, 1 mM DTT, 1 mM microcystin, and the inhibitor cocktails from Roche Phostop [#04906837001] and Complete [#11836145001]) using 80 µl buffer/million cells, and were sonicated in a cold water-bath for 10 min. Tissue samples were mechanically disrupted also in lysis buffer using a Precellys homogenizer. The supernatant was poured into a clean 1.5 ml tube and bath-sonicated for 10 min. Lysed cells were shaked, kept on ice for 15 min, and thereafter centrifuged at 1600*xg* for 15 min at 4°C. The supernatant was collected into a new tube and quantified in reference to a BSA-standard curve using the DC Protein assay kit (BioRad #5000112).

## Immunoblotting

Equal amounts of protein in Laemmli buffer were separated by SDS-polyacrylamide gel electrophoresis and transferred to a nitrocellulose membrane (Whatman #10401396) during 2 h at 200 mA using a wet-blotting transfer system (BioRad). Ponceau red staining was used to confirm the efficiency of transfer. The nitrocellulose membrane was blocked with 5% non-fat milk in PBS - 0.05% Tween for 1 h at RT. Specific proteins were labeled with the primary antibodies listed in **TABLE 8** at 4°C, rocking overnight. Excess of antibody was then washed with TBS and the secondary antibody was incubated for 1 h at RT in the dark. Tubulin was used as loading control and signal was visualized using Odyssey Infrared Imaging System (LiCor, Biosciences).

## Biostatistical analysis of lung cancer patient cohorts

The gene expression omnibus (GEO) repository *(Barrett et al., 2013)* was searched for microarray and survival data of NSCLC samples. The GEO

**TABLE 8.** Antibodies used for immunoblotting

| Antigen | Dilution | Host | Vendor (Reference) |
|---|---|---|---|
| **Primary antibodies** | | | |
| eCadherin | 1:1000 | mouse | BD Bioscience (610181) |
| HSP27 | 1:1000 | goat | Santa Cruz (1049) |
| MK2 | 1:1000 | rabbit | Cell Signaling (3042) |
| P-ERK | 1:1000 | rabbit | Cell Signaling (9101S) |
| P-HSP27 (S78) | 1:500 | rabbit | Cell Signaling (2401) |
| P-p38 (T180/Y182) | 1:2000 | rabbit | Cell Signaling (9211) |
| p38α | 1:1000 | rabbit | Cell Signaling (9218) |
| p38α | 1:1000 | goat | Santa Cruz (sc-535) |
| Tubulin | 1:5000 | mouse | Sigma (T9026) |
| **Secondary antibodies** | | | |
| Goat IgG- Alexa Fluor 680 | 1:5000 | donkey | Invitrogen (A21084) |
| Mouse IgG- Alexa Fluor 680 | 1:5000 | goat | Invitrogen (A21057) |
| Mouse IgG- Alexa Fluor 800 | 1:5000 | donkey | Rockland (610-731-124) |
| Rabbit IgG- Alexa Fluor 680 | 1:5000 | goat | Invitrogen (A21076) |
| Rabbit IgG- Alexa Fluor 800 | 1:5000 | goat | Rockland (611-131-122) |

data sets GSE30219 and GSE31210 included information about pathological stages. GSE10072 and GSE19188 were normalized and used for analyzing the expression levels of MAPK14, MAPKAPK2 and MAP2K6 in tumor samples and paired healthy parenchyma. The GEO data sets GSE8894 and GSE31210 were used for assessing the prognostic value of MAPK14, MAPKAPK2 and MAP2K6 corresponding to tumor progression. The probe set used for MAPK14 was 210449_x_at, for MAPKAPK2 was 201461_s_at, and for MAP2K6 was 205698_s_at. Lung adenocarcinoma patient samples were split by median expression level of each gene and the two patient cohorts were compared by Kaplan–Meier survival plot, using Cox regression with 95% confidence intervals and log-rank P value.

## Statistical methods

Data are presented as means ± standard error of the mean (SEM) or means ± standard deviation (SD) for in vitro data. Dataset statistics were analyzed with Prism 7 (GraphPad software). Groups were compared using the two tailed Mann-Whitney test or the analysis of variance (ANOVA). p values below 0.05 were considered statistically significant (*P<0.05, **P<0.01, ***P<0.001, ****P<0.0001).

# *Results*

## p38α, but not p38β, is required for lung homeostasis

To understand the role of p38 MAPK signaling in lung tumorigenesis, we first determined the contribution to homeostasis of the closely related p38α and p38β family members, which are expressed at detectable protein levels in mouse lungs *(del Barco Barrantes et al. 2011)*. To perform a loss of function study, we deleted both p38 MAPKs taking into account that constitutive p38β-deficient animals are viable but p38α null mice are embryonically lethal. For the genetic downregulation of p38α, we used adult mice expressing the ubiquitous and tamoxifen-inducible Ubiquitin-CreERT2 recombinase and floxed p38α alleles, in which the second and third exons, coding for the kinase domain of p38α, are flanked with LoxP sequences **(FIGURE 9A)**. These sequences are cleaved by the CreERT2 recombinase, whose activation depends on the administration of tamoxifen to the animal due to the fusion of the recombinase to the hormone-binding domain of the estrogen receptor. Animals were given daily intraperitoneal injections of tamoxifen during five consecutive days and nkilled two weeks later. The efficiency of p38α downregulation in p38α-$\Delta^{Ub}$ mice was assessed by western blot of whole-lung lysates **(FIGURE 9B)**.

To determine the contribution of each of these p38 MAPKs to lung homeostasis

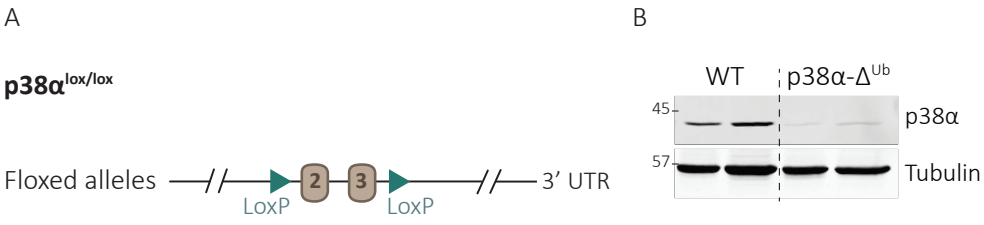


**FIGURE 9. p38α depletion by gene-targeting.** (A) After tamoxifen injection, active Cre recombinase cleaves the LoxP sites flanking exons 2 and 3 of the MAPK14 gene. (B) Immunoblot of p38α and α-tubulin of whole lysates from two independent samples of WT and p38α–$\Delta^{Ub}$ lungs.

and to rule out any redundancy between them, we checked the alveolar architecture in lungs of WT, p38α–$\Delta^{Ub}$, p38β-null and p38α–$\Delta^{Ub}$;p38β-null (double KO) animals. Inactivation of p38α in adult mouse lungs led to thickening of the alveolar septa **(FIGURE 10A)** due to hyperproliferation of SPC-expressing cells **(FIGURE 10B)**, as previously described *(Hui et al. 2007; Ventura et al. 2007)*. Interestingly, the lack of p38β did not affect the structure of the alveoli **(FIGURE 10)**. Furthermore, p38α depletion in p38β-null lungs produced an equivalent phenotype to that of the single p38α-$\Delta^{Ub}$ mice, suggesting that p38α, and not p38β, is in charge of maintaining distal airway homeostasis.

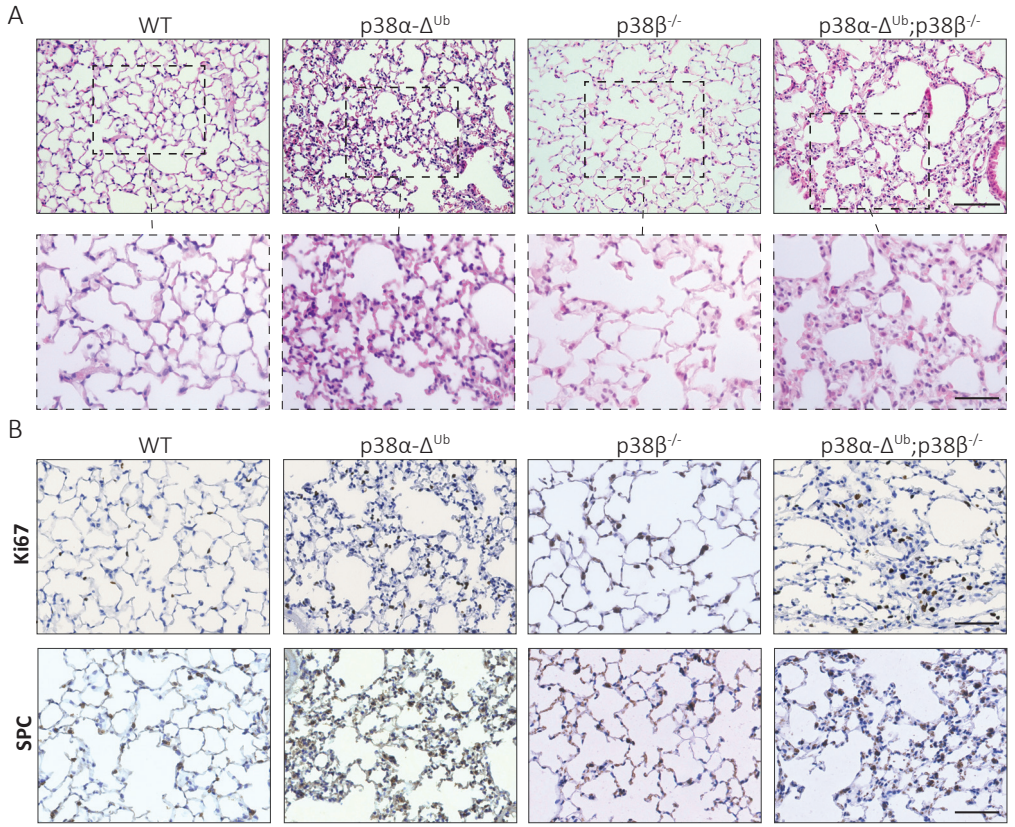


**FIGURE 10. p38α, but not p38β, maintains homeostasis in lungs.** (A) Representative pictures of H&E sections from WT, p38α–$\Delta^{Ub}$, p38β-null, and p38α–$\Delta^{Ub}$;p38β-null animals. Scale bars, 100 μm (upper panels) and 50 μm (lower panels). (B) Ki67- and SPC-labeled sections from WT p38α–$\Delta^{Ub}$, p38β-null, and p38α–$\Delta^{Ub}$;p38β-null lungs. Scale bars, 50 μm.

## Inactivation of p38α in alveolar epithelial type II cells enhances lung tumor initiation

The systemic loss of p38α, but not p38β, produces a hyperproliferation of SPC-expressing cells that disrupts the normal architecture of the alveoli *(Ventura et al. 2007)*. AE2 progenitors and BASC, both characterized by expressing SPC, are considered the tumor initiating cells of K-Ras$^{G12V}$-driven lung adenocarcinoma *(Jackson et al. 2001; Xu et al. 2012b)* so we next inquired whether the downregulation of p38α just in the SPC-expressing cells is sufficient to sensitize lungs to cancer development. First, we specifically downregulated p38α in the AE2 and BASC populations by injecting tamoxifen for 5 days to mice bearing SPC-CreER (p38α–Δ$^{Spc}$). The downregulation of p38α two weeks after tamoxifen injections was, as expected, specific to lung tissue **(FIGURE 11A)** and occurred in approximately 30% of AE2 progenitors, as determined by qPCR of sorted pneumocytes (CD31$^-$ CD45$^-$ ITGB2$^+$ SPC$^+$ like in *(Mukhametshina et al. 2013)*) **(FIGURE 11B)**. Mice were also engineered with a tdTomato/eGFP reporter *(Muzumdar et al. 2007)* to follow-up Cre recombinase activity and, therefore, the likely efficiency of p38α deletion. The tdTomato/eGFP reporter is expressed under the Rosa26 promoter so every cell constitutively expresses Tomato fluorescent protein, which in turn is flanked by LoxP sites. Thus, only those cells where Cre is active can cleave the LoxP sites inducing the expression of eGFP **(FIGURE 11C-D)**.

In order to study the role of p38α in the AE2 cells during the first steps of tumorigenesis, we needed to downregulate p38α in the tissue prior to tumor induction. Therefore, we designed a strategy that uncouples the inactivation of p38α from the expression of oncogenic K-Ras$^{G12V}$, based on the combination of the SPC-Cre – LoxP and the Flp – FRT systems. Expression of K-Ras$^{G12V}$ in mouse lungs triggers lung adenocarcinoma development *(Guerra et al. 2003)*. For the controlled induction of oncogenic K-Ras$^{G12V}$ we used mice with a knocked-in (KI) stop cassette flanked by FRT sites **(FIGURE 12A)**. This cassette precedes the open reading frame of the K-Ras$^{G12V}$ oncogene (K-Ras$^{+/FSFG12V}$) and is removed only upon intratracheal inoculation of adenovirus containing FlpO recombinase. This enables transcription of the oncogene, which can be detected

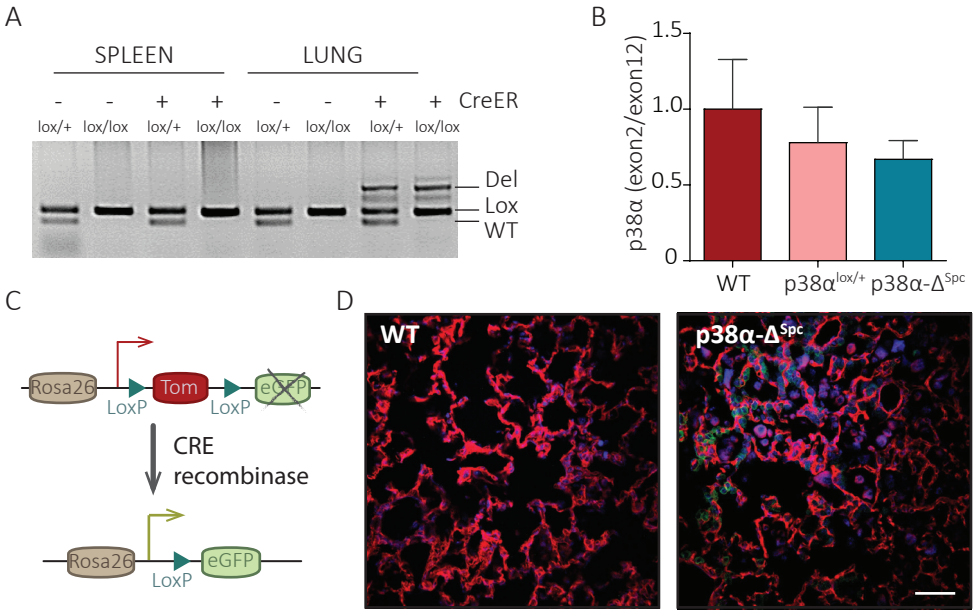


**FIGURE 11. p38α specific downregulation in AE2 cells.** (A) PCR of genomic DNA from whole lysates of spleen and lung samples one week after last tamoxifen injection. (B) Genomic DNA was isolated from AE2 cells sorted one week after five tamoxifen injections either from WT, p38α lox/+ or p38α-$\Delta^{Spc}$ mice, and analyzed by qPCR with specific primers for exon 2 and exon 12 of p38α. Relative copy number of exon 2 versus exon 12 of a representative experiment is shown. Values show average ± SD (n=3). (C) The double reporter gene tdTomato/GFP constitutively expresses Tomato fluorescent protein and blocks eGFP expression, until Cre-mediated excision enables eGFP transcription. (D) Representative confocal microscopy images of fixed lung tissue sections from WT and p38α-$\Delta^{Spc}$ mice showing Tomato (red) and eGFP (green) labeling (n=4). Nuclei were stained with DAPI (blue). Scale bar, 50 µm.

by RT-PCR **(FIGURE 12B)**. Hence, we downregulated p38α seven days before inducing the expression of the K-Ras$^{G12V}$ oncogene, and p38α–$\Delta^{Spc}$ animals were then maintained on a tamoxifen diet until the end of the experiment **(FIGURE 12C)**.

Twenty weeks after K-Ras$^{G12V}$ expression, p38α-$\Delta^{Spc}$ mice showed lungs with disrupted parenchyma and numerous lesions constituted by SPC$^{+}$ cells growing along the preexisting alveolar framework **(FIGURE 13A)**. Moreover, p38α-$\Delta^{Spc}$ lungs showed areas remarkably infiltrated by immune cells **(FIGURE**

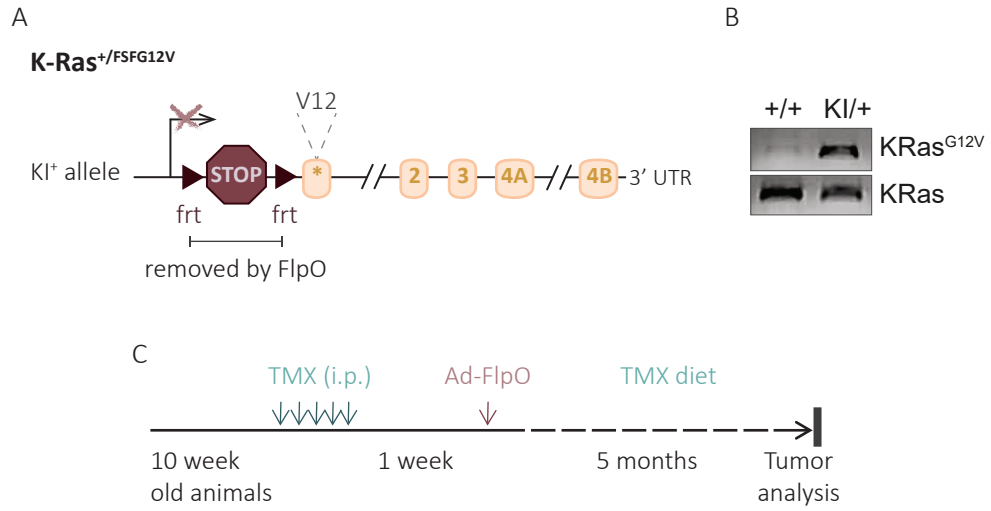


**FIGURE 12. K-Ras$^{G12V}$-driven lung tumor induction.** (A) Before intratracheal inoculation of FlpO recombinase, the STOP cassette introduced within the first intron of the K-Ras locus impairs its transcription. Following adeno-FlpO infection, the recombinase recognizes the FRT sites, removes the STOP cassette and allows expression of oncogenic K-Ras$^{G12V}$. (B) Semi-quantitative RT-PCR to check KRas$^{G12V}$ expression levels in whole lung lysates. (C) Scheme of the experimental design to study the role of p38α in lung tumor initiation. Ad-FlpO, adenovirus containing FlpO recombinase; TMX (i.p.), tamoxifen intraperitoneal injections.

**13B)**, accompanied by an increase in STAT3 phosphorylation **(FIGURE 13C)**, a known mediator of tumor-promoting inflammation *(Yu et al. 2009)*.

p38α-Δ$^{Spc}$ mice showed increased tumor burden and, accordingly, a significantly increased percentage of proliferative cells, as marked by Ki67$^{+}$ staining **(FIGURE 14A-B)**. The augmented tumor load was also evinced by the augmented weight of p38α-Δ$^{Spc}$ lungs in comparison to their WT counterparts **(FIGURE 14C)**. Therefore, the lack of p38α, even in 30% of the pneumocytes, is sufficient to sensitize lungs to tumor formation induced by K-Ras$^{G12V}$, indicating that p38α plays a cell autonomous tumor suppressor role in the healthy lung epithelia.

Noteworthy, p38α-Δ$^{Spc}$ lungs showed mostly hyperplasias, while WT animals had formed mainly adenomas with papillary structures. In other words, despite the increased tumor burden, the histopathological analysis showed fewer tumors in advanced stages in p38α-Δ$^{Spc}$ lungs **(FIGURE 14D)**, suggesting that p38α also plays a role in the progression of K-Ras$^{G12V}$-driven lung cancer.

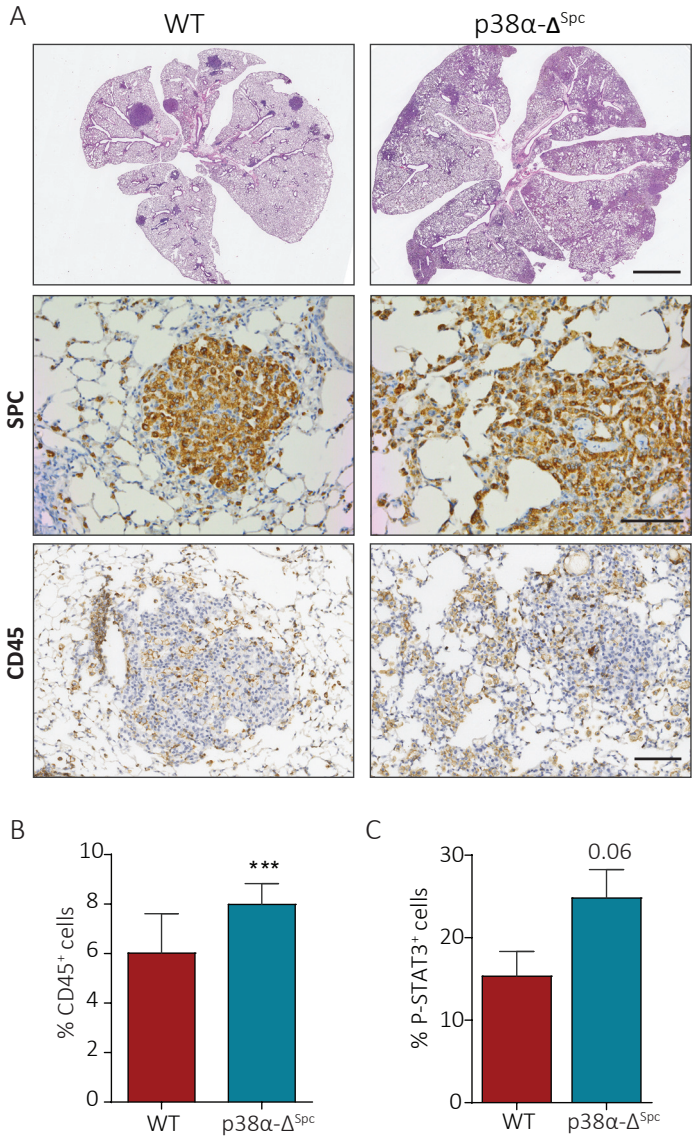


**FIGURE 13. Enhanced proliferation and inflammation in K-Ras$^{G12V}$ lungs with p38α-deficient AE2 progenitors.** (A) Upper, Representative H&E stainings of WT and p38α-Δ$^{Spc}$ lungs. Scale bar, 2 mm. Middle, SPC-labeled AE2 cells in sections from WT and p38α-Δ$^{Spc}$ lungs. Lower, representative pictures of WT and p38α-Δ$^{Spc}$ lungs stained for the hematopoietic cell marker CD45. Scale bar, 100 µm. (B) . The histogram shows the quantification of CD45$^{+}$ cells per field in lung tumors from WT and p38α-Δ$^{Spc}$ mice. Data shows average ± SEM (n=3 mice). (C) Quantification of pSTAT3+ cells in lung tumors from WT and p38α-Δ$^{Spc}$ mice. Data shows average ± SEM (n≥3 mice).

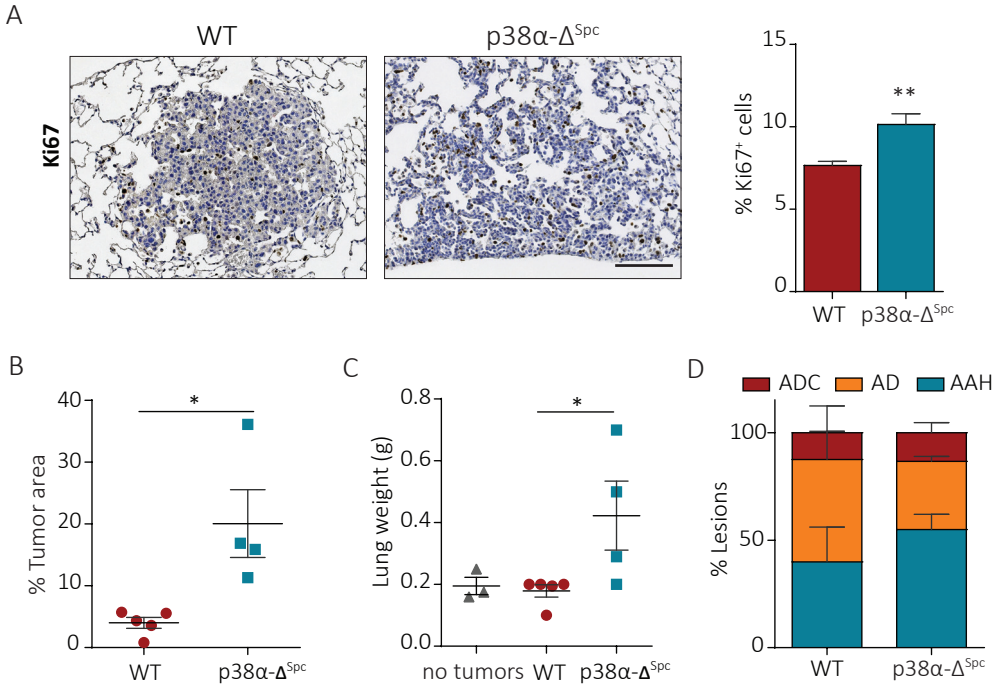


**FIGURE 14. p38α-Δ$^{Spc}$ mice show increased tumor burden but delayed progression to advanced stages.** (A) Lung sections were stained with Ki67 antibody to detect proliferative cells. The histogram shows the quantification of Ki67$^{+}$ cells in individual tumors. (B) Quantification of the tumor area relative to the total lung area. (C) Weight of the lungs of healthy mice and WT and p38α-Δ$^{Spc}$ animals with tumors. (D) Tumors were microscopically analyzed and classified according to their pathological stage: adenocarcinoma (ADC, red), adenoma (AD, yellow), atypical adenomatous hyperplasia (AAH, blue). Data in all graphs shows average ± SEM (n≥4 mice per group).

## p38 MAPK pathway is upregulated in lung adenocarcinomas and correlates with mortality rate in patients

The increased percentage of hyperplasias in p38α-Δ$^{Spc}$ mice hinted a putative role for epithelial p38α in the progression of lung tumors to more advanced stages.

Therefore, we analyzed the phosphorylation status of p38 MAPK in K-Ras$^{G12V}$-driven tumors developed 22 weeks after inoculation with adeno-FlpO. Given its tumor suppressor properties, we expected low levels of p38

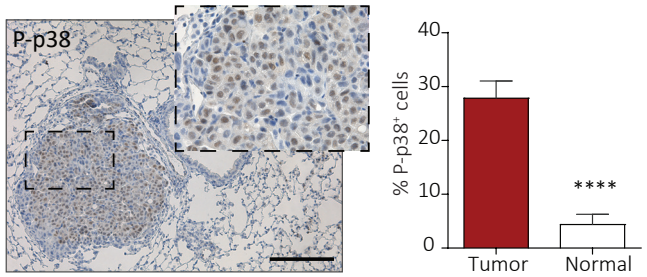


**FIGURE 15. p38 MAPK activation is enhanced in K-Ras$^{G12V}$-driven lung tumors.** Representative phospho-p38 MAPK staining of a murine K-Ras$^{G12V}$-driven tumor. Scale bar, 200 µm. The histogram shows the quantification of phospho-p38 MAPK positive cells per tumor as determined by IHC. Values correspond to average ± SEM (n=5 mice).

MAPK phosphorylation within the tumor masses. Strinkingly, we detected significantly increased phospho-p38 MAPK levels in the tumors in comparison to the healthy parenchyma **(FIGURE 15)**, indicating that tumor cells may take

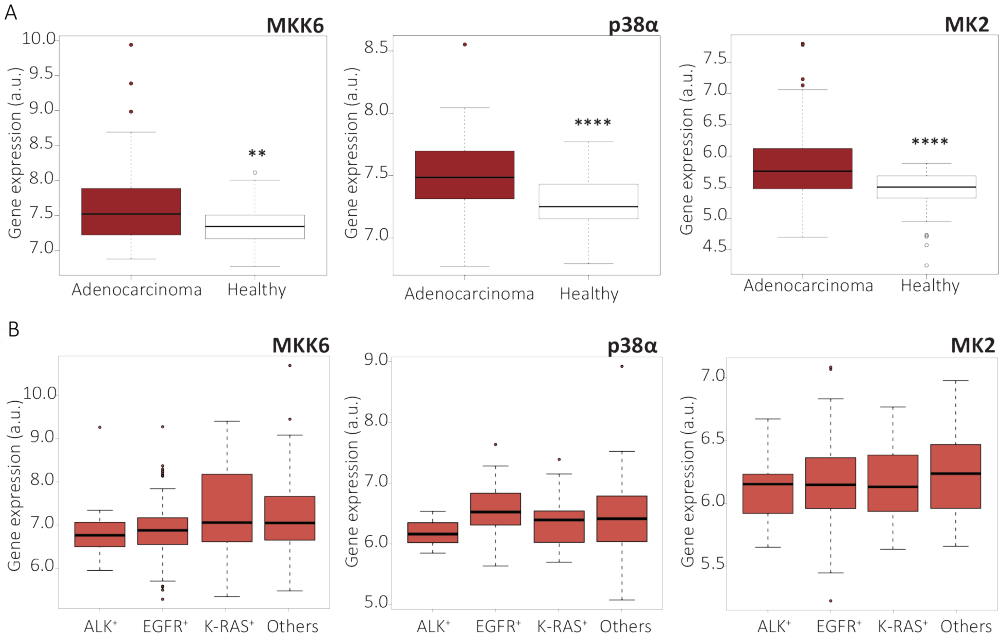


**FIGURE 16. Human lung adenocarcinomas show increased levels of p38 MAPK pathway components.** (A) Boxplots for mRNA expression levels of MKK6, p38α and MK2 comparing paired adenocarcinomas and healthy tissues (n≥49 per group). (B) Boxplots for mRNA expression levels of MKK6, p38α and MK2 for the different driver mutations in early stage lung adenocarcinoma (n≥11 per group).

advantage of this signaling pathway.

Having detected higher activity of p38 MAPK in mouse lung tumors, we analyzed the status of the p38 MAPK pathway in human lung adenocarcinomas in two different cohorts of patients formed by 122 and 156 samples, respectively, both containing tumor and non-tumor lung tissue. We found a significant increase in MKK6, p38α and MK2 mRNA expression levels in tumor tissue compared with paired healthy parenchyma **(FIGURE 16A)**, confirming the observations in mouse tissue. Nevertheless, this increase seemed independent from any particular driver mutation as we observed no difference in the expression levels of the components of the p38 MAPK pathway among the distinct subtypes of lung adenocarcinoma **(FIGURE 16B)**.

This activation of the pathway seemed to be enhanced with tumor progression, as we observed a direct correlation between MKK6 expression levels – probably reflecting p38α activation – and the tumor stage in a third cohort of lung adenocarcinoma patients **(FIGURE 17)**. As well, there was a modest but consistent increase in the p38α and MK2 mRNA expression levels correlating

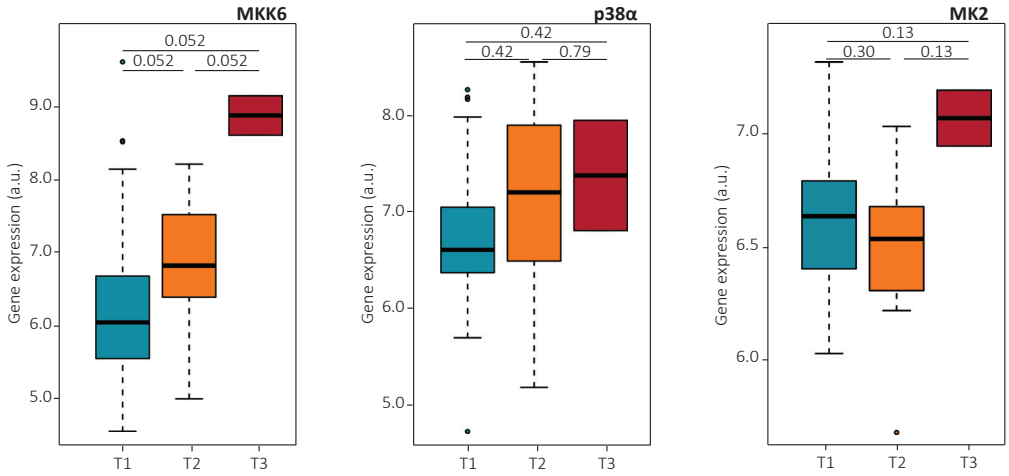


**FIGURE 17. MKK6, p38α and MK2 mRNA levels correlate with malignancy in human lung adenocarcinomas.** Boxplots correlating the MKK6, p38α and MK2 mRNA levels with the pathological stage of human lung adenocarcinoma samples (n=71 for T1, 12 for T2, 2 for T3)**.**

with the stage of tumor progression. Altogether, these observations in human samples support a tumor-promoting role of p38α in lung adenocarcinoma.

Additionally, we checked the p38 MAPK pathway status in patients with lung adenocarcinoma who have or not have suffered metastasis to the regional lymph nodes. MKK6 expression levels significantly correlated with enhanced lymph node metastasis, and these patients with metastasis also showed slightly higher levels of expression of p38α and MK2 in their primary tumors **(FIGURE 18)**.

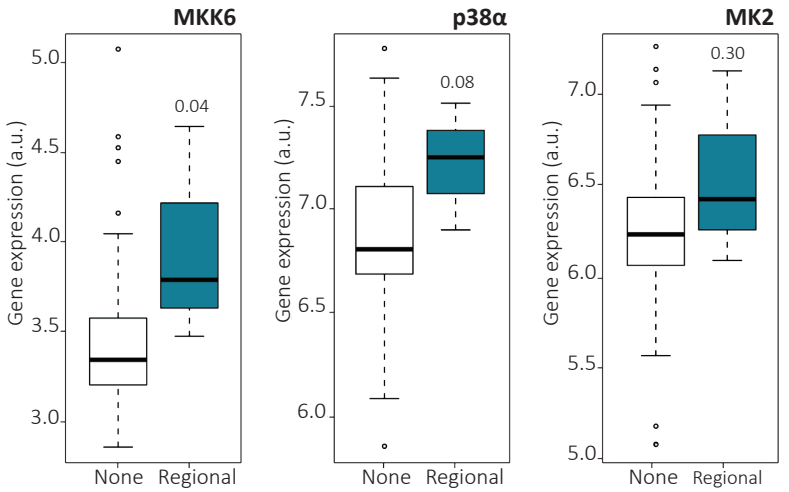


**FIGURE 18. MKK6 expression levels are higher in patients with lymph node metastasis.** Boxplots correlating MKK6, p38α and MK2 mRNA levels to the metastatic status N0 (none) and N1 (regional lymph nodes affected) in patients of lung adenocarcinoma (n=82 for N0 and n=3 for N1).

Next, we wondered whether p38α mRNA levels could be used as a prognostic factor, and performed a univariate analysis adjusting the data according to age, sex, smoking history, and pathological stage. We observed that, independently of tumor stage, highest levels of expression of the MKK6-p38α-MK2 axis correlated with a higher mortality rate **(FIGURE 19A)** and a higher relapse incidence **(FIGURE 19B)** in lung adenocarcinoma patients from the three different cohorts.

All these data suggest that high p38 MAPK signaling could be used as a

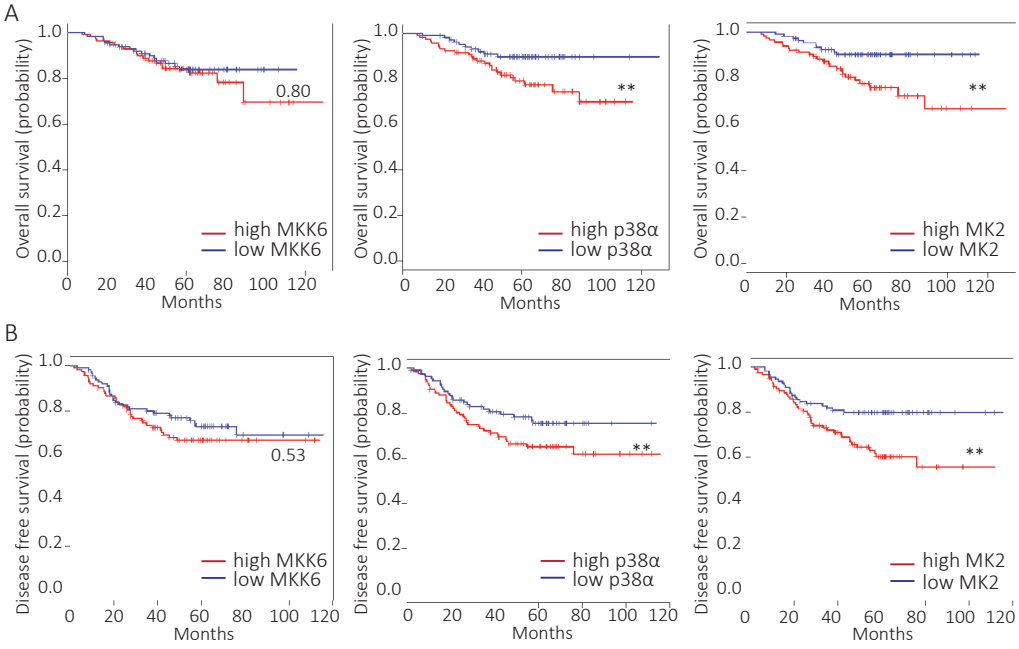


**FIGURE 19. p38α expression levels correlate with reduced survival.** (A) Kaplan–Meier plots showing overall survival of lung adenocarcinoma patients stratified by high or low MKK6, p38α, or MK2 mRNA expression (n≥105 per group). (B) Kaplan-Meier plots display recurrence-free survival over time of lung adenocarcinoma patients stratified by high or low MKK6, p38α, or MK2 mRNA expression (n≥105 per group).

prognostic factor of poor survival in lung adenocarcinoma. However, these correlations were not maintained in other subtypes of NSCLC. For instance, a univariate analysis of recurrence-free survival for squamous cell carcinoma patients did not correlate with the levels of MKK6, p38α or MK2 **(FIGURE 20)**.

In summary, tumor grade, metastasis to lymph nodes and poor prognosis correlate with the upregulation of p38α pathway components in lung adenocarcinoma patients, regardless of the driver mutation. However these features are not general for all NSCLC subtypes. Therefore, the progression of lung adenocarcinoma seems to be particularly dependent of p38α, suggesting that p38α activity could be a useful prognosis indicator for this disease.

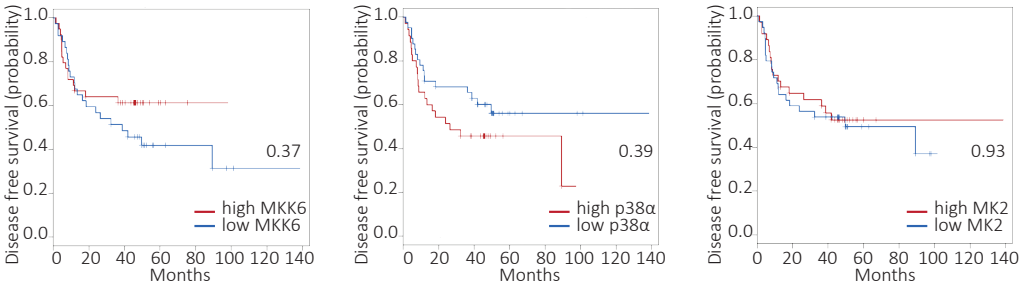


**FIGURE 20. p38 MAPK signaling in lung squamous cell carcinoma does not correlate with survival.** Kaplan-Meier plots showing disease free survival over time of lung squamous cell carcinoma patients stratified by high or low MKK6, p38α, or MK2 mRNA expression, respectively. Log rank P values are specified for each graph (n≥34 per group).

## Downregulation of p38α reduces tumor burden in K-Ras$^{G12V}$-driven NSCLC

As p38α has potential prognostic value in lung adenocarcinomas, we inquired whether the loss of p38α in tumors could impair their progression. This question is very relevant from a clinical perspective, and could help to design new therapeutic approaches for K-Ras$^{G12V}$-driven lung adenocarcinomas, currently an unmet medical need. To investigate whether lung adenocarcinomas need p38α to progress, we inoculated ten-week old p38α–$\Delta^{Ub}$ mice with adeno-FlpO and confirmed the presence of lung tumors 20 weeks later. These mice, both with or without Ubiquitin-CreERT2, were then injected intraperitoneally with tamoxifen during five consecutive days to downregulate p38α and were analyzed two weeks later **(FIGURE 21A)**. Surprisingly, mice with downregulated p38α showed a significant decrease in the number as well as in the size of macroscopic tumors **(FIGURE 21B)**, which we assessed for efficient p38α downregulation by both qPCR and western blot **(FIGURE 21C-D)**. Furthermore, we observed a remarkable decrease in the percentage of advanced lesions **(FIGURE 21E)**, in agreement to the *in vivo* experiment above **(FIGURE 14D)**. Hence, collectively these results indicate a pro-tumorigenic role of p38α in lung cancer cells.

Noteworthy, both the number of visible tumors and the average tumor size were increased in WT mice compared to those animals analyzed before p38α

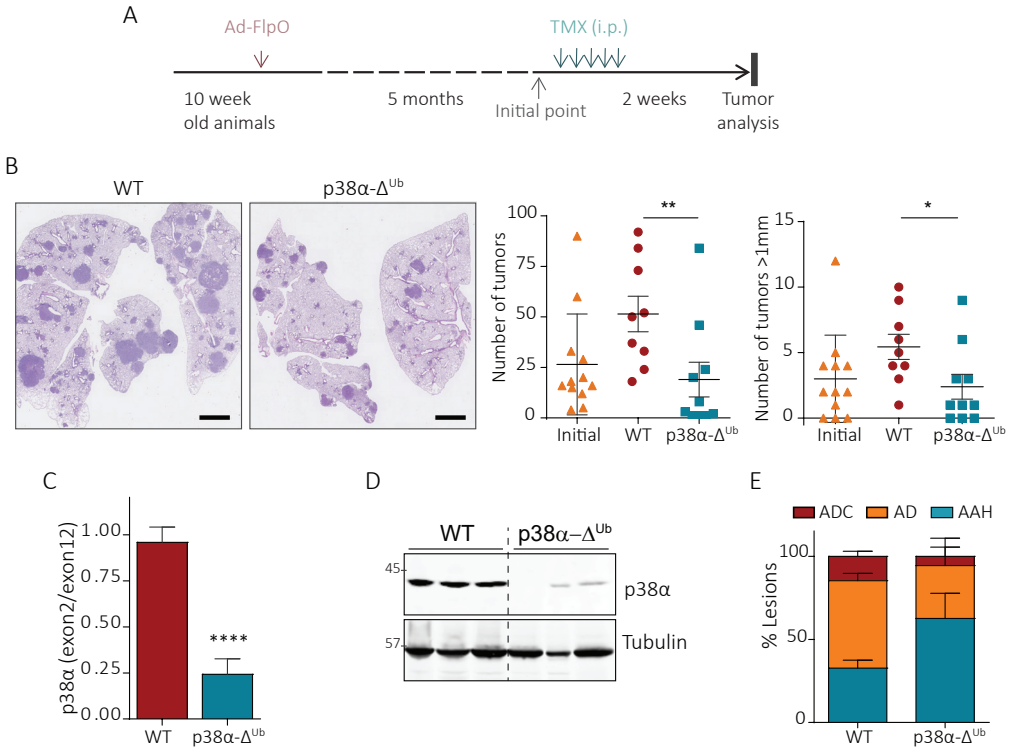


**FIGURE 21. p38α promotes NSCLC progression.** (A) Scheme of the experimental design to study the role of p38α in lung tumor maintenance. Ad-FlpO, adenovirus containing FlpO, TMX (i.p.), tamoxifen intraperitoneal injections. (B) Sections of WT and p38α–$\Delta^{Ub}$ lungs were stained with H&E. Bars, 2 mm. The histograms show the quantification of the tumor number and tumor size distribution per animal, before (yellow) and 2 weeks after tamoxifen treatment in WT (red) and p38α–$\Delta^{Ub}$ (blue) mice. Data represent means ± SEM (n≥9 mice per group). (C) Genomic DNA was isolated from individual tumors either from WT or p38α-$\Delta^{Ub}$ mice and the relative copy number of p38α exon 2 versus p38α exon 12 was analyzed by qPCR. Data represent means ± SD (n=4 WT and 16 p38α KO tumors). (D) Immunoblot of p38α and α-tubulin of individually isolated tumors at the experimental endpoint. (E) Tumors were microscopically analyzed and classified according to their pathological stage. AAH, atypical adenomatous hyperplasia; AD, adenoma; ADC, adenocarcinoma. Data shows average ± SEM (n≥6 mice per group).

downregulation, indicating that tamoxifen by itself does not interfere with tumor growth. Likewise, an equivalent experiment using animals bearing Ubiquitin-CreERT2 without floxed p38α, showed no significant differences neither in average number nor in tumor size, discarding any effect related to the Cre recombinase activity by itself **(FIGURE 22)**.

Noteworthy, both the number of visible tumors and the average tumor size were increased in WT mice compared to those animals analyzed before p38α downregulation, indicating that tamoxifen by itself does not interfere with tumor growth. Likewise, an equivalent experiment using animals bearing Ubiquitin-CreERT2 without floxed p38α, showed no significant differences neither in average number nor in tumor size, discarding any effect related to the Cre recombinase activity by itself **(FIGURE 22)**.

As both tumor number and tumor size decreased in p38α-$\Delta^{Ub}$ animals, we first checked apoptosis and proliferation markers. We did not observe any

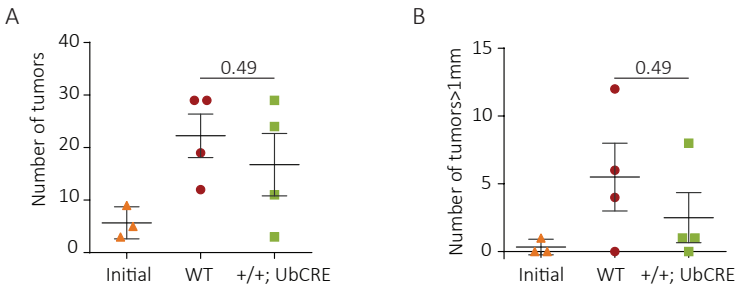


**FIGURE 22. Control experiment using animals only bearing Ubiquitin-CreERT2 showed no difference in tumor number or size.** Average tumor number and tumor size distribution in WT and Ubiquitin-CreERT2 mice, before and two weeks after tamoxifen treatment. Data represent means ± SEM (n≥3 mice per group).

difference in the number of apoptotic cells neither by cleaved-caspase 3 immunohistochemistry nor by TUNEL **(FIGURE 23,** upper pannels**)**. However, the number of proliferative cells, marked by Ki67 immunostaining, was diminished in p38α–$\Delta^{Ub}$ tumors **(FIGURE 23,** lower pannels**)**.

In conclusion, we have observed smaller tumors in p38α-$\Delta^{Ub}$ animals, which are similar in number and size to the tumors harvested prior to tamoxifen injections. We have not detected apoptotic cells, conversely we have observed a reduction in the percentage of $Ki67^{+}$ cells. Altogether, these observations strongly suggest that p38α has tumor promoting properties during lung adenocarcinoma progression and indicate that p38α downregulation produces a cytostatic effect in tumor cells.

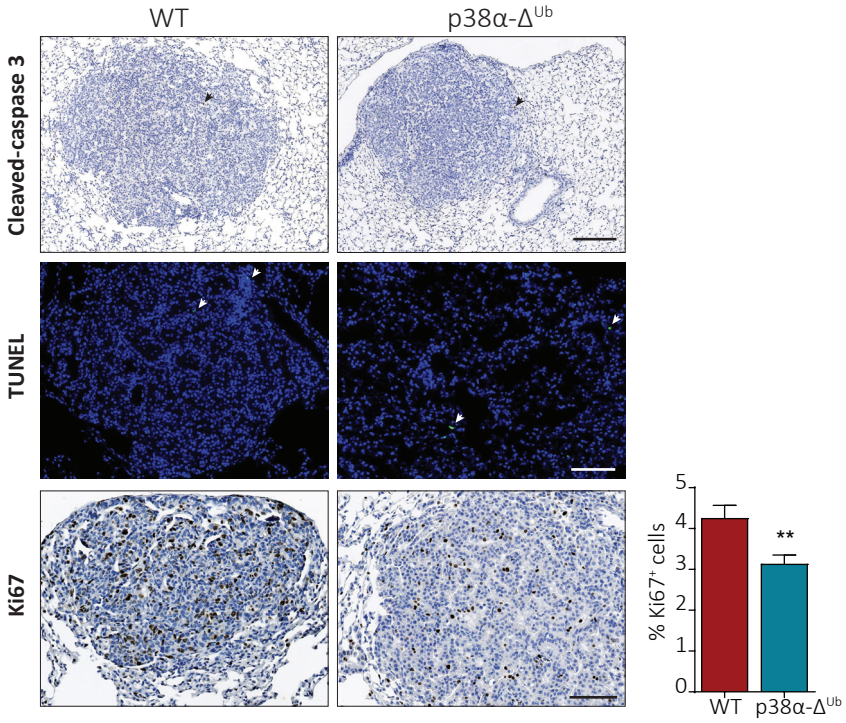


**FIGURE 23. p38α–Δ$^{Ub}$ tumors showed similar apoptosis ratios but reduced proliferation capacity.** Representative images of tumors stained for cleaved caspase 3. Scale bar, 200 µm. TUNEL staining of K-Ras$^{G12V}$-driven tumors from WT and p38α–Δ$^{Ub}$ mice. Positively stained cells are marked with arrowheads. Scale bar, 100 µm. Representative Ki67 staining of K-Ras$^{G12V}$-driven tumors from WT and p38α–Δ$^{Ub}$ mice. Scale bar, 100 µm. The histogram shows the quantification of proliferative cells (Ki67$^{+}$) per tumor. Values represent means ± SEM (n=3 mice).

## p38α kinase activity is necessary for tumor progression

To determine whether the pro-tumorigenic role of p38α relies on the catalytic function of the protein, we inhibited the kinase activity of p38α using the low molecular weight chemical compound PH797804. K-Ras$^{G12V}$ mice with 20-week old lung tumors were administered either PH797804 or vehicle solution for 14 days. After this period, we confirmed the inhibition of p38 MAPK signaling by western blot as the downstream target Hsp27 was not phosphorylated in the inhibitor treated samples.

Animals treated with the inhibitor showed a statistically significant decrease in the number and size of lung tumors in comparison to the vehicle-treated group **(FIGURE 24A-B)**. Again, a cytostatic effect was observed as the number and size of the tumors before the treatment resembles that of the inhibitor-treated group. The number of advanced lesions, as well as the percentage of Ki67$^{+}$ cells per tumor, was also reduced **(FIGURE 24C-D)**. These results phenocopied our observations using the tamoxifen-inducible mouse model, further confirming the pro-tumoral role of p38α in lung cancer cells. Moreover, these results show that the kinase activity of p38α is important for lung tumor progression and its inhibition could be potentially useful for NSCLC therapy.

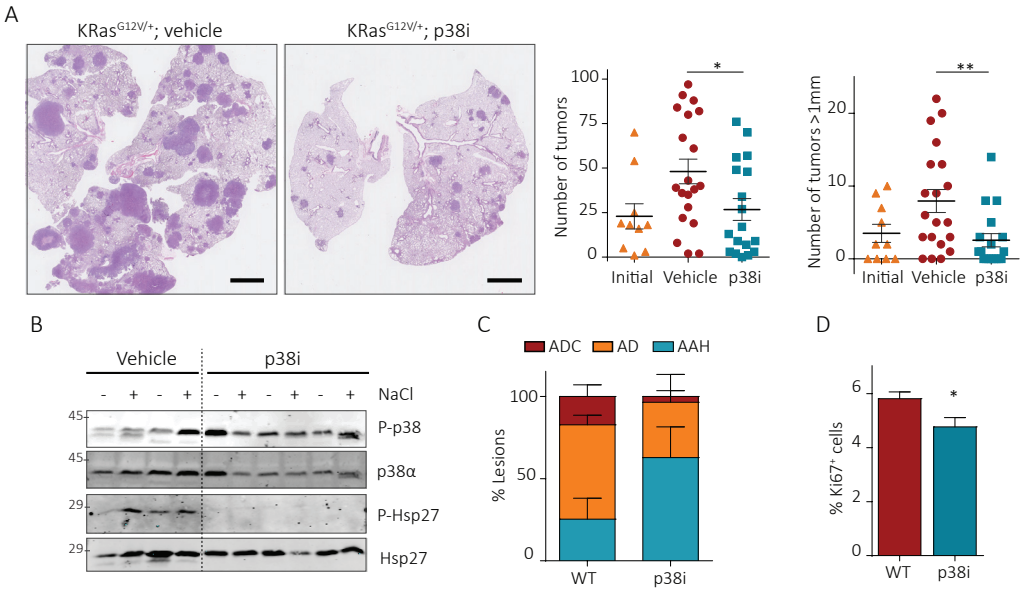


**FIGURE 24. Chemical inhibition of p38α kinase activity impairs tumor growth.** (A) Lung sections from vehicle- and inhibitor-treated animals were stained with H&E. Bars, 2 mm. The histograms show the quantifications of the average tumor number and the tumor size distribution, before and after 2 weeks of treatment. Data represent means ± SEM (n≥10 mice per group. Each dot represents one animal). (B) Individually isolated tumors were immunobloted with the indicated antibodies at the experimental endpoint. (C) Tumors were microscopically analyzed and classified according to their pathological stage. AAH, atypical adenomatous hyperplasia; AD, adenoma; ADC, adenocarcinoma. Data shows average ± SEM (n=3 mice per group). (D) Quantification of proliferative cells in individual tumors as determined by IHC staining for Ki67. Values represent means ± SEM (n≥5 mice).

## Lung tumor growth depends on epithelial p38α

The growth of solid tumors strongly depends of the interplay between tumor cells and their niche, as tumor cells continuously perceive and feed signals to the adjacent stroma which reprogram normal fibroblasts and recruit additional inflammatory cells, eminently from the myeloid cell lineage *(Barcellos-Hoff et al. 2013)*. Since we have observed that ubiquitous downregulation of p38α impairs lung tumor progression, we next studied the contribution of p38α in different cell populations of the TME, namely the epithelial, mesenchymal-derived and immune cell compartments.

To study the role of epithelial p38α in the tumor mass, we used the p38α-$\Delta^{Spc}$ mouse model. We injected tamoxifen in mice with 20-weeks old tumors that either expressed or not SPC-CreER and killed them two weeks after. No differences were observed between the downregulated and control groups, neither in the amount, nor the size of the lesions **(FIGURE 25)**.

As mentioned earlier, since the efficacy of deletion in this model accounted for about 30% of the pneumocytes in this model, we cannot rule out that the limited percentage of cells with downregulated p38α was insufficient to cause substantial effects on the established tumors.

As a complementary approach, we isolated lung adenocarcinomas from our K-Ras$^{G12V}$ mice, engrafted them into immunodeficient mice and put the

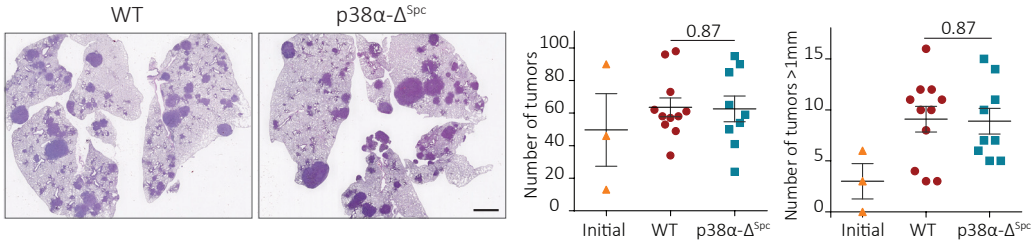


**FIGURE 25. Genetic deletion of p38α in a fraction of SPC$^+$ cells from K-Ras$^{G12V}$ tumors shows no difference in tumor burden.** Average tumor number and tumor size distribution in WT and p38α–$\Delta^{Spc}$ mice, before and two weeks after tamoxifen treatment. Data represent means ± SEM (n≥3 mice per group).

subsequent tumor cells in culture as previously described *(Ambrogio et al. 2014)*. This strategy allowed us to generate a murine K-Ras$^{G12V}$ lung cancer (mKLC) cell line carrying p38α-floxed alleles, in which p38α can be deleted by expressing Cre recombinase in the cells, for example using TatCre protein *(Peitz et al. 2002)*. These cells can be implanted orthotopically, ensuring p38α downregulation only in the epithelial cells that constitute the tumor mass.

We wanted to confirm that the immortalized cells retain the main characteristics of our lung cancer mouse model, which does not bear *Tp53* mutations. This fact is noteworthy because K-Ras$^{G12D}$; Tp53mut tumors are more aggressive than those carrying only mutations in *K-Ras (Jackson et al. 2005)*, and only half of human adenocarcinomas inactivate *Tp53 (Chen et al. 2014)*. Until recently, it was not possible to immortalize lung cancer cell lines from primary tumors that were Tp53-proficient, but the method of serial passaging into nude mice *(Ambrogio et al. 2014)* allows the immortalization of the cells, arguably by the acquisition of other tumor-promoting mutations. To test whether the mKLC cells with p38α-floxed alleles do maintain functional Tp53, they were treated with nutlin-3, a compound that blocks the interaction between the E3 ubiquitin ligase Mdm2 and Tp53, resulting in Tp53 accumulation. We also treated cells with cisplatin, a DNA damage-inducing agent that ultimately activates Tp53. In cells with functional Tp53, the activation of the pathway leads to the accumulation of both p21 and Mdm2. After 24 h treatment with nutlin-3 and cisplatin, we observed increased p21 and Mdm2 expression by qPCR **(FIGURE**

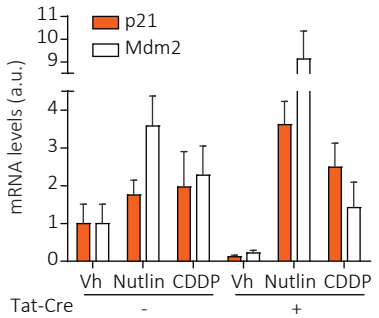


**FIGURE 26. Cells isolated from K-Ras$^{G12V}$ tumors maintain proficient Tp53.** Analysis by real-time qPCR of the mRNA levels for p21 and Mdm2 in WT and p38α KO mKLC (Tat-Cre treated) cells incubated for 24 h either with vehicle (Vh), nutlin-3 or cisplatin (CDDP). Data are means ± SD (n =3 replicates).

**26A)** as well as p21 accumulation by immunoblot **(FIGURE 26B)**, meaning that our mKLC cells are Tp53 proficient and resemble our GEMM.

Next, we inoculated WT and p38α KO mKLC cells intratracheally into the lungs of WT C57BL6/J mice. After 22 days, we observed an increased number of

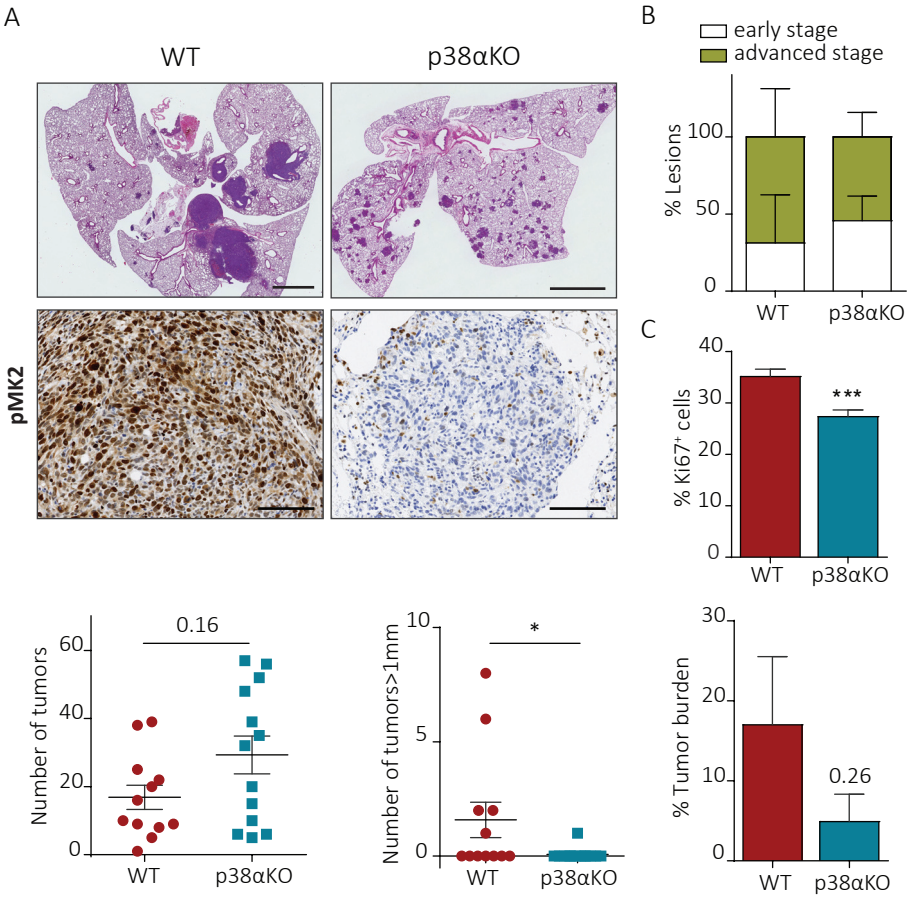


**FIGURE 27. p38α KO cells form smaller lung tumors when implanted orthotopically.** (A) Upper, Lung sections from WT animals that were intratracheally inoculated with either WT or p38α KO mKLC cells. Bars, 2 mm. Middle, pMK2 immunostainings of a WT and a p38α KO tumor. Scale bars, 100 µm. Lower, Average number of total tumors, of tumors bigger than 1 mm in diameter, and tumor burden 22 days after the implantation of WT and p38α KO mKLC cells. Data represent means ± SEM (n≥4 mice per group). (B) Tumors were microscopically analyzed and classified into benign and malignant lesions. Data shows average ± SEM (n≥3 mice per group). (C) Percentage of proliferative cells in individual tumors as determined by IHC staining for Ki67. Values represent means ± SEM (n≥5 mice).

tumors, but of smaller size, in animals injected with p38α KO cells, leading to a diminished tumor load **(FIGURE 27A)**. Again, most of p38α KO lesions were at earlier stages of tumor development than WT lesions **(FIGURE 27B)** and showed a decreased number of proliferative cells **(FIGURE 27C)**, recapitulating our previous observations in the p38α-$\Delta^{Ub}$ mouse model.

As a complementary experiment to rule out any contribution from differences in the colonization ability of WT and p38α KO mKLC cells, we generated a mKLC cell line expressing both p38α lox/lox and CreERT2 **(FIGURE 28A)**. This way, p38α could be deleted in a time-controlled manner. Analogously to the previous experiment, cells were orthotopically implanted in the lungs and allow to grow for 22 days. At this time, animals were injected or not with tamoxifen for 5 days. Fifteen days after the first tamoxifen injection we could observe a significant decrease in both tumor number and size, resulting in

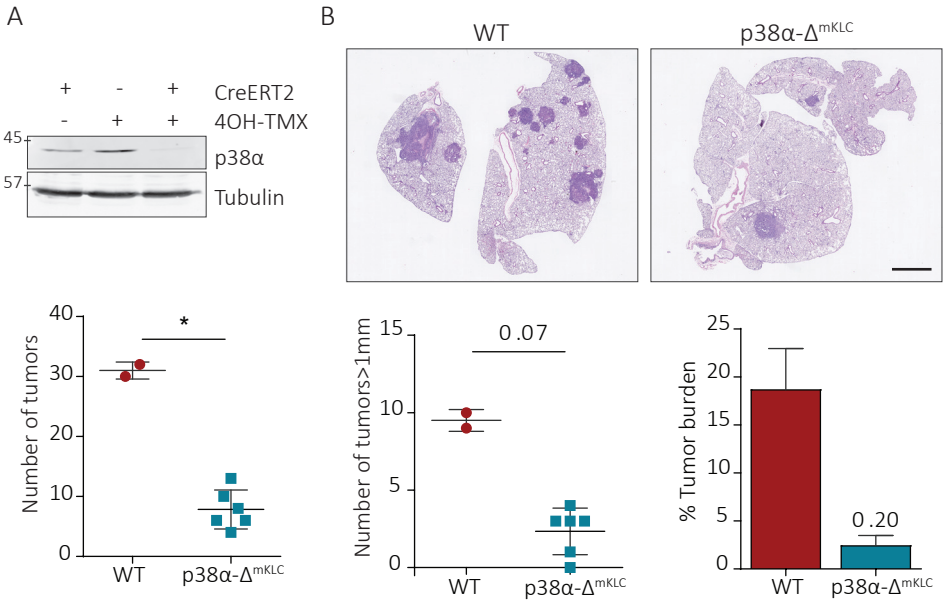


**FIGURE 28. Downregulation of p38α in cancer cells reduces lung tumor burden.** (A) Immunoblot for p38α of mKLC cells treated or not with 4-hydroxy-tamoxifen (4OH-TMX). Tubulin was blotted as loading control. (B) Lung sections from WT animals inoculated with floxed p38α and CreERT2 mKLC cells and injected (p38α-$\Delta^{mKLC}$) or not (WT) with tamoxifen. Scale bar, 2 mm. Average number of total tumors, tumors bigger than 1 mm diameter, and tumor burden 22 days after implantation. Data represent means ± SEM (n≥2 mice per group).

diminished total tumor burden **(FIGURE 28B)**. Altogether, these data show that epithelial p38α is necessary for the progression of lung tumors.

## p38α-deficient tumors show impaired vascularization

In order to check whether the ubiquitous downregulation of p38α particularly affects any of the components of the tumor stroma beyond the epithelial cancer cells, we performed a histopathology analysis of the lung tumors from WT and p38α-$\Delta^{Ub}$ mice. The lung is a highly vascularized tissue and, accordingly, blood vessels are an important component of the tumor mass. The area covered by endothelial cells, positively stained for the von Willebrand factor, was statistically decreased in p38α-$\Delta^{Ub}$ tumors; and so it was the area stained for Pdgfrβ, which mainly marks pericytes **(FIGURE 29A)**. The reduced vascularization correlates with the decreased number of advanced tumors in p38α-$\Delta^{Ub}$ mice as angiogenesis is determinant for tumor progression.

On the other hand, we analyzed the immune cell infiltration in the tumors. Same numbers of lymphoid (CD3-expressing) cells associated to the tumor masses of both genotypes and remained mainly on the periphery. We did not observe changes either in the number of macrophages (CD68-positive cells) between the WT and p38α-$\Delta^{Ub}$ tumors. These results suggest that p38α is necessary for the proper vascularization of lung tumors and does not interfere with immune cell infiltration.

## Myeloid p38α supports lung tumor growth

To determine more accurately the contribution of p38α individually in the stromal cell compartments, we inoculated WT mKLC cells orthotopically into animals constitutively expressing either Fsp-Cre or LysM-Cre. The FSP1 promoter is useful for targeting CAF, as it is active in fibroblasts, cells undergoing early steps of epithelial-to-mesenchymal transition and also some bone marrow derived macrophages *(Trimboli et al. 2008; Osterreicher et al. 2011)*. On the other hand, the Lysozyme-M gene is specific for myeloid cell lineages, particularly granulocytes and macrophages *(Clausen et al. 1999)*.

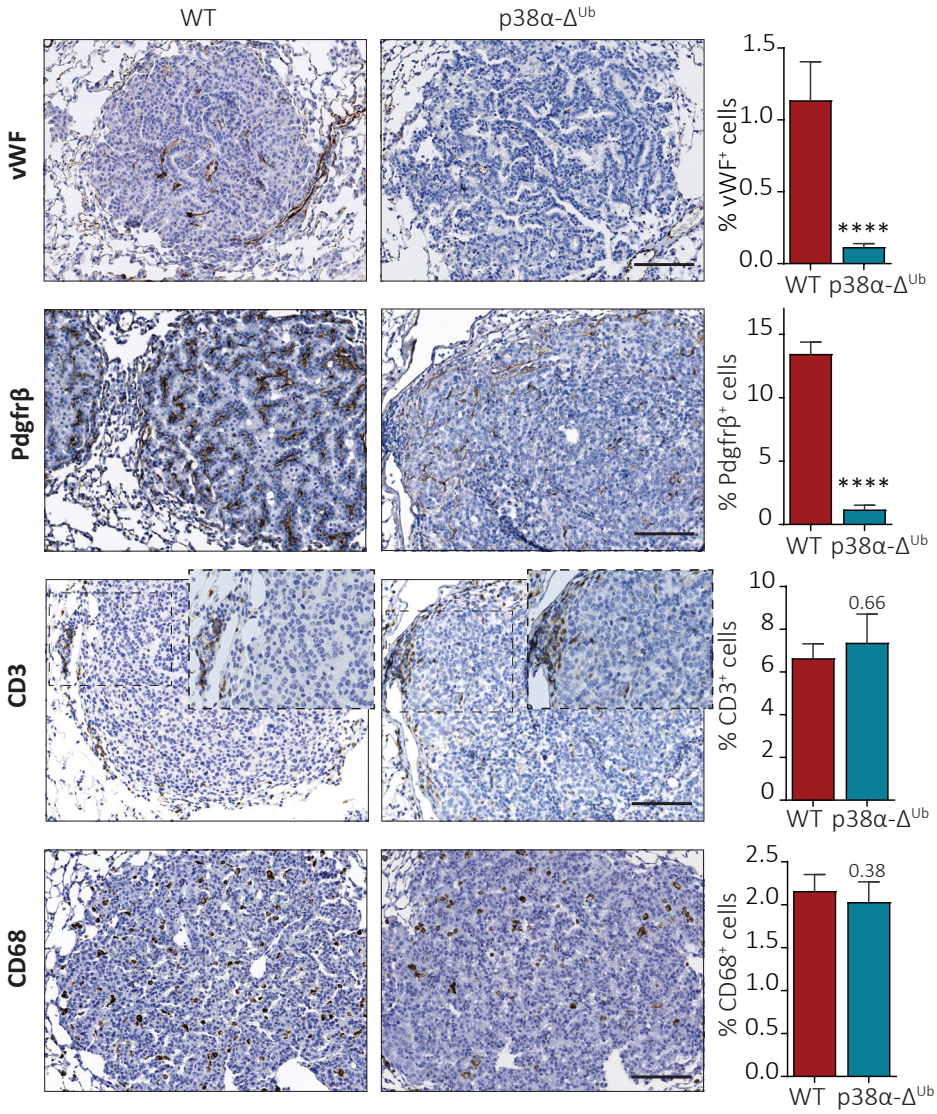


**FIGURE 29. p38α-Δ$^{Ub}$ mice show impaired vasculature.** Representative IHC stainings of WT and p38α-Δ$^{Ub}$ lung sections for the indicated markers of TME cell components. The histograms show the respective quantifications of several tumors of similar size from each animal. Values were obtained in a completely automated manner, represent the relative percentage of stained surface per tumor, and correspond to average ± SEM (n=3 mice per group). Scale bars, 100 µm, and 50 µm for magnifications.

First, we implanted mKLC cells in both p38α-$\Delta^{Fsp}$ mice and the WT control group, consisting of mice expressing Fsp-Cre without floxed p38α. These mice all carried the tdTomato/eGFP reporter, so we could determine the efficiency of p38α deletion by sorting the GFP-positive population. We sorted the GFP-positive fibroblasts (Pdgfrα$^{+}$ GFP$^{+}$ cells), which constituted about 15% of the total Pdgfrα-expressing cells, and analyzed them by quantitative PCR. The sorted GFP-positive fibroblasts showed a 50% p38α-deletion **(FIGURE 30A)**.

Twenty-two days after the implantation we did not observe any difference between the tumors formed in each group of animals **(FIGURE 30B)**, but we cannot discard that a more extensive depletion of p38α in fibroblasts could have affected tumor progression.

Secondly, we implanted mice with floxed p38α, which either carried or not

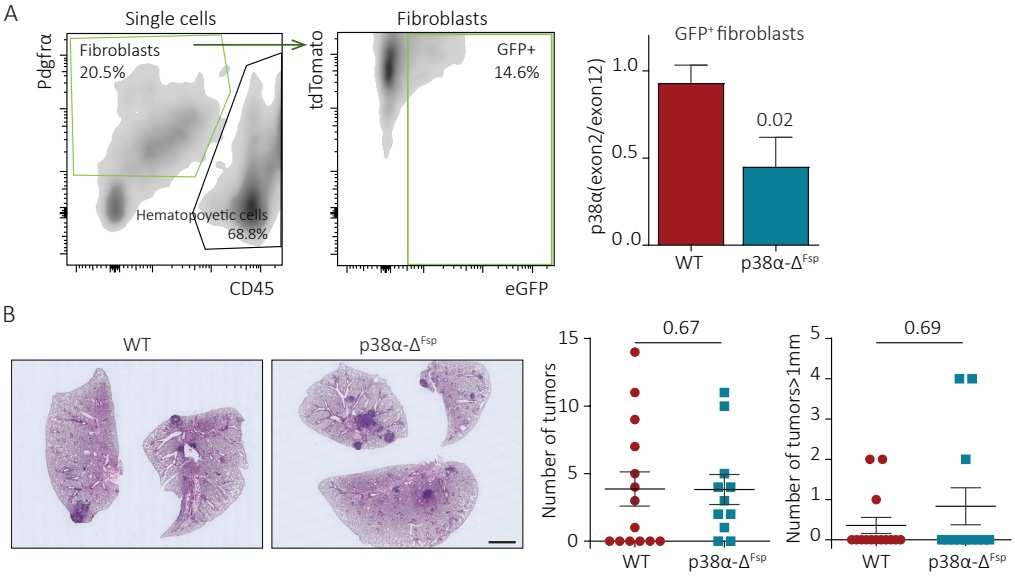


**FIGURE 30. p38α might not contribute to CAF tumor-promoting activity.** (A) Scheme of the multicolor flow cytometry analysis of pulmonary GFP-positive fibroblasts. The genomic DNA was analyzed by qPCR for the relative amount of p38α exon 2 versus p38α exon 12. Data represent means ± SD (n=4). (B) ) Lung sections from WT and p38α-$\Delta^{Fsp}$ animals 22 days after being inoculated with WT mKLC. Scale bar, 2 mm. Average tumor number and tumors bigger than 1 mm diameter 22 days after implantation. Data represent means ± SEM (n≥11 mice per group).

carried the LysM-Cre transgene. We confirmed the deletion in peritoneal macrophages by western blot **(FIGURE 31A)** and also by qPCR of sorted myeloid population from lungs, within which alveolar macrophages and dendritic cells showed the most efficient deletion of p38α **(FIGURE 31B)**. Twenty-two days after the implantation we observed a decrease in the number, the size and the

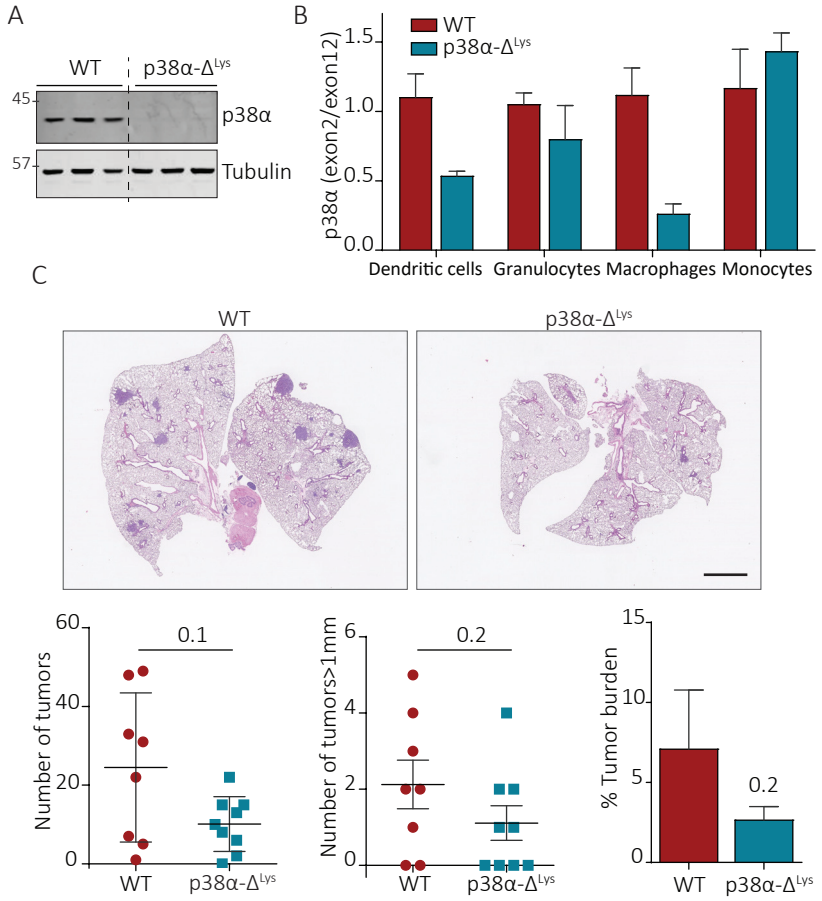


**FIGURE 31. Lungs deficient for myeloid p38α show decreased tumor growth.** (A) Immunoblot of p38α and α-tubulin in peritoneal macrophages from three independent samples of WT and p38α-$\Delta^{Lys}$ mice. (B) Genomic DNA was isolated from sorted lung resident myeloid populations either from WT or p38α-$\Delta^{Lys}$ mice, and the amount of p38α exon 2 versus exon 12 was analyzed by qPCR. Data represent means ± SD (n=3). (C) Lung sections from WT and p38α-$\Delta^{Lys}$ animals 22 days after being inoculated with WT mKLC. Scale bar, 2 mm. Average number of total tumors, tumors bigger than 1 mm diameter, and tumor burden 22 days after the implantation. Data represent means ± SEM (n≥4 mice per group).

tumor burden in the p38α-$\Delta^{Lys}$ mice **(FIGURE 31C)**, indicating that p38α might play a pro-tumorigenic role in macrophages and dendritic cells. Taken together, our results suggest that the strong tumor reduction observed upon ubiquitous downregulation of p38α is the result of pro-tumorigenic p38α functions in both the epithelial and myeloid cell compartments.

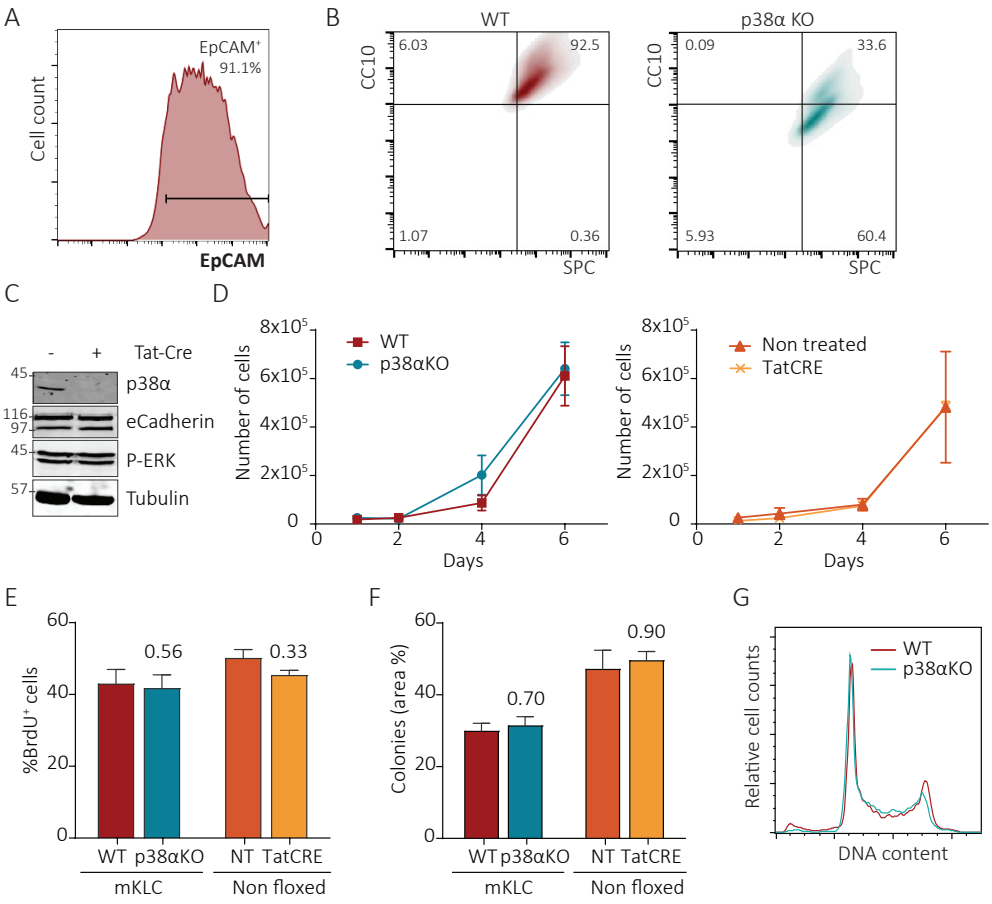


**FIGURE 32. p38α-deficient mKLC cells conserve their proliferation capability *ex vivo*.** (A-B) FACs of mKLC cells for EpCAM epithelial marker (A) and double staining for CCSP and SPC (B). (C) Immunoblot of WT and p38α KO mKLC cells with the indicated antibodies. (D) Cell-doubling curves of WT, p38α KO and mKLC control cells without floxed p38α, either treated or not with Tat-Cre protein; n=3. (E) WT, p38α KO, and non-floxed mKLC cells were labelled with BrdU and analyzed by flow cytometry; n=8. (F) Colony-formation assay of WT, p38α KO and non-floxed mKLC cell lines; n=3. (G) Representative cell cycle profiles from WT and p38α KO cells. All data represent means ± SD.

## WT and p38α KO mKLC cells can proliferate similarly *ex vivo*

Since lung tumors depend on epithelial p38α to progress, we examined the characteristics and the proliferation capacity of WT and p38α KO mKLC cells *ex vivo*. We confirmed that these cells were epithelial **(FIGURE 32A)** and negative for mesenchymal markers such as CD90.2. They also expressed the alveolar epithelium markers SPC and CCSP **(FIGURE 32B)**. We checked by western blot that mKLC cells retained the expression of e-Cadherin after treatment with Tat-Cre protein **(FIGURE 32C)**. We also inquired whether the oncogenic K-Ras-Erk1/2 signaling pathway had been altered upon p38α depletion. In fact, p38α has been reported to negatively feedback onto Erk1/2 signaling (*Chen et al. 2000; Li et al. 2003)* but immunoblot of the WT and p38α KO cells showed similar Erk1/2 phosphorylation levels in both cases **(FIGURE 32C)**.

Next, we performed cell doubling assays which, strikingly, showed similar proliferation curves for WT and p38α KO cells **(FIGURE 32D)**. Consistently, BrdU stainings and clonogenic assays were also comparable between WT and p38α KO cells **(FIGURE 32E-F)**. Indeed, the cell cycle profiles of both genotypes overlapped, and had comparable apoptotic levels of $subG_0$ cell populations **(FIGURE 32G)**.

We then treated mKLC cells with two different p38 MAPK chemical inhibitors, SB203580 and PH797804 **(FIGURE 33A)**. Similar to the previous observations in the genetic model, the chemical inhibition of p38α kinase activity did not affect the proliferation capacity of mKLC cells *ex vivo* as shown by the proliferation curves **(FIGURE 33B)** or colony formation assays **(FIGURE 33C)**. Therefore, we conclude that the downregulation or the inhibition of p38α does not change the ability of lung tumor cells to grow *ex vivo* in standard culturing conditions.

## The lack of p38α attenuates the inflammatory network in lung tumors

To promote tumor growth, cancer cells not only rely on their proliferation capacities, but also need a permissive ecosystem which provides them with growth factors and immunosuppressive mediators *(Barcellos-Hoff et al. 2013)*.

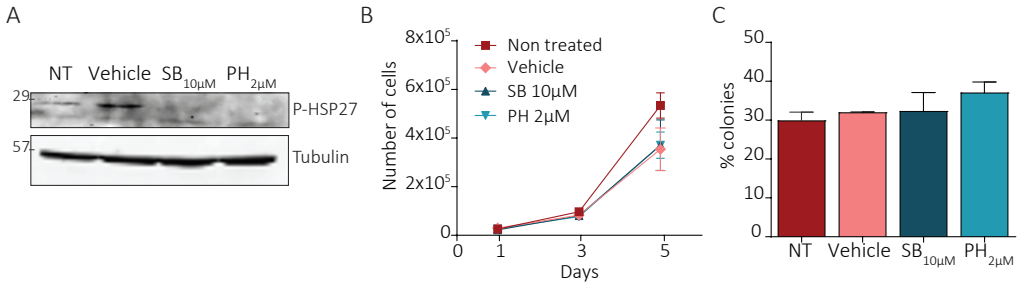


**FIGURE 33. Inhibition of p38 MAPK activity does not influence lung tumor cell proliferation *ex vivo*.** (A) Immunoblot of phosphorylated Hsp27 and the loading control α-tubulin in mKLC cells that were either treated or not with the p38 MAPK inhibitors SB203580 (SB) and PH797804 (PH) for four days. (B) Proliferation curves of mKLC cells treated with the indicated p38 MAPK inhibitors for five days; n=3. (C) Colony-formation assays with mKLC cell line treated with the indicated p38MAPK inhibitors for 15 days; n=2. All data represent means ± SD.

p38α depletion did not change the proliferation potential of mKLC cells *ex vivo*, suggesting that the pro-tumorigenic role of p38α in tumor epithelial cells might rely on a non-cell autonomous function *in vivo*.

Tumor-stroma communication, induction of proliferative signals and immunosuppression are usually carried out by cytokines. Moreover, cytokines are also intimately related to tumor-promoting inflammation. p38α plays a pivotal role in inflammatory processes and has been extensively reported to both regulate the secretion and mediate the signaling by cytokines *(Cuadrado and Nebreda 2010)*. Therefore, we evaluated the contribution of p38α to the cytokine network in the K-Ras$^{G12V}$-driven model of lung adenocarcinomas.

We first compared the levels of 40 different cytokines between WT and p38α KO mKLC cells in culture, to look for intrinsic differences in cytokine secretion driven just by the lack of p38α. We observed that the expression of most cytokines in the p38α KO cells array was reduced, up to 30% and none of them was upregulated **(FIGURE 34A)**. p38α partially controls cytokine secretion in tumor epithelial cells, although the general downregulation of both anti- and pro-inflammatory cytokines suggests that, in the absence of stimuli or extracellular stress, epithelial p38α downregulation does not strongly alter the balance towards a more cytotoxic or less immunosuppressive immune environment.

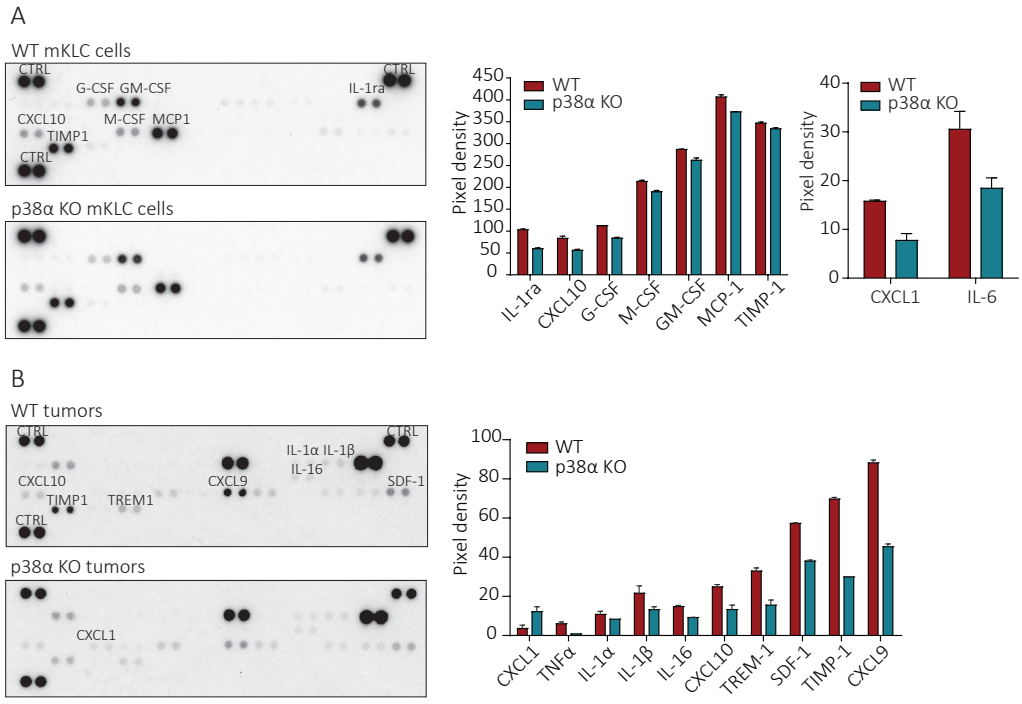


**FIGURE 34. p38α KO mKLC cells secrete decreased levels of cytokines.** (A) WT and p38α KO mKLC cells were cultured for 48h and supernatants were pooled together on a cytokine array. The histograms show pixel density quantification of highly expressed cytokines after a 5 minute and a 30 minutes exposition, respectively. (B) Five tumors from four different mice for each genotype were lysed together and loaded onto a cytokine array. The histogram shows pixel density quantification of the ten most highly expressed cytokines on the array panel. All data represent means ± SD.

Next, we checked the status of the cytokine network in the TME context. The same cytokines were evaluated in tumors that had been generated by orthothopical implantation of WT and p38α KO lung cancer cells in immunocompetent mice. The analysis of the tumor lysates showed a general and even stronger downregulation of the secreted cytokines in p38α KO tumors, reduced on average to half of the levels in WT tumors **(FIGURE 34B)**. Interestingly, CXCL9 and the tissue inhibitor of metalloproteases (TIMP) 1 were among the most significantly reduced cytokines. CXCL9 is a T cell chemoattractant cytokine that can be degraded by neutrophil collagenase (MMP-8), and cleaved by MMP-9 *(Van den Steen et al. 2003)*. TIMP-1 is an inhibitor of MMPs that can also promote

lung tumor growth through activation of Erk1/2 signaling. Moreover, TIMP1 is usually upregulated in advanced lung-cancer patients with poor prognosis *(Xia et al. 2012)*.

In summary, the general reduction in the cytokine levels might impair intercellular communication and also reduce inflammation-mediated promotion of tumor growth. Furthermore, the enhanced differences between cytokine levels in the tumors strengthens the hypothesis of p38α being involved in non-cell autonomous functions in K-Ras$^{G12V}$–driven cancer.

## Lung tumor cells deficient in p38α generate smaller metastasis

The final stages of cancer progression eventually lead to metastasis. Activated p38 MAPK has been reported to enhance several metastatic processes: epithelial-to-mesenchymal transition, invasion, cell migration and extravasation. Conversely, p38 MAPK has been shown to induce anoikis in circulating tumor cells and cancer cell dormancy in disseminated cells *[reviewed in (del Barco Barrantes and Nebreda 2012)]*.

To study the role of p38α in the metastasis of lung cancer cells, we first looked at some of these features in vitro. We checked cell heterologous attachment using fibronectin- and collagen-coated plates. WT and p38α KO cells showed equivalent abilities to adhere **(FIGURE 35A)**, suggesting that p38α KO cells do not have any intrinsic advantage to adhere to the niche. Moreover, cell migration assays in Boyden chambers did not show any difference between WT and p38α KO mKLC cells **(FIGURE 35B)**. We next seeded cells in low-attachment plates to evaluate anoikis resistance for 48h. The survival of detached cells did not change in the absence of p38α **(FIGURE 35C)**.

Furthermore, we checked the anchorage-independent growth using soft agar. After 20 days we observed that a similar number of colonies had formed, thus both WT and p38α KO mKLC cells can survive to non-adherence conditions, in agreement with the aforesaid anoikis experiment. However, the colony size was significantly reduced when p38α was depleted **(FIGURE 35D)**, highlighting the reduced tumorigenic potential of the cells upon p38α depletion. This

observation correlates with our *in vivo* results and again points towards a supportive role of p38α in the progression of lung tumors.

The K-Ras$^{G12V}$ mouse model does not develop metastasis from the lung primary tumors *(Jackson et al. 2001)*. Therefore, to check the metastatic potential of K-Ras$^{G12V}$-driven lung tumors *in vivo*, we injected subcutaneously WT and p38α KO mKLC cells into the back flanks of immunocompromised mice and let them grow for 14 days until tumors were about 0.9 cm$^3$. At this

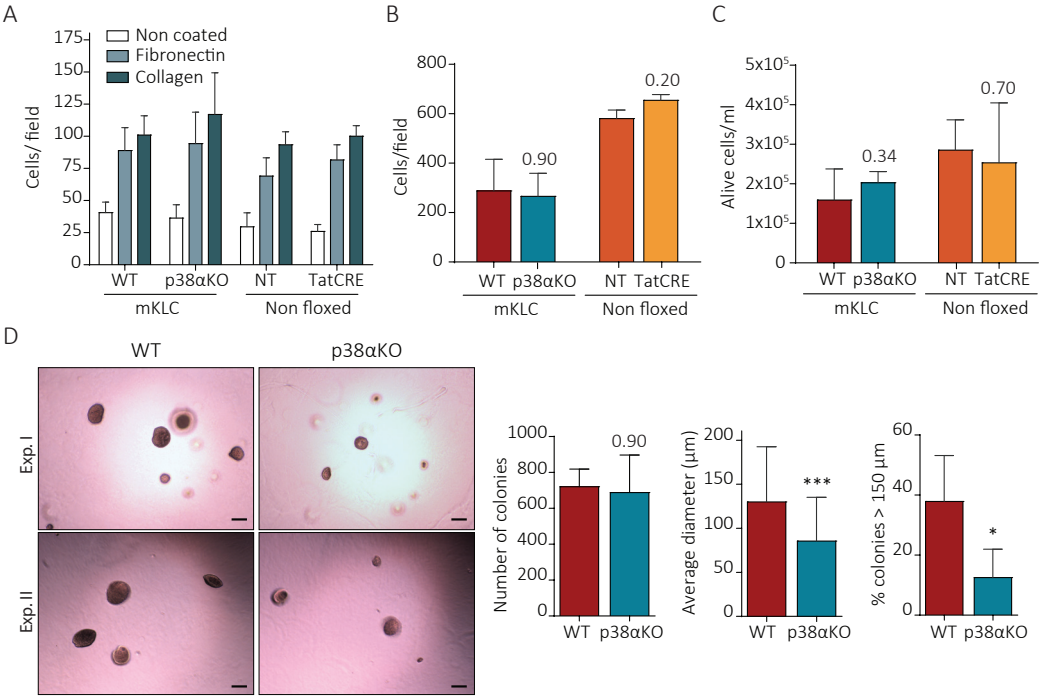


**FIGURE 35. Depletion of p38α does not change the metastatic properties of mKLC cells but reduces their growth potential in soft agar.** (A) Average number of mKLC cells attached to non-coated, fibronectin-coated and collagen-coated plates 90 min after seeding; n=8. Non-floxed cells were used as control for any side-effect of the Tat-Cre treatment. (B) Cells were seeded on top of a Boyden chamber and those migrated to the lower chamber were counted after 20 h; n=3. (C) Cells were cultured for 48 h in non-adherent conditions and then counted in a Neubauer chamber using trypan-blue; n= 4. (D) Representative pictures of WT and p38α KO cells from two independent soft agar assays. Scale bars, 150 µm. The histograms show the quantification of the average number, average size and percentage of colonies bigger than 150 µm in a well; n=4. All data represent means ± SD.

time, primary tumors were resected and 15 days later lungs were checked for metastatic foci. The number of metastatic tumors was similar for WT and p38α KO mKLC cells **(FIGURE 36A)**. However, when p38α KO mKLC cells were injected intravenously into immunodeficient mice, we observed a decrease in lung tumor burden compared with mice injected with WT cells **(FIGURE 36B)**. Noteworthy, no metastasis to brain, bone, or liver was detected in either of the groups. These results are consistent with the observations in soft agar. Therefore, our results suggest that p38α contributes to the ability of mKLC cells to metastasize, probably during the late stages of the process.

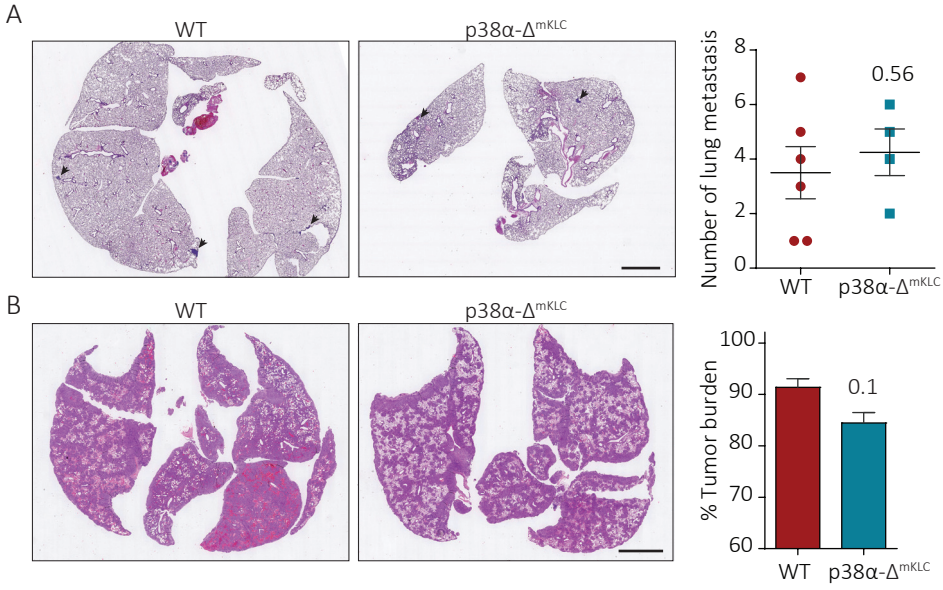


**FIGURE 36. p38α depletion diminishes the burden of metastatic foci.** (A) Nude mice which were injected with mKLC cells subcutaneously into their back flanks, tumors were resected and metastatic foci were counted 15 days later; n≥4 mice. (B) Representative H&E sections and quantification of the tumor burden of lungs from nude mice which had been injected with mKLC cells intravenously and were analyzed 20 days later; n=3 mice. All data represent means ± SEM.

# *Discussion*

p38α has been attributed tumor suppressor properties based on its ability to arrest the cell cycle, induce cell differentiation and trigger apoptosis *(Bulavin and Fornace 2004)*. However, increased levels of phosphorylated p38 MAPK have been related to malignancy in several human tumor types, like NSCLC *(Greenberg et al. 2002)*, follicular lymphoma *(Elenitoba-Johnson et al. 2003)*, breast carcinoma *(Esteva et al. 2004)*, hepatocellular carcinoma *(Wang et al. 2012)* or head and neck squamous cell carcinoma *(Leelahavanichkul et al. 2014)*.

In this thesis, I have studied the contribution of p38α to different steps of lung tumor development and have demonstrated that the initial tumor suppressor role of p38α in lung epithelial cells, interfering with K-Ras$^{G12V}$–driven malignant transformation, is not maintained during advanced tumor stages, in which p38α acts as a tumor promoter.

## p38α plays a dual role in lung tumorigenesis

The ubiquitous downregulation of p38α in the lung leads to distorted alveolar architecture due to hyperproliferation of AE2 progenitors *(Hui et al. 2007)*. Nevertheless, p38β KO lungs do not present hyperplasia and p38α and p38β double KO animals do not show an aggravated phenotype in comparison with p38α KO littermates **(FIGURE 10)**, suggesting that p38β is not involved in lung homeostasis maintenance, in agreement with previous studies in p38β KO mice *(Beardmore et al. 2005)*. The alveolar architecture relies on p38α, as shown by the increased percentages of proliferating SPC-positive cells in p38α KO lungs **(FIGURE 10)**.

p38α KO AE2 cells also become dysplastic as they lose the expression of

differentiation markers and become more susceptible to oncogenic insults like K-Ras$^{G12V}$, giving rise to oversized lungs with numerous tumors *(Ventura et al. 2007)*. These observations are based on models of ubiquitous p38α downregulation, but it is known that the tumor stroma controls stem cell self-renewal and their compartment size *(Bondar and Medzhitov 2013)*, thus a possible stromal contribution to the enhanced tumorigenesis in p38α-deficient lungs remained to be investigated. Here, we show that the downregulation of p38α specifically in AE2 cells is enough to sensitize lungs to K-Ras$^{G12V}$–driven tumorigenesis despite maintaining a WT niche. The increase in both tumor burden and Ki67-positive cells **(FIGURE 13A and 14)** indicate that this hyperproliferation is due to a cell-autonomous effect.

It is worth mentioning that tumors formed from p38α KO AE2 cells were remarkably more infiltrated by immune cells than WT lesions, probably enhancing tumor-promoting inflammation as shown by the increase in STAT3 phosphorylation **(FIGURE 13B-C)**, which stimulates tumor growth. The increased infiltration that we observe confirms previous observations in a constitutive p38α KO model *(Hui et al. 2007)* and suggests that the lack of p38α in tumor initiating cells might change their ability to recruit immune cells.

The tumor suppressor function of p38α in lung epithelial cells is probably connected to both CCAAT enhancer binding protein α (C/EBPα) and protein kinase C α (PKCα). The transcription factor C/EBPα controls proliferation and differentiation in several cell types, and C/EBPα KO animals show a very similar phenotype to that of the p38α KO in AE2 cells *(Basseres et al. 2006; Martis et al. 2006)*. Moreover, p38α has been proposed to phosphorylate C/EBPβ, which in turn regulates the expression of C/EBPα *(Ventura et al. 2007)*. On the other hand, PKCα also acts as a tumor suppressor in lung epithelial cells, through a PKCα-p38α-TGF-β axis that enforces oncogene induced senescence avoiding K-Ras-driven transformation *(Hill et al. 2014)*.

The *in vivo* studies performed by *Hui et al. (2007)* and *Ventura et al. (2007)* analyzed the role of p38α only in the early stages of lung tumorigenesis because the experimental models used could not uncouple K-Ras induction from p38α downregulation. Lung tumors could have been induced with chemical carcinogens like urethane, but tumorigenesis in that case depends on a random

mutagenesis process that adds an extra layer of variability to the study. Thus, we have designed an *in vivo* strategy combining the Flp-FRT system with different promoter-driven Cre recombinases. This way, both the cell type and the time point in which each genetic modification takes place can be controlled, allowing us to address the role of p38α in different cell compartments and at different stages of K-Ras$^{G12V}$-driven lung cancer development **(FIGURE 12C and 21A)**. Using this strategy, we first induced K-Ras$^{G12V}$-driven tumors and 20 weeks later induced systemic p38α downregulation. The acute downregulation of p38α in mice with established lung tumors clearly impaired tumor growth, in agreement with a recent publication *(Brichkina et al. 2016b)*, and impaired progression to more advanced stages **(FIGURE 21B and 21E)**. The smaller lung tumors observed upon systemic downregulation of p38α were similar in number and size to the tumors harvested prior to tamoxifen injections, and had a reduced percentage of Ki67-positive cells than WT tumors but no difference in apoptotic markers **(FIGURE 23)**. These data suggest that p38α pathway mediates proliferation signals and its downregulation induces a cytostatic effect.

Additionally, tumors in mice with ubiquitously downregulated p38α showed impaired vascularization **(FIGURE 29)**, which probably also contributes to the halted tumor progression to more advanced stages. The decrease in tumor vasculature can be due to the disruption of two axis in endothelial cells, one enabling cell proliferation (Ras-p38α-GATA2) *(Katsumura et al. 2014)*, and a second one enabling cell migration (VEGFR2-p38α-PRAK) *(Yoshizuka et al. 2012)*, which are both necessary to form new blood vessels. Also, in non-endothelial cells, p38α downregulation might have impaired the secretion of extracellular factors which normally impinge on endothelial cells, affecting therfore the induction of vasculature development.

It should be noted that a former report showed that p38α simultaneous depletion to K-Ras$^{G12D}$ induction, made lung tumors progress faster to the adenoma and adenocarcinoma stages, and animals die earlier *(Ventura et al. 2007)*. The differences in tumor progression in both cases could be due to the time point of p38α downregulation. In this case tumors in p38α KO animals are formed without p38α from the outset. In our case, WT tumors probably

develop an addiction to p38α signaling that is halted upon acute genetic downregulation, so they would need to readapt for resuming growth. Aside from that, it is also possible that some tumors in *Ventura et al. (2007)* contained progressively increasing numbers of p38α-proficient cells as tumor evolves, surpassing the p38α KO cancer cells and enhancing even more the progression of an initially bigger tumor burden.

How p38α performs tumor-promoting functions in K-Ras$^{G12V}$-driven lung cancer cells is still unknown. The mechanism could go through downstream targets of p38α, like Il-6, which has also showed a dual role during lung tumor development. Il-6 maintains lung homeostasis, reduces iNOS production by alveolar macrophages, and activates cytotoxic T cells upon K-Ras$^{G12D}$ oncogenic stress. However, it promotes lung cancer growth through induction of the cell proliferation regulator cyclin D1 *(Qu et al. 2015)*. Additionally, the systemic blockade of Il-6 with a monoclonal antibody has been shown to significantly inhibit lung cancer progression and angiogenesis, and to reprogram the immune cells towards an anti-tumor phenotype *(Caetano et al. 2016)*. Accordingly, the NFκB pathway, which also controls the secretion of Il-6 *(Libermann and Baltimore 1990)* and whose activity can be positively regulated by p38 MAPK signaling *(Cuadrado and Nebreda 2010)*, has been proven to mediate K-Ras-induced lung tumorigenesis *(Meylan et al. 2009; Basseres et al. 2010)*. Here we show that p38α-depleted lung cancer cells form smaller tumors when implanted intratracheally **(FIGURE 27)**. In those tumors Il-6 secretion is reduced, and so it is in the supernatant of the p38α KO cancer cells cultured *ex vivo* **(FIGURE 34)**; hence the pro-tumorigenic contribution of Il-6 signaling could be affected by the downregulation of p38α.

Our results on the dual role of p38α in NSCLC extend a recent study on intestinal tumorigenesis *(Gupta et al. 2014)* and, in agreement with the upregulated levels of phospho-p38 MAPK generally observed in human tumors *(Wagner and Nebreda 2009)*, it seems likely that this dual function might be conserved in tumors originating in different tissues. Further studies using other inducible tissue specific-deletion models should be performed to confirm this hypothesis.

To sum up, this thesis shows that the p38α pathway plays two opposing functions in lung cancer development **(FIGURE 37)**. During the early stages

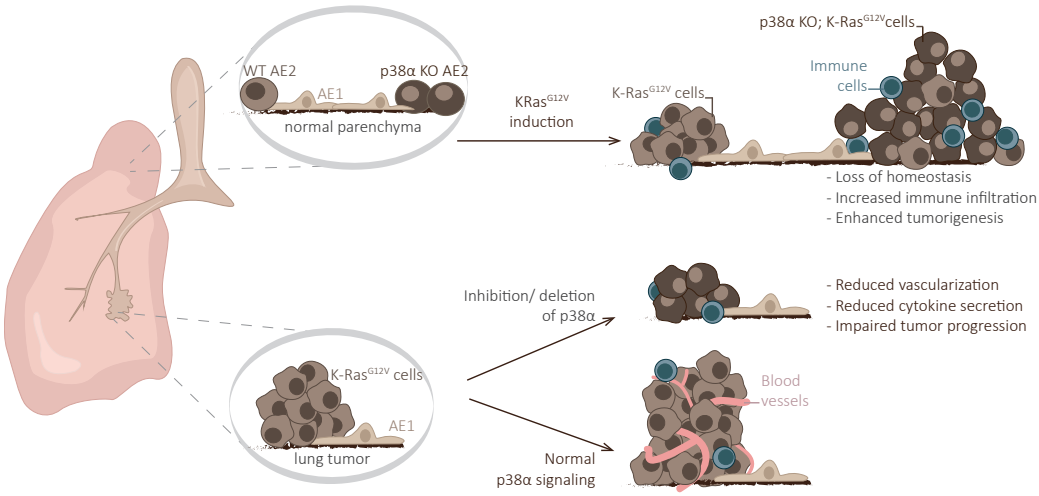


**FIGURE 37. Dual role of p38α in lung tumorigenesis.** Upper, p38α KO pneumocytes are more sensitive to oncogenic insults like K-Ras$^{G12V}$ expression, leading to enhanced tumorigenesis. Lower, the inhibition of p38α impairs the progression of Kras$^{G12V}$-driven tumors.

of malignant transformation, p38α has an intrinsic antitumor role in epithelial cells controlling differentiation and stem cell self-renewal **(FIGURE 10, 14A and** *(Ventura et al. 2007)***)**. However, as tumors evolve, they become addicted to p38α signaling, which favors cancer cell proliferation, angiogenesis, and pro-tumorigenic cytokine expression **(FIGURES 23, 29 and 34)**.

## Both epithelial and myeloid p38α promote lung tumor progression

Systemic expression of a non-phosphorylatable p38α mutant, which is expected to function in a dominant negative manner, has been recently shown to reduce the number and size of K-Ras-induced lung tumors *(Brichkina et al. 2016b)*. Specifically, p38α has been proposed to regulate the synthesis of hyaluronic acid by CAF, which in turn induces lung cancer cell proliferation *(Brichkina et al. 2016a)*. Interestingly, the latter study discarded any tumor promoting role of epithelial p38α due to enhanced proliferation of the mutant p38α cells when inoculated into nude mice, and so then focused in the p38α-mediated signaling in CAF using a fibroblast specific Cre system. However, our results indicate that

lung epithelial tumor cells require p38α signaling to proliferate in anchorage-independent conditions and within the pulmonary niche *in vivo*. Although cell proliferation *ex vivo* is not affected by the absence of p38α **(FIGURES 32 and 33)**, there are clear differences in soft agar colony size **(FIGURE 35D)**. This discrepancy might be explained because adhesion signals in 2D cultures are sufficient to support cell growth independently of p38α; whereas in reduced adhesion conditions, cells depend on p38α to produce and/or transduce mitogenic signals that enhance tumor growth. Moreover, the differences in tumor burden upon orthotopic implantation **(FIGURE 27 and 28)** point to a role of p38α in tumor cell-stroma interactions.

Given that tumor cells rely on the associated stroma and the paracrine signaling that interconnects them, one option is that p38α signaling in epithelial tumor cells controls the establishment of a supportive interplay with the tumor microenvironment **(FIGURE 38)**. Consistent with this possibility, human lung stem cells have been reported to depend on p38α to orchestrate a paracrine network that forms the pulmonary niche. In particular, p38α regulates the secretion of stromal cell-derived factor (SDF) 1, which in turn activates and recruits fibroblasts that secrete TNFα and IL8, subsequently recruiting endothelial cells *(Ruiz et al. 2014)*. We have explored the epithelial cell-secreted inflammatory network within the lung tumor context and observed that p38α partially controls the secretion of several inflammatory cytokines, including SDF-1 and Il-1 **(FIGURE 34),** which may potentially promote tumor growth. In the p38α KO lung tumors and cancer cells, we observed an important decrease particularly in Timp-1 **(FIGURE 34)**, an inhibitor of MMPs which positively correlates with bad prognosis in NSCLC *(Pesta et al. 2011)*. TIMP-1 was previously linked to p38α signaling, as its expression can be induced by IL-1 via both the IKK/NF-κB and p38/ATF-2 pathways in astrocytes *(Wilczynska et al. 2006)*. Reduced expression of TIMP-1 might allow an accumulation of MMPs, which degrade other cytokines such as CXCL9, explaining the concomitant decrease that we observed in the latter protein. Aside of its MMP inhibitor activity, Timp-1 can bind CD63 and activate FAK and Erk phosphorylation, that enhance cell proliferation *(Xia et al. 2012; Park et al. 2015)*.

A recent publication has shown that p38α signaling in CAF plays a crucial role

in breast tumorigenesis by controlling the activity of AUF1, which induces the post-transcriptional stabilization of tumor-promoting inflammatory cytokines *(Alspach et al. 2014)*. Unfortunately, we could not confirm a role for p38α in the mesenchymal-derived cell compartment of lung tumors, due to the limited deletion capacity of the Fsp-Cre system in our mouse lines **(FIGURE 30)**. The

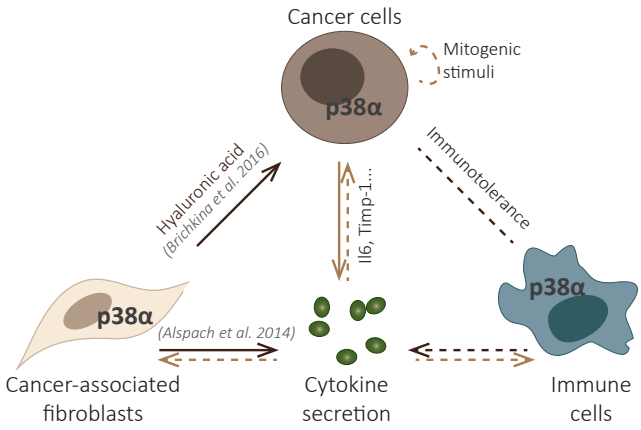


**FIGURE 38. p38α signaling in cancer cells establishes a supportive interplay with the tumor microenvironment that promotes lung cancer progression.** p38α controls the secretion of cytokines by epithelial cancer cells and other cells of the tumor microenvironment. p38α can also control the secretion of extracellular matrix components by cancer-associated fibroblasts, as well as tumor immunosuppression by myeloid cells, which ultimately impact on tumor progression.

use of other fibroblast specific Cre lines, like Pdgfrα-Cre or Col1a2-Cre, would be needed to investigate possible functions of p38α signaling in CAF during lung tumorigenesis.

Additionally, we investigated the contribution of p38α in immune cells. The number of infiltrating lymphocytes and macrophages does not change between tumors with or without p38α **(FIGURE 29)**, although we cannot discard possible differences in their commitment to type I or type II immune responses. Particularly, we show that p38α in myeloid cells plays an important role supporting lung tumor progression **(FIGURE 31)**. The underlying mechanism for this phenotype remains elusive but, based on previous data that relates

p38α to tumor-promoting immune responses in dendritic cells *(Wang et al. 2006a)*, it is possible that myeloid p38α facilitates tumor immune tolerance in K-Ras-driven lung cancer *(Lu et al. 2014)*.

Regarding the lymphoid lineage, it has been shown that tumor infiltrating lymphocytes can exert type II responses, and also that interfering with non-canonic p38α activation in $CD4^+$ T cells impairs pancreatic cancer *(Alam et al. 2015)*. Therefore, the function of p38α in lymphocytes could also contribute to the difference in lung tumor burden observed in mice with induced ubiquitous downregulation of p38α. Aside of the tumor-promoting ability of p38α in the T cells, we know from other studies in our group that epithelial p38α is important for the tumor-lymphoid cells interplay. While p38α KO lung cancer cells form substantially smaller tumors than WT cells when implanted into immunocompetent mice, the difference is less clear when the same lung cancer cells are implanted into the lungs of immunodeficient mice *(Real S, unpublished data)*. This observation suggests that signals produced by infiltrating T cells could impinge differently on epithelial tumor cells with or without p38α, promoting stronger growth in lung tumors that are p38α proficient.

In summary, our results show that p38α can perform pro-tumorigenic functions both in the malignant lung epithelial cells and in immune cells, especially by controlling the cytokine release and possibly by inducing immune-tolerance.

## p38α as a potential therapeutic target in lung adenocarcinoma

In this study, we have addressed the role of p38α in lung tumors that are Tp53 proficient. For this, we have generated Tp53 proficient cell lines **(FIGURE 26)** that can deplete p38α *ex vivo* using a recently developed immortalization method *(Ambrogio et al. 2014)*. Importantly, Tp53 is a known target downstream of the p38 MAPK pathway, so these lung cancer cell lines will allow the study of cues that impinge on this protein through p38α signaling.

Constitutively active p38 MAPK has been proposed to increase the selective pressure in cancer cells to inactivate downstream targets with tumor suppressor functions like Tp53 or p16 *(Bulavin and Fornace 2004)*, prompting tumors to more

advanced stages, and making them more aggressive. Given that half of human adenocarcinomas inactivate the TP53 gene *(Chen et al. 2014)* it is also useful to ask whether Tp53-deficient lung tumors are sensitive to p38α downregulation. As p38α depletion affects the progression to advanced lung cancer stages **(FIGURE 21E and 24C)**, and K-Ras$^{G12V}$; Tp53$^{null}$ tumors can progress more quickly, it is likely that p38α depletion in the Tp53$^{null}$ context would have shown stronger effects in tumor burden and progression. In fact, it has been recently shown that systemic downregulation of p38α signaling in mice with K-Ras$^{G12D}$; Tp53$^{null}$ lung tumors significantly reduces tumor burden *(Brichkina et al. 2016a)*, and another study has showed a synthetic lethality between the p38α effector MK2 and Tp53 in K-Ras$^{G12D}$-driven lung tumors *(Morandell et al. 2013)*. Therefore, the depletion of p38α could be beneficial for adenocarcinoma treatment in both Tp53-proficient and -deficient scenarios.

Several inhibitors of p38 MAPK are undergoing clinical trials for treating inflammatory diseases *(Goldstein et al. 2010; MacNee et al. 2013)*. Previous studies have shown that the chemical inhibitor of p38α PH797804 impairs growth of patient-derived colorectal tumors *(Gupta et al. 2015)*. In agreement with this result, we show that p38α kinase function is necessary for K-Ras$^{G12V}$-driven lung tumor progression into more advanced stages, based on the treatment of mice with PH797804 **(FIGURE 24)**.

In addition, p38α inhibition can potentiate the effect of chemotherapeutic drugs like cisplatin or doxorubicin. For instance, the combination of PH797804 and cisplatin significantly impairs mammary tumor progression in mice expressing polyomavirus middle T-antigen *(Pereira et al. 2013)*, and p38 MAPK has been related to cancer cell survival and resistance to doxorubicin treatment in gastric cancer *(Tan et al. 2014)*. This synergy also applies in the case of lung cancer, as a recent study reported a significant reduction in K-Ras$^{G12D}$-induced lung tumor burden upon ubiquitous expression of the kinase inactive p38α mutant P224I, and an increase in the number of apoptotic cells when combined with cisplatin *(Brichkina et al. 2016b)*. As well, MK2$^{-/-}$ Tp53$^{-/-}$ double KO tumors showed increased sensitivity to cisplatin in a K-Ras$^{G12D}$-driven NSCLC mouse model *(Morandell et al. 2013)*. Taken together all these results strongly support the therapeutic interest of p38α inhibition for lung cancer treatment, alone or

in combination with cisplatin.

Furthermore, we have shown that p38α inhibition affects both tumor cells **(FIGURE 27 and 28)** and the tumor associated stromal cells **(FIGURE 31 and** *(Brichkina and Bulavin 2017)***)**. Stromal cells are genetically more stable than the heterogeneous cancer cells, thus the systemic inhibition of p38α might avoid the development of resistance, which is a current struggle of other currently available chemotherapies.

Nevertheless, p38 MAPK inhibition has been reported to occasionally enhance metastatic features *(del Barco Barrantes and Nebreda 2012)*, thus it is important to study if the treatment of primary tumors with p38α inhibitors could carry undesirable consequences. For example, one aspect to take into consideration is that p38α activity is recovered upon withdrawal of the p38α inhibitor; therefore, the use of a K-Ras$^{G12V}$; Tp53$^{null}$ mouse model, which does eventually develop metastasis to lymph nodes and distant organs *(Jackson et al. 2005)* would be useful for evaluating metastasis latency upon treatment of the primary tumors with p38α inhibitors. At the moment, our research shows that p38α depletion in mKLC cells has a net negative effect on the growth of metastatic lesions in the lung **(FIGURE 36)**. We demonstrate *in vitro* that p38α downregulation does not change the migratory abilities of tumor cells **(FIGURE 35C)** therefore it does not seem likely that p38α inhibition in the primary tumor cells could enhance their dissemination through the body. Furthermore, the comparable behavior of WT and KO cells in anoikis assays **(FIGURES 35A and 35B)**, but the differences in the size of soft agar colonies **(FIGURE 35D)** and in the burden of the metastasis upon intravenous injection of lung cancer cells **(FIGURE 36B)** indicate that p38α signaling might facilitate lung tumor growth in the metastatic site. Indeed, studies injecting WT Lewis lung carcinoma cells in p38α KO animals, i.e. with a p38α KO pre-metastatic niche, show strongly reduced colonization of the lungs *(Matsuo et al. 2006; Brichkina et al. 2016a)*. On the other hand, p38α in the cancer-cell has also been shown to influence pre-metastatic niche formation in the lung, through the expression of the inflammatory chemoattractants S100A8 and S100A9 by the primary tumor *(Hiratsuka et al. 2006)*. Therefore, we hypothesize that inhibiting p38α would potentially hinder metastasis, improving the 5-year survival expectancy of lung cancer patients.

## p38α mRNA levels have clinical prognostic value

p38α has been identified as an influential gene deregulated in gene expression networks generated from the sequencing data of primary NSCLC *(Kalari et al. 2012; Choi et al. 2015; Brichkina et al. 2016a)*. Moreover, the copy number of MK2 has been proposed as a risk and prognosis biomarker for lung cancer *(Liu et al. 2012)*. Here, we further extend these predictions to the whole signaling axis, by performing a bioinformatics analysis in three different cohorts of human lung adenocarcinoma samples. We show that the expression of MK2, p38α and MKK6 are increased in lung adenocarcinomas compared to paired healthy parenchyma, suggesting a likely enhanced activity of the p38 MAPK cascade in lung tumors **(FIGURE 16A)**. The upregulation correlates with the tumor stage **(FIGURE 17)** and is independent of the driver mutation **(FIGURE 16B)**. Altogether it is likely that p38α is not a downstream target activated by K-Ras signaling but an orthogonal collaborator, i.e. a common pathway activated upon the oncogenic stress induced in lung cancer cells, and therefore applicable to many subtypes of adenocarcinoma. Moreover, adjusting the data to the different tumor stages, we observed that the overall and the relapse-free survival over time are statistically increased in patients with low levels of these mRNAs **(FIGURE 19)**. Therefore, we conclude that the mRNA levels of p38α pathway components may have prognostic value in lung adenocarcinoma patients. Accordingly, p38 MAPK phosphorylation levels were found increased in mouse K-Ras$^{G12V}$-driven lung tumors **(FIGURE 15 and** *(Brichkina et al. 2016b)***)**, and human NSCLC tumors *(Greenberg et al. 2002)*, especially in those of never smokers *(Mountzios et al. 2008)*.

However, it must be taken into account that the correlation between mRNA expression levels and survival in lung adenocarcinoma did not apply to squamous cell carcinoma **(FIGURE 20)**. In fact, poorly phosphorylated p38 MAPK has been reported in advanced squamous cell carcinoma, and its downregulation in cells of lung squamous cell carcinomas promotes the S phase to G2 phase transition *(Nan et al. 2017)*. Hence, it will be important to determine which lung cancer types can use p38α mRNA levels as a prognostic factor and benefit from p38α inhibition.

## Final remarks and future perspectives

Our results show that p38α signaling can exert opposite functions in lung tumorigenesis depending on the cell transformation stage. On one hand, p38α contributes to the homeostasis of lung progenitor cells interfering with oncogene-induced malignant transformation. On the other hand, it contributes to lung tumor progression by favoring vascularization and the establishment of a cytokine network. We also show that p38α does not influence the early events of the metastatic process, but rather supports progression of lung cancer cells once they have metastasized the lung. Therefore, targeting this pathway alone or in combination with chemotherapy may provide novel opportunities for the treatment of lung adenocarcinomas.

It would be interesting to check whether other K-Ras-driven tumors, such as pancreatic ductal adenocarcinomas, depend on p38α signaling for their progression using GEMM. As well, although our understanding of the *in vivo* roles of p38α signaling in tumors has considerably improved, more mechanistic studies, including the use of high-throughput screening technologies are required to identify key regulators of p38α and the targets that exert its tumor-promoting functions. This information will be fundamental for the design of more efficient therapeutic strategies with reduced secondary effects to be ultimately used in the clinics.

# *Conclusions*

p38α signaling in lung epithelial cells maintains lung homeostasis and negatively regulates lung tumor initiation.

Enhanced mRNA expression levels of the MKK6, p38α and MK2 correlate with advanced tumoral stages, reduced survival, and increased relapse incidence in lung adenocarcinoma patients.

Systemic downregulation or inhibition of p38α reduces K-Ras$^{G12V}$–driven lung tumorigenesis and the formation of tumor-associated vasculature.

K-Ras$^{G12V}$-driven lung tumors depend on p38α signaling in epithelial and myeloid cells to progress into advanced stages.

p38α signaling controls cytokine secretion by lung cancer epithelial cells, promotes their growth in anchorage-independent culture conditions, and facilitates growth of metastatic *foci*.

# *Bibliography*

Adams RH, Porras A, Alonso G, Jones M, Vintersten K, Panelli S, Valladares A, Perez L, Klein R, Nebreda AR. 2000. Essential role of p38alpha MAP kinase in placental but not embryonic cardiovascular development. Molecular cell 6: 109-116.

Aguirre-Ghiso JA, Liu D, Mignatti A, Kovalski K, Ossowski L. 2001. Urokinase receptor and fibronectin regulate the ERK(MAPK) to p38(MAPK) activity ratios that determine carcinoma cell proliferation or dormancy in vivo. Molecular biology of the cell 12: 863-879.

Alam MS, Gaida MM, Bergmann F, Lasitschka F, Giese T, Giese NA, Hackert T, Hinz U, Hussain SP, Kozlov SV et al. 2015. Selective inhibition of the p38 alternative activation pathway in infiltrating T cells inhibits pancreatic cancer progression. Nature medicine 21: 1337-1343.

Allen M, Svensson L, Roach M, Hambor J, McNeish J, Gabel CA. 2000. Deficiency of the stress kinase p38alpha results in embryonic lethality: characterization of the kinase dependence of stress responses of enzyme-deficient embryonic stem cells. The Journal of experimental medicine 191: 859-870.

Alspach E, Flanagan KC, Luo X, Ruhland MK, Huang H, Pazolli E, Donlin MJ, Marsh T, Piwnica-Worms D, Monahan J et al. 2014. p38MAPK plays a crucial role in stromal-mediated tumorigenesis. Cancer discovery 4: 716-729.

Ambrogio C, Carmona FJ, Vidal A, Falcone M, Nieto P, Romero OA, Puertas S, Vizoso M, Nadal E, Poggio T et al. 2014. Modeling lung cancer evolution and preclinical response by orthotopic mouse allografts. Cancer research 74: 5978-5988.

Aouadi M, Bost F, Caron L, Laurent K, Le Marchand Brustel Y, Binetruy B. 2006. p38 mitogen-activated protein kinase activity commits embryonic stem cells to either neurogenesis or cardiomyogenesis. Stem Cells 24: 1399-1406.

Balkwill F, Mantovani A. 2001. Inflammation and cancer: back to Virchow? Lancet 357: 539-545.

Barbacid M. 2012. Opening a new GATAway for treating KRAS-driven lung tumors. Cancer cell 21: 598-600.

Barbie DA, Tamayo P, Boehm JS, Kim SY, Moody SE, Dunn IF, Schinzel AC, Sandy P, Meylan E, Scholl C et al. 2009. Systematic RNA interference reveals that oncogenic KRAS-driven cancers require TBK1. Nature 462: 108-112.

Barcellos-Hoff MH, Lyden D, Wang TC. 2013. The evolution of the cancer niche during multistage carcinogenesis. Nature reviews Cancer 13: 511-518.

Barrett JC. 1993. Mechanisms of multistep carcinogenesis and carcinogen risk assessment. Environmental health perspectives 100: 9-20.

Basseres DS, Ebbs A, Levantini E, Baldwin AS. 2010. Requirement of the NF-kappaB subunit p65/RelA for K-Ras-induced lung tumorigenesis. Cancer research 70:

3537-3546.

Basseres DS, Levantini E, Ji H, Monti S, Elf S, Dayaram T, Fenyus M, Kocher O, Golub T, Wong KK et al. 2006. Respiratory failure due to differentiation arrest and expansion of alveolar cells following lung-specific loss of the transcription factor C/EBPalpha in mice. Molecular and cellular biology 26: 1109-1123.

Beardmore VA, Hinton HJ, Eftychi C, Apostolaki M, Armaka M, Darragh J, McIlrath J, Carr JM, Armit LJ, Clacher C et al. 2005. Generation and characterization of p38beta (MAPK11) gene-targeted mice. Molecular and cellular biology 25: 10454-10464.

Bhowmick NA, Zent R, Ghiassi M, McDonnell M, Moses HL. 2001. Integrin beta 1 signaling is necessary for transforming growth factor-beta activation of p38MAPK and epithelial plasticity. The Journal of biological chemistry 276: 46707-46713.

Blasco RB, Francoz S, Santamaria D, Canamero M, Dubus P, Charron J, Baccarini M, Barbacid M. 2011. c-Raf, but not B-Raf, is essential for development of K-Ras oncogene-driven non-small cell lung carcinoma. Cancer cell 19: 652-663.

Bode AM, Dong Z. 2009. Cancer prevention research - then and now. Nature reviews Cancer 9: 508-516.

Bondar T, Medzhitov R. 2013. The origins of tumor-promoting inflammation. Cancer cell 24: 143-144.

Boulton TG, Cobb MH. 1991. Identification of multiple extracellular signal-regulated kinases (ERKs) with antipeptide antibodies. Cell regulation 2: 357-371.

Boveri T. 2008. Concerning the origin of malignant tumours by Theodor Boveri. Translated and annotated by Henry Harris. Journal of cell science 121 Suppl 1: 1-84.

Brabletz T. 2012. To differentiate or not -- routes towards metastasis. Nature reviews Cancer 12: 425-436.

Brambilia E, Travis WD. 2014. Lung cancer. in World Cancer Report 2014 (eds. BW Stewart, CP Wild), pp. 350-361. International Agency for Research on Cancer, Lyon.

Brancho D, Tanaka N, Jaeschke A, Ventura JJ, Kelkar N, Tanaka Y, Kyuuma M, Takeshita T, Flavell RA, Davis RJ. 2003. Mechanism of p38 MAP kinase activation in vivo. Genes & development 17: 1969-1978.

Brichkina A, Bertero T, Loh HM, Nguyen NT, Emelyanov A, Rigade S, Ilie M, Hofman P, Gaggioli C, Bulavin DV. 2016a. p38MAPK builds a hyaluronan cancer niche to drive lung tumorigenesis. Genes & development 30: 2623-2636.

Brichkina A, Bulavin DV. 2017. Cancer suppression by systemic inactivation of p38MAPK. Oncotarget 8: 14275-14276.

Brichkina A, Nguyen NT, Baskar R, Wee S, Gunaratne J, Robinson RC, Bulavin DV. 2016b. Proline isomerisation as a novel regulatory mechanism for p38MAPK activation and functions. Cell death and differentiation 23: 1592-1601.

Bulavin DV, Demidov ON, Saito S, Kauraniemi P, Phillips C, Amundson SA, Ambrosino C, Sauter G, Nebreda AR, Anderson CW et al. 2002. Amplification of PPM1D in human tumors abrogates p53 tumor-suppressor activity. Nature genetics 31: 210-215.

Bulavin DV, Fornace AJ, Jr. 2004. p38 MAP kinase's emerging role as a tumor suppressor. Advances in cancer research 92: 95-118.

Bulavin DV, Higashimoto Y, Popoff IJ, Gaarde WA, Basrur V, Potapova O, Appella E, Fornace AJ, Jr. 2001. Initiation of a G2/M checkpoint after ultraviolet radiation requires p38 kinase. Nature 411: 102-107.

Bulavin DV, Phillips C, Nannenga B, Timofeev O, Donehower LA, Anderson CW, Appella E, Fornace AJ, Jr. 2004. Inactivation of the Wip1 phosphatase inhibits mammary tumorigenesis through p38 MAPK-mediated activation of the p16(Ink4a)-p19(Arf) pathway. Nature genetics 36: 343-350.

Caetano MS, Zhang H, Cumpian AM, Gong L, Unver N, Ostrin EJ, Daliri S, Chang SH, Ochoa CE, Hanash S et al. 2016. IL6 Blockade Reprograms the Lung Tumor Microenvironment to Limit the Development and Progression of K-ras-Mutant Lung Cancer. Cancer research 76: 3189-3199.

Campbell JD, Alexandrov A, Kim J, Wala J, Berger AH, Pedamallu CS, Shukla SA, Guo G, Brooks AN, Murray BA et al. 2016. Distinct patterns of somatic genome alterations in lung adenocarcinomas and squamous cell carcinomas. Nature genetics 48: 607-616.

Cappellini A, Tazzari PL, Mantovani I, Billi AM, Tassi C, Ricci F, Conte R, Martelli AM. 2005. Antiapoptotic role of p38 mitogen activated protein kinase in Jurkat T cells and normal human T lymphocytes treated with 8-methoxypsoralen and ultraviolet-A radiation. Apoptosis : an international journal on programmed cell death 10: 141-152.

Chaube B, Malvi P, Singh SV, Mohammad N, Viollet B, Bhat MK. 2015. AMPK maintains energy homeostasis and survival in cancer cells via regulating p38/PGC-1alpha-mediated mitochondrial biogenesis. Cell death discovery 1: 15063.

Chen B, Johanson L, Wiest JS, Anderson MW, You M. 1994. The second intron of the K-ras gene contains regulatory elements associated with mouse lung tumor susceptibility. Proceedings of the National Academy of Sciences of the United States of America 91: 1589-1593.

Chen C, Chen YH, Lin WW. 1999. Involvement of p38 mitogen-activated protein kinase in lipopolysaccharide-induced iNOS and COX-2 expression in J774 macrophages.

Immunology 97: 124-129.

Chen G, Hitomi M, Han J, Stacey DW. 2000. The p38 pathway provides negative feedback for Ras proliferative signaling. The Journal of biological chemistry 275: 38973-38980.

Chen Z, Cheng K, Walton Z, Wang Y, Ebi H, Shimamura T, Liu Y, Tupper T, Ouyang J, Li J et al. 2012. A murine lung cancer co-clinical trial identifies genetic modifiers of therapeutic response. Nature 483: 613-617.

Chen Z, Fillmore CM, Hammerman PS, Kim CF, Wong KK. 2014. Non-small-cell lung cancers: a heterogeneous set of diseases. Nature reviews Cancer 14: 535-546.

Chen Z, Sasaki T, Tan X, Carretero J, Shimamura T, Li D, Xu C, Wang Y, Adelmant GO, Capelletti M et al. 2010. Inhibition of ALK, PI3K/MEK, and HSP90 in murine lung adenocarcinoma induced by EML4-ALK fusion oncogene. Cancer research 70: 9827-9836.

Cheung PC, Campbell DG, Nebreda AR, Cohen P. 2003. Feedback control of the protein kinase TAK1 by SAPK2a/p38alpha. The EMBO journal 22: 5793-5805.

Cheung WK, Nguyen DX. 2015. Lineage factors and differentiation states in lung cancer progression. Oncogene 34: 5771-5780.

Chiacchiera F, Grossi V, Cappellari M, Peserico A, Simonatto M, Germani A, Russo S, Moyer MP, Resta N, Murzilli S et al. 2012. Blocking p38/ERK crosstalk affects colorectal cancer growth by inducing apoptosis in vitro and in preclinical mouse models. Cancer letters 324: 98-108.

Chiacchiera F, Matrone A, Ferrari E, Ingravallo G, Lo Sasso G, Murzilli S, Petruzzelli M, Salvatore L, Moschetta A, Simone C. 2009. p38alpha blockade inhibits colorectal cancer growth in vivo by inducing a switch from HIF1alpha- to FoxO-dependent transcription. Cell death and differentiation 16: 1203-1214.

Choi H, Sheng J, Gao D, Li F, Durrans A, Ryu S, Lee SB, Narula N, Rafii S, Elemento O et al. 2015. Transcriptome analysis of individual stromal cell populations identifies stroma-tumor crosstalk in mouse lung cancer model. Cell reports 10: 1187-1201.

Clausen BE, Burkhardt C, Reith W, Renkawitz R, Forster I. 1999. Conditional gene targeting in macrophages and granulocytes using LysMcre mice. Transgenic research 8: 265-277.

Collado M, Gil J, Efeyan A, Guerra C, Schuhmacher AJ, Barradas M, Benguria A, Zaballos A, Flores JM, Barbacid M et al. 2005. Tumour biology: senescence in premalignant tumours. Nature 436: 642.

Cosaceanu D, Budiu RA, Carapancea M, Castro J, Lewensohn R, Dricu A. 2007. Ionizing radiation activates IGF-1R triggering a cytoprotective signaling by interfering with Ku-DNA binding and by modulating Ku86 expression via a p38 kinase-

dependent mechanism. Oncogene 26: 2423-2434.

Coulombe P, Meloche S. 2007. Atypical mitogen-activated protein kinases: structure, regulation and functions. Biochimica et biophysica acta 1773: 1376-1387.

Coulthard LR, White DE, Jones DL, McDermott MF, Burchill SA. 2009. p38(MAPK): stress responses from molecular mechanisms to therapeutics. Trends in molecular medicine 15: 369-379.

Coussens LM, Werb Z. 2002. Inflammation and cancer. Nature 420: 860-867.

Cuadrado A, Lafarga V, Cheung PC, Dolado I, Llanos S, Cohen P, Nebreda AR. 2007. A new p38 MAP kinase-regulated transcriptional coactivator that stimulates p53-dependent apoptosis. The EMBO journal 26: 2115-2126.

Cuadrado A, Nebreda AR. 2010. Mechanisms and functions of p38 MAPK signalling. The Biochemical journal 429: 403-417.

Cuenda A, Rousseau S. 2007. p38 MAP-kinases pathway regulation, function and role in human diseases. Biochimica et biophysica acta 1773: 1358-1375.

Cuevas BD, Abell AN, Johnson GL. 2007. Role of mitogen-activated protein kinase kinase kinases in signal integration. Oncogene 26: 3159-3171.

Davies KD, Le AT, Theodoro MF, Skokan MC, Aisner DL, Berge EM, Terracciano LM, Cappuzzo F, Incarbone M, Roncalli M et al. 2012. Identifying and targeting ROS1 gene fusions in non-small cell lung cancer. Clinical cancer research : an official journal of the American Association for Cancer Research 18: 4570-4579.

De Chiara G, Marcocci ME, Torcia M, Lucibello M, Rosini P, Bonini P, Higashimoto Y, Damonte G, Armirotti A, Amodei S et al. 2006. Bcl-2 Phosphorylation by p38 MAPK: identification of target sites and biologic consequences. The Journal of biological chemistry 281: 21353-21361.

de Nadal E, Posas F. 2010. Multilayered control of gene expression by stress-activated protein kinases. The EMBO journal 29: 4-13.

del Barco Barrantes I, Coya JM, Maina F, Arthur JS, Nebreda AR. 2011. Genetic analysis of specific and redundant roles for p38alpha and p38beta MAPKs during mouse development. Proceedings of the National Academy of Sciences of the United States of America 108: 12764-12769.

del Barco Barrantes I, Nebreda AR. 2012. Roles of p38 MAPKs in invasion and metastasis. Biochemical Society transactions 40: 79-84.

Derijard B, Hibi M, Wu IH, Barrett T, Su B, Deng T, Karin M, Davis RJ. 1994. JNK1: a protein kinase stimulated by UV light and Ha-Ras that binds and phosphorylates the c-Jun activation domain. Cell 76: 1025-1037.

Desai S, Laskar S, Pandey BN. 2013. Autocrine IL-8 and VEGF mediate epithelial-mesenchymal transition and invasiveness via p38/JNK-ATF-2 signalling in A549

lung cancer cells. Cellular signalling 25: 1780-1791.

Desideri E, Vegliante R, Cardaci S, Nepravishta R, Paci M, Ciriolo MR. 2014. MAPK14/p38alpha-dependent modulation of glucose metabolism affects ROS levels and autophagy during starvation. Autophagy 10: 1652-1665.

Dhillon AS, Hagan S, Rath O, Kolch W. 2007. MAP kinase signalling pathways in cancer. Oncogene 26: 3279-3290.

Dickinson SE, Olson ER, Zhang J, Cooper SJ, Melton T, Criswell PJ, Casanova A, Dong Z, Hu C, Saboda K et al. 2011. p38 MAP kinase plays a functional role in UVB-induced mouse skin carcinogenesis. Molecular carcinogenesis 50: 469-478.

Dolado I, Nebreda AR. 2008. Regulation of tumorigenesis by p38αMAP kinase. in Stress-Activated Protein Kinases (eds. F Posas, AR Nebreda), pp. 99-128. Springer, Berlin Heidelberg.

Dolado I, Swat A, Ajenjo N, De Vita G, Cuadrado A, Nebreda AR. 2007. p38alpha MAP kinase as a sensor of reactive oxygen species in tumorigenesis. Cancer cell 11: 191-205.

Doll R, Hill AB. 1956. Lung cancer and other causes of death in relation to smoking; a second report on the mortality of British doctors. British medical journal 2: 1071-1081.

Doll SR. 2000. Smoking and lung cancer. American journal of respiratory and critical care medicine 162: 4-6.

Doroshow JH, Kummar S. 2014. Translational research in oncology--10 years of progress and future prospects. Nature reviews Clinical oncology 11: 649-662.

Dosaka-Akita H, Hu SX, Fujino M, Harada M, Kinoshita I, Xu HJ, Kuzumaki N, Kawakami Y, Benedict WF. 1997. Altered retinoblastoma protein expression in nonsmall cell lung cancer: its synergistic effects with altered ras and p53 protein status on prognosis. Cancer 79: 1329-1337.

Dreissigacker U, Mueller MS, Unger M, Siegert P, Genze F, Gierschik P, Giehl K. 2006. Oncogenic K-Ras down-regulates Rac1 and RhoA activity and enhances migration and invasion of pancreatic carcinoma cells through activation of p38. Cellular signalling 18: 1156-1168.

Elenitoba-Johnson KS, Jenson SD, Abbott RT, Palais RA, Bohling SD, Lin Z, Tripp S, Shami PJ, Wang LY, Coupland RW et al. 2003. Involvement of multiple signaling pathways in follicular lymphoma transformation: p38-mitogen-activated protein kinase as a target for therapy. Proceedings of the National Academy of Sciences of the United States of America 100: 7259-7264.

Emerling BM, Platanias LC, Black E, Nebreda AR, Davis RJ, Chandel NS. 2005. Mitochondrial reactive oxygen species activation of p38 mitogen-activated protein

kinase is required for hypoxia signaling. Molecular and cellular biology 25: 4853-4862.

Engelman JA, Chen L, Tan X, Crosby K, Guimaraes AR, Upadhyay R, Maira M, McNamara K, Perera SA, Song Y et al. 2008. Effective use of PI3K and MEK inhibitors to treat mutant Kras G12D and PIK3CA H1047R murine lung cancers. Nature medicine 14: 1351-1356.

Engelman JA, Zejnullahu K, Mitsudomi T, Song Y, Hyland C, Park JO, Lindeman N, Gale CM, Zhao X, Christensen J et al. 2007. MET amplification leads to gefitinib resistance in lung cancer by activating ERBB3 signaling. Science 316: 1039-1043.

Enslen H, Raingeaud J, Davis RJ. 1998. Selective activation of p38 mitogen-activated protein (MAP) kinase isoforms by the MAP kinase kinases MKK3 and MKK6. The Journal of biological chemistry 273: 1741-1748.

Erez N, Truitt M, Olson P, Arron ST, Hanahan D. 2010. Cancer-Associated Fibroblasts Are Activated in Incipient Neoplasia to Orchestrate Tumor-Promoting Inflammation in an NF-kappaB-Dependent Manner. Cancer cell 17: 135-147.

Esteva FJ, Sahin AA, Smith TL, Yang Y, Pusztai L, Nahta R, Buchholz TA, Buzdar AU, Hortobagyi GN, Bacus SS. 2004. Prognostic significance of phosphorylated P38 mitogen-activated protein kinase and HER-2 expression in lymph node-positive breast carcinoma. Cancer 100: 499-506.

Faccio L, Chen A, Fusco C, Martinotti S, Bonventre JV, Zervos AS. 2000. Mxi2, a splice variant of p38 stress-activated kinase, is a distal nephron protein regulated with kidney ischemia. American journal of physiology Cell physiology 278: C781-790.

Faust D, Dolado I, Cuadrado A, Oesch F, Weiss C, Nebreda AR, Dietrich C. 2005. p38alpha MAPK is required for contact inhibition. Oncogene 24: 7941-7945.

Faust D, Schmitt C, Oesch F, Oesch-Bartlomowicz B, Schreck I, Weiss C, Dietrich C. 2012. Differential p38-dependent signalling in response to cellular stress and mitogenic stimulation in fibroblasts. Cell communication and signaling : CCS 10: 6.

Fong KM, Sekido Y, Gazdar AF, Minna JD. 2003. Lung cancer. 9: Molecular biology of lung cancer: clinical implications. Thorax 58: 892-900.

Freshney NW, Rawlinson L, Guesdon F, Jones E, Cowley S, Hsuan J, Saklatvala J. 1994. Interleukin-1 activates a novel protein kinase cascade that results in the phosphorylation of Hsp27. Cell 78: 1039-1049.

Freund A, Patil CK, Campisi J. 2011. p38MAPK is a novel DNA damage response-independent regulator of the senescence-associated secretory phenotype. The EMBO journal 30: 1536-1548.

Gao N, Jiang BH, Leonard SS, Corum L, Zhang Z, Roberts JR, Antonini J, Zheng JZ, Flynn DC, Castranova V et al. 2002. p38 Signaling-mediated hypoxia-inducible

factor 1alpha and vascular endothelial growth factor induction by Cr(VI) in DU145 human prostate carcinoma cells. The Journal of biological chemistry 277: 45041-45048.

Ge B, Gram H, Di Padova F, Huang B, New L, Ulevitch RJ, Luo Y, Han J. 2002. MAPKK-independent activation of p38alpha mediated by TAB1-dependent autophosphorylation of p38alpha. Science 295: 1291-1294.

Geest CR, Buitenhuis M, Laarhoven AG, Bierings MB, Bruin MC, Vellenga E, Coffer PJ. 2009. p38 MAP kinase inhibits neutrophil development through phosphorylation of C/EBPalpha on serine 21. Stem Cells 27: 2271-2282.

Goldstein DM, Kuglstatter A, Lou Y, Soth MJ. 2010. Selective p38alpha inhibitors clinically evaluated for the treatment of chronic inflammatory disorders. Journal of medicinal chemistry 53: 2345-2353.

Gonzalez-Roca E, Garcia-Albeniz X, Rodriguez-Mulero S, Gomis RR, Kornacker K, Auer H. 2010. Accurate expression profiling of very small cell populations. PloS one 5: e14418.

Graves JD, Krebs EG. 1999. Protein phosphorylation and signal transduction. Pharmacology & therapeutics 82: 111-121.

Greenberg AK, Basu S, Hu J, Yie TA, Tchou-Wong KM, Rom WN, Lee TC. 2002. Selective p38 activation in human non-small cell lung cancer. American journal of respiratory cell and molecular biology 26: 558-564.

Guay J, Lambert H, Gingras-Breton G, Lavoie JN, Huot J, Landry J. 1997. Regulation of actin filament dynamics by p38 map kinase-mediated phosphorylation of heat shock protein 27. Journal of cell science 110 ( Pt 3): 357-368.

Gubern A, Joaquin M, Marques M, Maseres P, Garcia-Garcia J, Amat R, Gonzalez-Nunez D, Oliva B, Real FX, de Nadal E et al. 2016. The N-Terminal Phosphorylation of RB by p38 Bypasses Its Inactivation by CDKs and Prevents Proliferation in Cancer Cells. Molecular cell 64: 25-36.

Guerra C, Mijimolle N, Dhawahir A, Dubus P, Barradas M, Serrano M, Campuzano V, Barbacid M. 2003. Tumor induction by an endogenous K-ras oncogene is highly dependent on cellular context. Cancer cell 4: 111-120.

Guinot A, Oeztuerk-Winder F, Ventura JJ. 2016. miR-17-92/p38alpha Dysregulation Enhances Wnt Signaling and Selects Lgr6+ Cancer Stem-like Cells during Lung Adenocarcinoma Progression. Cancer research 76: 4012-4022.

Gupta J, del Barco Barrantes I, Igea A, Sakellariou S, Pateras IS, Gorgoulis VG, Nebreda AR. 2014. Dual function of p38alpha MAPK in colon cancer: suppression of colitis-associated tumor initiation but requirement for cancer cell survival. Cancer cell 25: 484-500.

Gupta J, Igea A, Papaioannou M, Lopez-Casas PP, Llonch E, Hidalgo M, Gorgoulis VG, Nebreda AR. 2015. Pharmacological inhibition of p38 MAPK reduces tumor growth in patient-derived xenografts from colon tumors. Oncotarget 6: 8539-8551.

Gupta S, Ramjaun AR, Haiko P, Wang Y, Warne PH, Nicke B, Nye E, Stamp G, Alitalo K, Downward J. 2007. Binding of ras to phosphoinositide 3-kinase p110alpha is required for ras-driven tumorigenesis in mice. Cell 129: 957-968.

Gutierrez-Uzquiza A, Arechederra M, Bragado P, Aguirre-Ghiso JA, Porras A. 2012. p38alpha mediates cell survival in response to oxidative stress via induction of antioxidant genes: effect on the p70S6K pathway. The Journal of biological chemistry 287: 2632-2642.

Hahn WC, Weinberg RA. 2002. Modelling the molecular circuitry of cancer. Nature reviews Cancer 2: 331-341.

Halawani D, Mondeh R, Stanton LA, Beier F. 2004. p38 MAP kinase signaling is necessary for rat chondrosarcoma cell proliferation. Oncogene 23: 3726-3731.

Halazonetis TD, Gorgoulis VG, Bartek J. 2008. An oncogene-induced DNA damage model for cancer development. Science 319: 1352-1355.

Han J, Lee JD, Bibbs L, Ulevitch RJ. 1994. A MAP kinase targeted by endotoxin and hyperosmolarity in mammalian cells. Science 265: 808-811.

Han X, Li F, Fang Z, Gao Y, Fang R, Yao S, Sun Y, Li L, Zhang W, Ma H et al. 2014. Transdifferentiation of lung adenocarcinoma in mice with Lkb1 deficiency to squamous cell carcinoma. Nature communications 5: 3261.

Hanahan D, Coussens LM. 2012. Accessories to the crime: functions of cells recruited to the tumor microenvironment. Cancer cell 21: 309-322.

Hanahan D, Weinberg RA. 2000. The hallmarks of cancer. Cell 100: 57-70.

Hanahan D, Weinberg RA. 2011. Hallmarks of cancer: the next generation. Cell 144: 646-674.

Heinrichsdorff J, Luedde T, Perdiguero E, Nebreda AR, Pasparakis M. 2008. p38 alpha MAPK inhibits JNK activation and collaborates with IkappaB kinase 2 to prevent endotoxin-induced liver failure. EMBO reports 9: 1048-1054.

Heist RS, Engelman JA. 2012. SnapShot: non-small cell lung cancer. Cancer cell 21: 448 e442.

Hill KS, Erdogan E, Khoor A, Walsh MP, Leitges M, Murray NR, Fields AP. 2014. Protein kinase Calpha suppresses Kras-mediated lung tumor formation through activation of a p38 MAPK-TGFbeta signaling axis. Oncogene 33: 2134-2144.

Hiratsuka S, Duda DG, Huang Y, Goel S, Sugiyama T, Nagasawa T, Fukumura D, Jain RK. 2011. C-X-C receptor type 4 promotes metastasis by activating p38 mitogen-activated protein kinase in myeloid differentiation antigen (Gr-1)-positive cells.

Proceedings of the National Academy of Sciences of the United States of America 108: 302-307.

Hiratsuka S, Watanabe A, Aburatani H, Maru Y. 2006. Tumour-mediated upregulation of chemoattractants and recruitment of myeloid cells predetermines lung metastasis. Nature cell biology 8: 1369-1375.

Hirsch FR, Scagliotti GV, Mulshine JL, Kwon R, Curran WJ, Jr., Wu YL, Paz-Ares L. 2017. Lung cancer: current therapies and new targeted treatments. Lancet 389: 299-311.

Hong J, Zhou J, Fu J, He T, Qin J, Wang L, Liao L, Xu J. 2011. Phosphorylation of serine 68 of Twist1 by MAPKs stabilizes Twist1 protein and promotes breast cancer cell invasiveness. Cancer research 71: 3980-3990.

Hu M, Polyak K. 2008. Microenvironmental regulation of cancer development. Current opinion in genetics & development 18: 27-34.

Huber S, Schrader J, Fritz G, Presser K, Schmitt S, Waisman A, Luth S, Blessing M, Herkel J, Schramm C. 2008. P38 MAP kinase signaling is required for the conversion of CD4+CD25- T cells into iTreg. PloS one 3: e3302.

Hui L, Bakiri L, Mairhorfer A, Schweifer N, Haslinger C, Kenner L, Komnenovic V, Scheuch H, Beug H, Wagner EF. 2007. p38alpha suppresses normal and cancer cell proliferation by antagonizing the JNK-c-Jun pathway. Nature genetics 39: 741-749.

Huntly BJ, Gilliland DG. 2005. Leukaemia stem cells and the evolution of cancer-stem-cell research. Nature reviews Cancer 5: 311-321.

IARC Working Group on the Evaluation of Carcinogenic Risks to Humans. 2004. Tobacco smoke and involuntary smoking. IARC monographs on the evaluation of carcinogenic risks to humans 83: 1-1438.

Iwasa H, Han J, Ishikawa F. 2003. Mitogen-activated protein kinase p38 defines the common senescence-signalling pathway. Genes to cells : devoted to molecular & cellular mechanisms 8: 131-144.

Jackson EL, Olive KP, Tuveson DA, Bronson R, Crowley D, Brown M, Jacks T. 2005. The differential effects of mutant p53 alleles on advanced murine lung cancer. Cancer research 65: 10280-10288.

Jackson EL, Willis N, Mercer K, Bronson RT, Crowley D, Montoya R, Jacks T, Tuveson DA. 2001. Analysis of lung tumor initiation and progression using conditional expression of oncogenic K-ras. Genes & development 15: 3243-3248.

Ji H, Li D, Chen L, Shimamura T, Kobayashi S, McNamara K, Mahmood U, Mitchell A, Sun Y, Al-Hashem R et al. 2006. The impact of human EGFR kinase domain mutations on lung tumorigenesis and in vivo sensitivity to EGFR-targeted therapies. Cancer cell 9: 485-495.

Ji H, Ramsey MR, Hayes DN, Fan C, McNamara K, Kozlowski P, Torrice C, Wu MC, Shimamura T, Perera SA et al. 2007. LKB1 modulates lung cancer differentiation and metastasis. Nature 448: 807-810.

Johansson N, Ala-aho R, Uitto V, Grenman R, Fusenig NE, Lopez-Otin C, Kahari VM. 2000. Expression of collagenase-3 (MMP-13) and collagenase-1 (MMP-1) by transformed keratinocytes is dependent on the activity of p38 mitogen-activated protein kinase. Journal of cell science 113 Pt 2: 227-235.

Jones RG, Thompson CB. 2009. Tumor suppressors and cell metabolism: a recipe for cancer growth. Genes & development 23: 537-548.

Jonkers J, Berns A. 2002. Conditional mouse models of sporadic cancer. Nature reviews Cancer 2: 251-265.

Joyce JA, Pollard JW. 2009. Microenvironmental regulation of metastasis. Nature reviews Cancer 9: 239-252.

Juneja VR, McGuire KA, Manguso RT, LaFleur MW, Collins N, Haining WN, Freeman GJ, Sharpe AH. 2017. PD-L1 on tumor cells is sufficient f or i mmune e vasion in immunogenic tumors and inhibits CD8 T cell cytotoxicity. The Journal of experimental medicine 214: 895-904.

Kalari KR, Rossell D, Necela BM, Asmann YW, Nair A, Baheti S, Kachergus JM, Younkin CS, Baker T, Carr JM et al. 2012. Deep Sequence Analysis of Non-Small Cell Lung Cancer: Integrated Analysis of Gene Expression, Alternative Splicing, and Single Nucleotide Variations in Lung Adenocarcinomas with and without Oncogenic KRAS Mutations. Frontiers in oncology 2: 12.

Kalogeraki A, Bouros D, Zoras O, Karabekios S, Chalkiadakis G, Stathopoulos E, Siafakas N, Delides GS. 2003. E-cadherin expression on fine-needle aspiration biopsies in primary lung adenocarcinomas is related to tumor differentiation and invasion. Anticancer research 23: 3367-3371.

Kan Z, Jaiswal BS, Stinson J, Janakiraman V, Bhatt D, Stern HM, Yue P, Haverty PM, Bourgon R, Zheng J et al. 2010. Diverse somatic mutation patterns and pathway alterations in human cancers. Nature 466: 869-873.

Kaplan RN, Rafii S, Lyden D. 2006. Preparing the "soil": the premetastatic niche. Cancer research 66: 11089-11093.

Kaplan RN, Riba RD, Zacharoulis S, Bramley AH, Vincent L, Costa C, MacDonald DD, Jin DK, Shido K, Kerns SA et al. 2005. VEGFR1-positive haematopoietic bone marrow progenitors initiate the pre-metastatic niche. Nature 438: 820-827.

Karpozilos A, Pavlidis N. 2004. The treatment of cancer in Greek antiquity. Eur J Cancer 40: 2033-2040.

Kato S, Yokoyama S, Hayakawa Y, Li L, Iwakami Y, Sakurai H, Saiki I. 2016. P38

pathway as a key downstream signal of connective tissue growth factor to regulate metastatic potential in non-small-cell lung cancer. Cancer science 107: 1416-1421.

Katsumura KR, Yang C, Boyer ME, Li L, Bresnick EH. 2014. Molecular basis of crosstalk between oncogenic Ras and the master regulator of hematopoiesis GATA-2. EMBO reports 15: 938-947.

Kawano O, Sasaki H, Endo K, Suzuki E, Haneda H, Yukiue H, Kobayashi Y, Yano M, Fujii Y. 2006. PIK3CA mutation status in Japanese lung cancer patients. Lung Cancer 54: 209-215.

Keil E, Hocker R, Schuster M, Essmann F, Ueffing N, Hoffman B, Liebermann DA, Pfeffer K, Schulze-Osthoff K, Schmitz I. 2013. Phosphorylation of Atg5 by the Gadd45beta-MEKK4-p38 pathway inhibits autophagy. Cell death and differentiation 20: 321-332.

Keohavong P, DeMichele MA, Melacrinos AC, Landreneau RJ, Weyant RJ, Siegfried JM. 1996. Detection of K-ras mutations in lung carcinomas: relationship to prognosis. Clinical cancer research : an official j ournal o f t he A merican A ssociation f or Cancer Research 2: 411-418.

Kerr KM. 2001. Pulmonary preinvasive neoplasia. Journal of clinical pathology 54: 257-271.

Keshet Y, Seger R. 2010. The MAP kinase signaling cascades: a system of hundreds of components regulates a diverse array of physiological functions. Methods Mol Biol 661: 3-38.

Kessenbrock K, Plaks V, Werb Z. 2010. Matrix metalloproteinases: regulators of the tumor microenvironment. Cell 141: 52-67.

Khurana A, Nakayama K, Williams S, Davis RJ, Mustelin T, Ronai Z. 2006. Regulation of the ring finger E3 ligase Siah2 by p38 MAPK. The Journal of biological chemistry 281: 35316-35326.

Kim CF, Jackson EL, Woolfenden AE, Lawrence S, Babar I, Vogel S, Crowley D, Bronson RT, Jacks T. 2005. Identification of bronchioalveolar stem cells in normal lung and lung cancer. Cell 121: 823-835.

Kim D, Dai J, Park YH, Fai LY, Wang L, Pratheeshkumar P, Son YO, Kondo K, Xu M, Luo J et al. 2016. Activation of Epidermal Growth Factor Receptor/p38/Hypoxia-inducible Factor-1alpha Is Pivotal for Angiogenesis and Tumorigenesis of Malignantly Transformed Cells Induced by Hexavalent Chromium. The Journal of biological chemistry 291: 16271-16281.

Kim YH, Yoo KC, Cui YH, Uddin N, Lim EJ, Kim MJ, Nam SY, Kim IG, Suh Y, Lee SJ. 2014. Radiation promotes malignant progression of glioma cells through HIF-1alpha stabilization. Cancer letters 354: 132-141.

Knauf U, Tschopp C, Gram H. 2001. Negative regulation of protein translation by mitogen-activated protein kinase-interacting kinases 1 and 2. Molecular and cellular biology 21: 5500-5511.

Knebel A, Haydon CE, Morrice N, Cohen P. 2002. Stress-induced regulation of eukaryotic elongation factor 2 kinase by SB 203580-sensitive and -insensitive pathways. The Biochemical journal 367: 525-532.

Kobayashi M, Nishita M, Mishima T, Ohashi K, Mizuno K. 2006. MAPKAPK-2-mediated LIM-kinase activation is critical for VEGF-induced actin remodeling and cell migration. The EMBO journal 25: 713-726.

Kondoh K, Sunadome K, Nishida E. 2007. Notch signaling suppresses p38 MAPK activity via induction of MKP-1 in myogenesis. The Journal of biological chemistry 282: 3058-3065.

Kopper F, Bierwirth C, Schon M, Kunze M, Elvers I, Kranz D, Saini P, Menon MB, Walter D, Sorensen CS et al. 2013. Damage-induced DNA replication stalling relies on MAPK-activated protein kinase 2 activity. Proceedings of the National Academy of Sciences of the United States of America 110: 16856-16861.

Kotton DN, Morrisey EE. 2014. Lung regeneration: mechanisms, applications and emerging stem cell populations. Nature medicine 20: 822-832.

Krishna M, Narang H. 2008. The complexity of mitogen-activated protein kinases (MAPKs) made simple. Cellular and molecular life sciences : CMLS 65: 3525-3544.

Kumar MS, Hancock DC, Molina-Arcas M, Steckel M, East P, Diefenbacher M, Armenteros-Monterroso E, Lassailly F, Matthews N, Nye E et al. 2012. The GATA2 transcriptional network is requisite for RAS oncogene-driven non-small cell lung cancer. Cell 149: 642-655.

Kurosu T, Takahashi Y, Fukuda T, Koyama T, Miki T, Miura O. 2005. p38 MAP kinase plays a role in G2 checkpoint activation and inhibits apoptosis of human B cell lymphoma cells treated with etoposide. Apoptosis : an international journal on programmed cell death 10: 1111-1120.

Kwon MC, Berns A. 2013. Mouse models for lung cancer. Molecular oncology 7: 165-177.

Kyriakis JM, Avruch J. 2001. Mammalian mitogen-activated protein kinase signal transduction pathways activated by stress and inflammation. Physiological reviews 81: 807-869.

Kyriakis JM, Banerjee P, Nikolakaki E, Dai T, Rubie EA, Ahmad MF, Avruch J, Woodgett JR. 1994. The stress-activated protein kinase subfamily of c-Jun kinases. Nature 369: 156-160.

Lafarga V, Cuadrado A, Lopez de Silanes I, Bengoechea R, Fernandez-Capetillo O,

Nebreda AR. 2009. p38 Mitogen-activated protein kinase- and HuR-dependent stabilization of p21(Cip1) mRNA mediates the G(1)/S checkpoint. Molecular and cellular biology 29: 4341-4351.

Lavoie JN, L'Allemain G, Brunet A, Muller R, Pouyssegur J. 1996. Cyclin D1 expression is regulated positively by the p42/p44MAPK and negatively by the p38/HOGMAPK pathway. The Journal of biological chemistry 271: 20608-20616.

Lee JC, Laydon JT, McDonnell PC, Gallagher TF, Kumar S, Green D, McNulty D, Blumenthal MJ, Heys JR, Landvatter SW et al. 1994. A protein kinase involved in the regulation of inflammatory cytokine biosynthesis. Nature 372: 739-746.

Lee JD, Ulevitch RJ, Han J. 1995. Primary structure of BMK1: a new mammalian map kinase. Biochemical and biophysical research communications 213: 715-724.

Leelahavanichkul K, Amornphimoltham P, Molinolo AA, Basile JR, Koontongkaew S, Gutkind JS. 2014. A role for p38 MAPK in head and neck cancer cell growth and tumor-induced angiogenesis and lymphangiogenesis. Molecular oncology 8: 105-118.

Levental KR, Yu H, Kass L, Lakins JN, Egeblad M, Erler JT, Fong SF, Csiszar K, Giaccia A, Weninger W et al. 2009. Matrix crosslinking forces tumor progression by enhancing integrin signaling. Cell 139: 891-906.

Lewis JS, Vijayanathan V, Thomas TJ, Pestell RG, Albanese C, Gallo MA, Thomas T. 2005. Activation of cyclin D1 by estradiol and spermine in MCF-7 breast cancer cells: a mechanism involving the p38 MAP kinase and phosphorylation of ATF-2. Oncology research 15: 113-128.

Lewis PD, Parry JM. 2004. In silico p53 mutation hotspots in lung cancer. Carcinogenesis 25: 1099-1107.

Li J, Yang Y, Peng Y, Austin RJ, van Eyndhoven WG, Nguyen KC, Gabriele T, McCurrach ME, Marks JR, Hoey T et al. 2002. Oncogenic properties of PPM1D located within a breast cancer amplification epicenter at 17q23. Nature genetics 31: 133-134.

Li SP, Junttila MR, Han J, Kahari VM, Westermarck J. 2003. p38 Mitogen-activated protein kinase pathway suppresses cell survival by inducing dephosphorylation of mitogen-activated protein/extracellular signal-regulated kinase kinase1,2. Cancer research 63: 3473-3477.

Libermann TA, Baltimore D. 1990. Activation of interleukin-6 gene expression through the NF-kappa B transcription factor. Molecular and cellular biology 10: 2327-2334.

Liu B, Yang L, Huang B, Cheng M, Wang H, Li Y, Huang D, Zheng J, Li Q, Zhang X et al. 2012. A functional copy-number variation in MAPKAPK2 predicts risk and prognosis of lung cancer. American journal of human genetics 91: 384-390.

Liu K, Yu D, Cho YY, Bode AM, Ma W, Yao K, Li S, Li J, Bowden GT, Dong Z et al. 2013.

Sunlight UV-induced skin cancer relies upon activation of the p38alpha signaling pathway. Cancer research 73: 2181-2188.

Llopis A, Salvador N, Ercilla A, Guaita-Esteruelas S, Barrantes Idel B, Gupta J, Gaestel M, Davis RJ, Nebreda AR, Agell N. 2012. The stress-activated protein kinases p38alpha/beta and JNK1/2 cooperate with Chk1 to inhibit mitotic entry upon DNA replication arrest. Cell Cycle 11: 3627-3637.

Lou-Qian Z, Rong Y, Ming L, Xin Y, Feng J, Lin X. 2013. The prognostic value of epigenetic silencing of p16 gene in NSCLC patients: a systematic review and meta-analysis. PloS one 8: e54970.

Lu H, Ouyang W, Huang C. 2006. Inflammation, a key event in cancer development. Molecular cancer research : MCR 4: 221-233.

Lu Y, Zhang M, Wang S, Hong B, Wang Z, Li H, Zheng Y, Yang J, Davis RE, Qian J et al. 2014. p38 MAPK-inhibited dendritic cells induce superior antitumour immune responses and overcome regulatory T-cell-mediated immunosuppression. Nature communications 5: 4229.

Luo J, Emanuele MJ, Li D, Creighton CJ, Schlabach MR, Westbrook TF, Wong KK, Elledge SJ. 2009a. A genome-wide RNAi screen identifies multiple synthetic lethal interactions with the Ras oncogene. Cell 137: 835-848.

Luo J, Solimini NL, Elledge SJ. 2009b. Principles of cancer therapy: oncogene and non-oncogene addiction. Cell 136: 823-837.

MacNee W, Allan RJ, Jones I, De Salvo MC, Tan LF. 2013. Efficacy and safety of the oral p38 inhibitor PH-797804 in chronic obstructive pulmonary disease: a randomised clinical trial. Thorax 68: 738-745.

Maher P. 1999. p38 mitogen-activated protein kinase activation is required for fibroblast growth factor-2-stimulated cell proliferation but not differentiation. The Journal of biological chemistry 274: 17491-17498.

Mahtani KR, Brook M, Dean JL, Sully G, Saklatvala J, Clark AR. 2001. Mitogen-activated protein kinase p38 controls the expression and posttranslational modification of tristetraprolin, a regulator of tumor necrosis factor alpha mRNA stability. Molecular and cellular biology 21: 6461-6469.

Mainardi S, Mijimolle N, Francoz S, Vicente-Duenas C, Sanchez-Garcia I, Barbacid M. 2014. Identification of cancer initiating cells in K-Ras driven lung adenocarcinoma. Proceedings of the National Academy of Sciences of the United States of America 111: 255-260.

Malkinson AM. 2001. Primary lung tumors in mice as an aid for understanding, preventing, and treating human adenocarcinoma of the lung. Lung Cancer 32: 265-279.

Malumbres M, Barbacid M. 2003. RAS oncogenes: the first 30 years. Nature reviews Cancer 3: 459-465.

Mantovani A, Allavena P, Sica A, Balkwill F. 2008. Cancer-related inflammation. Nature 454: 436-444.

Mantovani A, Cassatella MA, Costantini C, Jaillon S. 2011. Neutrophils in the activation and regulation of innate and adaptive immunity. Nature reviews Immunology 11: 519-531.

Marks JL, Gong Y, Chitale D, Golas B, McLellan MD, Kasai Y, Ding L, Mardis ER, Wilson RK, Solit D et al. 2008. Novel MEK1 mutation identified by mutational analysis of epidermal growth factor receptor signaling pathway genes in lung adenocarcinoma. Cancer research 68: 5524-5528.

Marshall C. 1999. How do small GTPase signal transduction pathways regulate cell cycle entry? Current opinion in cell biology 11: 732-736.

Martis PC, Whitsett JA, Xu Y, Perl AK, Wan H, Ikegami M. 2006. C/EBPalpha is required for lung maturation at birth. Development 133: 1155-1164.

Mascaux C, Iannino N, Martin B, Paesmans M, Berghmans T, Dusart M, Haller A, Lothaire P, Meert AP, Noel S et al. 2005. The role of RAS oncogene in survival of patients with lung cancer: a systematic review of the literature with meta-analysis. British journal of cancer 92: 131-139.

Masiero M, Minuzzo S, Pusceddu I, Moserle L, Persano L, Agnusdei V, Tosello V, Basso G, Amadori A, Indraccolo S. 2011. Notch3-mediated regulation of MKP-1 levels promotes survival of T acute lymphoblastic leukemia cells. Leukemia 25: 588-598.

Masuya D, Huang C, Liu D, Kameyama K, Hayashi E, Yamauchi A, Kobayashi S, Haba R, Yokomise H. 2001. The intratumoral expression of vascular endothelial growth factor and interleukin-8 associated with angiogenesis in nonsmall cell lung carcinoma patients. Cancer 92: 2628-2638.

Matsumoto T, Turesson I, Book M, Gerwins P, Claesson-Welsh L. 2002. p38 MAP kinase negatively regulates endothelial cell survival, proliferation, and differentiation in FGF-2-stimulated angiogenesis. The Journal of cell biology 156: 149-160.

Matsuo Y, Amano S, Furuya M, Namiki K, Sakurai K, Nishiyama M, Sudo T, Tatsumi K, Kuriyama T, Kimura S et al. 2006. Involvement of p38alpha mitogen-activated protein kinase in lung metastasis of tumor cells. The Journal of biological chemistry 281: 36767-36775.

Meuwissen R, Linn SC, van der Valk M, Mooi WJ, Berns A. 2001. Mouse model for lung tumorigenesis through Cre/lox controlled sporadic activation of the K-Ras oncogene. Oncogene 20: 6551-6558.

Meylan E, Dooley AL, Feldser DM, Shen L, Turk E, Ouyang C, Jacks T. 2009. Requirement

for NF-kappaB signalling in a mouse model of lung adenocarcinoma. Nature 462: 104-107.

Mitsudomi T, Hamajima N, Ogawa M, Takahashi T. 2000. Prognostic significance of p53 alterations in patients with non-small cell lung cancer: a meta-analysis. Clinical cancer research: an official journal of the American Association for Cancer Research 6: 4055-4063.

Morandell S, Reinhardt HC, Cannell IG, Kim JS, Ruf DM, Mitra T, Couvillon AD, Jacks T, Yaffe MB. 2013. A reversible gene-targeting strategy identifies synthetic lethal interactions between MK2 and p53 in the DNA damage response in vivo. Cell reports 5: 868-877.

Mountzios G, Planchard D, Besse B, Validire P, Girard P, Devisme C, Dimopoulos MA, Soria JC, Fouret P. 2008. Mitogen-activated protein kinase activation in lung adenocarcinoma: a comparative study between ever smokers and never smokers. Clinical cancer research: an official journal of the American Association for Cancer Research 14: 4096-4102.

Mudgett JS, Ding J, Guh-Siesel L, Chartrain NA, Yang L, Gopal S, Shen MM. 2000. Essential role for p38alpha mitogen-activated protein kinase in placental angiogenesis. Proceedings of the National Academy of Sciences of the United States of America 97: 10454-10459.

Mukhametshina RT, Ruhs A, Singh I, Hasan D, Contreras A, Mehta A, Nikam VS, Ahlbrecht K, Carraro G, Cabrera-Fuentes HA et al. 2013. Quantitative proteome analysis of alveolar type-II cells reveals a connection of integrin receptor subunits beta 2/6 and WNT signaling. Journal of proteome research 12: 5598-5608.

Mukherjee S. 2010. The emperor of all maladies : a biography of cancer. Scribner, New York.

Muzumdar MD, Tasic B, Miyamichi K, Li L, Luo L. 2007. A global double-fluorescent Cre reporter mouse. Genesis 45: 593-605.

Nan Y, Chang R, Jiang H, Yang S, Jin F, Xie Y. 2017. Downregulation of P38 phosphorylation correlates with low-grade differentiation and proliferation of lung squamous cell carcinoma. American journal of translational research 9: 1922-1933.

Osterreicher CH, Penz-Osterreicher M, Grivennikov SI, Guma M, Koltsova EK, Datz C, Sasik R, Hardiman G, Karin M, Brenner DA. 2011. Fibroblast-specific protein 1 identifies an inflammatory subpopulation of macrophages in the liver. Proceedings of the National Academy of Sciences of the United States of America 108: 308-313.

Otsuka M, Kang YJ, Ren J, Jiang H, Wang Y, Omata M, Han J. 2010. Distinct effects of p38alpha deletion in myeloid lineage and gut epithelia in mouse models of inflammatory bowel disease. Gastroenterology 138: 1255-1265, 1265 e1251-1259.

Owens TW, Valentijn AJ, Upton JP, Keeble J, Zhang L, Lindsay J, Zouq NK, Gilmore AP. 2009. Apoptosis commitment and activation of mitochondrial Bax during anoikis is regulated by p38MAPK. Cell death and differentiation 16: 1551-1562.

Paez JG, Janne PA, Lee JC, Tracy S, Greulich H, Gabriel S, Herman P, Kaye FJ, Lindeman N, Boggon TJ et al. 2004. EGFR mutations in lung cancer: correlation with clinical response to gefitinib therapy. Science 304: 1497-1500.

Paget S. 1889. The distribution of secondary growths in cancer of the breast. The Lancet 133: 571-573.

Paik PK, Arcila ME, Fara M, Sima CS, Miller VA, Kris MG, Ladanyi M, Riely GJ. 2011. Clinical characteristics of patients with lung adenocarcinomas harboring BRAF mutations. Journal of clinical oncology : official journal of the American Society of Clinical Oncology 29: 2046-2051.

Paillas S, Causse A, Marzi L, de Medina P, Poirot M, Denis V, Vezzio-Vie N, Espert L, Arzouk H, Coquelle A et al. 2012. MAPK14/p38alpha confers irinotecan resistance to TP53-defective cells by inducing survival autophagy. Autophagy 8: 1098-1112.

Pan CQ, Sudol M, Sheetz M, Low BC. 2012. Modularity and functional plasticity of scaffold proteins as p(l)acemakers in cell signaling. Cellular signalling 24: 2143-2165.

Pao W, Miller V, Zakowski M, Doherty J, Politi K, Sarkaria I, Singh B, Heelan R, Rusch V, Fulton L et al. 2004. EGF receptor gene mutations are common in lung cancers from "never smokers" and are associated with sensitivity of tumors to gefitinib and erlotinib. Proceedings of the National Academy of Sciences of the United States of America 101: 13306-13311.

Park SA, Kim MJ, Park SY, Kim JS, Lim W, Nam JS, Yhong Sheen Y. 2015. TIMP-1 mediates TGF-beta-dependent crosstalk between hepatic stellate and cancer cells via FAK signaling. Scientific reports 5: 16492.

Pedraza-Alva G, Koulnis M, Charland C, Thornton T, Clements JL, Schlissel MS, Rincon M. 2006. Activation of p38 MAP kinase by DNA double-strand breaks in V(D)J recombination induces a G2/M cell cycle checkpoint. The EMBO journal 25: 763-773.

Peinado H, Lavotshkin S, Lyden D. 2011. The secreted factors responsible for pre-metastatic niche formation: old sayings and new thoughts. Seminars in cancer biology 21: 139-146.

Peitz M, Pfannkuche K, Rajewsky K, Edenhofer F. 2002. Ability of the hydrophobic FGF and basic TAT peptides to promote cellular uptake of recombinant Cre recombinase: a tool for efficient g enetic e ngineering o f m ammalian g enomes. Proceedings of the National Academy of Sciences of the United States of America 99: 4489-4494.

Perdiguero E, Muñoz-Cánoves P. 2008. Transcriptional regulation by the p38 MAPK signaling pathway in mammalian cells. in Stress-Activated Protein Kinases (eds. F Posas, AR Nebreda), pp. 51-79. Springer, Verlag Berlin Heidelberg.

Perdiguero E, Ruiz-Bonilla V, Serrano AL, Munoz-Canoves P. 2007. Genetic deficiency of p38alpha reveals its critical role in myoblast cell cycle exit: the p38alpha-JNK connection. Cell Cycle 6: 1298-1303.

Pereira L, Igea A, Canovas B, Dolado I, Nebreda AR. 2013. Inhibition of p38 MAPK sensitizes tumour cells to cisplatin-induced apoptosis mediated by reactive oxygen species and JNK. EMBO molecular medicine 5: 1759-1774.

Pesta M, Kulda V, Kucera R, Pesek M, Vrzalova J, Liska V, Pecen L, Treska V, Safranek J, Prazakova M et al. 2011. Prognostic significance of TIMP-1 in non-small cell lung cancer. Anticancer research 31: 4031-4038.

Pietras K, Ostman A. 2010. Hallmarks of cancer: interactions with the tumor stroma. Experimental cell research 316: 1324-1331.

Polyak K, Haviv I, Campbell IG. 2009. Co-evolution of tumor cells and their microenvironment. Trends in genetics : TIG 25: 30-38.

Porras A, Zuluaga S, Black E, Valladares A, Alvarez AM, Ambrosino C, Benito M, Nebreda AR. 2004. P38 alpha mitogen-activated protein kinase sensitizes cells to apoptosis induced by different stimuli. Molecular biology of the cell 15: 922-933.

Puri PL, Wu Z, Zhang P, Wood LD, Bhakta KS, Han J, Feramisco JR, Karin M, Wang JY. 2000. Induction of terminal differentiation by constitutive activation of p38 MAP kinase in human rhabdomyosarcoma cells. Genes & development 14: 574-584.

Puyol M, Martin A, Dubus P, Mulero F, Pizcueta P, Khan G, Guerra C, Santamaria D, Barbacid M. 2010. A synthetic lethal interaction between K-Ras oncogenes and Cdk4 unveils a therapeutic strategy for non-small cell lung carcinoma. Cancer cell 18: 63-73.

Pylayeva-Gupta Y, Grabocka E, Bar-Sagi D. 2011. RAS oncogenes: weaving a tumorigenic web. Nature reviews Cancer 11: 761-774.

Qu Z, Sun F, Zhou J, Li L, Shapiro SD, Xiao G. 2015. Interleukin-6 Prevents the Initiation but Enhances the Progression of Lung Cancer. Cancer research 75: 3209-3215.

Re FC, Manenti G, Borrello MG, Colombo MP, Fisher JH, Pierotti MA, Della Porta G, Dragani TA. 1992. Multiple molecular alterations in mouse lung tumors. Molecular carcinogenesis 5: 155-160.

Recio JA, Merlino G. 2002. Hepatocyte growth factor/scatter factor activates proliferation in melanoma cells through p38 MAPK, ATF-2 and cyclin D1. Oncogene 21: 1000-1008.

Reissmann PT, Koga H, Takahashi R, Figlin RA, Holmes EC, Piantadosi S, Cordon-

Cardo C, Slamon DJ. 1993. Inactivation of the retinoblastoma susceptibility gene in non-small-cell lung cancer. The Lung Cancer Study Group. Oncogene 8: 1913-1919.

Remy G, Risco AM, Inesta-Vaquera FA, Gonzalez-Teran B, Sabio G, Davis RJ, Cuenda A. 2010. Differential activation of p38MAPK isoforms by MKK6 and MKK3. Cellular signalling 22: 660-667.

Reunanen N, Li SP, Ahonen M, Foschi M, Han J, Kahari VM. 2002. Activation of p38 alpha MAPK enhances collagenase-1 (matrix metalloproteinase (MMP)-1) and stromelysin-1 (MMP-3) expression by mRNA stabilization. The Journal of biological chemistry 277: 32360-32368.

Reynolds CH, Betts JC, Blackstock WP, Nebreda AR, Anderton BH. 2000. Phosphorylation sites on tau identified by nanoelectrospray mass spectrometry: differences in vitro between the mitogen-activated protein kinases ERK2, c-Jun N-terminal kinase and P38, and glycogen synthase kinase-3beta. Journal of neurochemistry 74: 1587-1595.

Rikova K, Guo A, Zeng Q, Possemato A, Yu J, Haack H, Nardone J, Lee K, Reeves C, Li Y et al. 2007. Global survey of phosphotyrosine signaling identifies oncogenic kinases in lung cancer. Cell 131: 1190-1203.

Rock JR, Hogan BL. 2011. Epithelial progenitor cells in lung development, maintenance, repair, and disease. Annual review of cell and developmental biology 27: 493-512.

Rodenhuis S, Slebos RJ. 1992. Clinical significance of ras oncogene activation in human lung cancer. Cancer research 52: 2665s-2669s.

Rosen K, Shi W, Calabretta B, Filmus J. 2002. Cell detachment triggers p38 mitogen-activated protein kinase-dependent overexpression of Fas ligand. A novel mechanism of Anoikis of intestinal epithelial cells. The Journal of biological chemistry 277: 46123-46130.

Rouse J, Cohen P, Trigon S, Morange M, Alonso-Llamazares A, Zamanillo D, Hunt T, Nebreda AR. 1994. A novel kinase cascade triggered by stress and heat shock that stimulates MAPKAP kinase-2 and phosphorylation of the small heat shock proteins. Cell 78: 1027-1037.

Rousseau S, Dolado I, Beardmore V, Shpiro N, Marquez R, Nebreda AR, Arthur JS, Case LM, Tessier-Lavigne M, Gaestel M et al. 2006. CXCL12 and C5a trigger cell migration via a PAK1/2-p38alpha MAPK-MAPKAP-K2-HSP27 pathway. Cellular signalling 18: 1897-1905.

Roux PP, Blenis J. 2004. ERK and p38 MAPK-activated protein kinases: a family of protein kinases with diverse biological functions. Microbiology and molecular biology reviews : MMBR 68: 320-344.

Rudalska R, Dauch D, Longerich T, McJunkin K, Wuestefeld T, Kang TW, Hohmeyer

A, Pesic M, Leibold J, von Thun A et al. 2014. In vivo RNAi screening identifies a mechanism of sorafenib resistance in liver cancer. Nature medicine 20: 1138-1146.

Ruiz-Bonilla V, Perdiguero E, Gresh L, Serrano AL, Zamora M, Sousa-Victor P, Jardi M, Wagner EF, Munoz-Canoves P. 2008. Efficient adult skeletal muscle regeneration in mice deficient in p38beta, p38gamma and p38delta MAP kinases. Cell Cycle 7: 2208-2214.

Ruiz EJ, Oeztuerk-Winder F, Ventura JJ. 2014. A paracrine network regulates the cross-talk between human lung stem cells and the stroma. Nature communications 5: 3175.

Saba-El-Leil MK, Fremin C, Meloche S. 2016. Redundancy in the World of MAP Kinases: All for One. Frontiers in cell and developmental biology 4: 67.

Saccani S, Pantano S, Natoli G. 2002. p38-Dependent marking of inflammatory genes for increased NF-kappa B recruitment. Nature immunology 3: 69-75.

Saklatvala J. 2004. The p38 MAP kinase pathway as a therapeutic target in inflammatory disease. Current opinion in pharmacology 4: 372-377.

Sakurai T, He G, Matsuzawa A, Yu GY, Maeda S, Hardiman G, Karin M. 2008. Hepatocyte necrosis induced by oxidative stress and IL-1 alpha release mediate carcinogen-induced compensatory proliferation and liver tumorigenesis. Cancer cell 14: 156-165.

Sanchez-Cespedes M, Parrella P, Esteller M, Nomoto S, Trink B, Engles JM, Westra WH, Herman JG, Sidransky D. 2002. Inactivation of LKB1/STK11 is a common event in adenocarcinomas of the lung. Cancer research 62: 3659-3662.

Sanchez-Prieto R, Rojas JM, Taya Y, Gutkind JS. 2000. A role for the p38 mitogen-acitvated protein kinase pathway in the transcriptional activation of p53 on genotoxic stress by chemotherapeutic agents. Cancer research 60: 2464-2472.

Schuster DP, Brody SL, Zhou Z, Bernstein M, Arch R, Link D, Mueckler M. 2007. Regulation of lipopolysaccharide-induced increases in neutrophil glucose uptake. American journal of physiology Lung cellular and molecular physiology 292: L845-851.

Shi Y, Gaestel M. 2002. In the cellular garden of forking paths: how p38 MAPKs signal for downstream assistance. Biological chemistry 383: 1519-1536.

Shimkin MB, Stoner GD. 1975. Lung tumors in mice: application to carcinogenesis bioassay. Advances in cancer research 21: 1-58.

Slebos RJ, Kibbelaar RE, Dalesio O, Kooistra A, Stam J, Meijer CJ, Wagenaar SS, Vanderschueren RG, van Zandwijk N, Mooi WJ et al. 1990. K-ras oncogene activation as a prognostic marker in adenocarcinoma of the lung. The New England journal of medicine 323: 561-565.

Soda M, Choi YL, Enomoto M, Takada S, Yamashita Y, Ishikawa S, Fujiwara S, Watanabe H, Kurashina K, Hatanaka H et al. 2007. Identification of the transforming EML4-ALK fusion gene in non-small-cell lung cancer. Nature 448: 561-566.

Soeda A, Lathia J, Williams BJ, Wu Q, Gallagher J, Androutsellis-Theotokis A, Giles AJ, Yang C, Zhuang Z, Gilbert MR et al. 2017. The p38 signaling pathway mediates quiescence of glioma stem cells by regulating epidermal growth factor receptor trafficking. Oncotarget 8: 33316-33328.

Soloaga A, Thomson S, Wiggin GR, Rampersaud N, Dyson MH, Hazzalin CA, Mahadevan LC, Arthur JS. 2003. MSK2 and MSK1 mediate the mitogen- and stress-induced phosphorylation of histone H3 and HMG-14. The EMBO journal 22: 2788-2797.

Soucek L, Whitfield J, Martins CP, Finch AJ, Murphy DJ, Sodir NM, Karnezis AN, Swigart LB, Nasi S, Evan GI. 2008. Modelling Myc inhibition as a cancer therapy. Nature 455: 679-683.

Srinivasa SP, Doshi PD. 2002. Extracellular signal-regulated kinase and p38 mitogen-activated protein kinase pathways cooperate in mediating cytokine-induced proliferation of a leukemic cell line. Leukemia 16: 244-253.

Stalheim L, Johnson G. 2008. MAPK Kinase Kinase Regulation of SAPK/JNK Pathways. in Stress-Activated Protein Kinases (eds. F Posas, AR Nebreda), pp. 1-15. Springer, Berlin Heidelberg.

Stephens P, Hunter C, Bignell G, Edkins S, Davies H, Teague J, Stevens C, O'Meara S, Smith R, Parker A et al. 2004. Lung cancer: intragenic ERBB2 kinase mutations in tumours. Nature 431: 525-526.

Stokoe D, Engel K, Campbell DG, Cohen P, Gaestel M. 1992. Identification of MAPKAP kinase 2 as a major enzyme responsible for the phosphorylation of the small mammalian heat shock proteins. FEBS letters 313: 307-313.

Sui X, Kong N, Ye L, Han W, Zhou J, Zhang Q, He C, Pan H. 2014. p38 and JNK MAPK pathways control the balance of apoptosis and autophagy in response to chemotherapeutic agents. Cancer letters 344: 174-179.

Sun H, Xu B, Inoue H, Chen QM. 2008. P38 MAPK mediates COX-2 gene expression by corticosterone in cardiomyocytes. Cellular signalling 20: 1952-1959.

Sun P, Yoshizuka N, New L, Moser BA, Li Y, Liao R, Xie C, Chen J, Deng Q, Yamout M et al. 2007. PRAK is essential for ras-induced senescence and tumor suppression. Cell 128: 295-308.

Sutherland KD, Song JY, Kwon MC, Proost N, Zevenhoven J, Berns A. 2014. Multiple cells-of-origin of mutant K-Ras-induced mouse lung adenocarcinoma. Proceedings of the National Academy of Sciences of the United States of America 111: 4952-4957.

Swat A, Dolado I, Rojas JM, Nebreda AR. 2009. Cell density-dependent inhibition of epidermal growth factor receptor signaling by p38alpha mitogen-activated protein kinase via Sprouty2 downregulation. Molecular and cellular biology 29: 3332-3343.

Tamura K, Sudo T, Senftleben U, Dadak AM, Johnson R, Karin M. 2000. Requirement for p38alpha in erythropoietin expression: a role for stress kinases in erythropoiesis. Cell 102: 221-231.

Tan W, Yu HG, Luo HS. 2014. Inhibition of the p38 MAPK pathway sensitizes human gastric cells to doxorubicin treatment in vitro and in vivo. Molecular medicine reports 10: 3275-3281.

Tanno M, Bassi R, Gorog DA, Saurin AT, Jiang J, Heads RJ, Martin JL, Davis RJ, Flavell RA, Marber MS. 2003. Diverse mechanisms of myocardial p38 mitogen-activated protein kinase activation: evidence for MKK-independent activation by a TAB1-associated mechanism contributing to injury during myocardial ischemia. Circulation research 93: 254-261.

Thompson SL, Compton DA. 2010. Proliferation of aneuploid human cells is limited by a p53-dependent mechanism. The Journal of cell biology 188: 369-381.

Thornton TM, Pedraza-Alva G, Deng B, Wood CD, Aronshtam A, Clements JL, Sabio G, Davis RJ, Matthews DE, Doble B et al. 2008. Phosphorylation by p38 MAPK as an alternative pathway for GSK3beta inactivation. Science 320: 667-670.

Timmerman R, Paulus R, Galvin J, Michalski J, Straube W, Bradley J, Fakiris A, Bezjak A, Videtic G, Johnstone D et al. 2010. Stereotactic body radiation therapy for inoperable early stage lung cancer. Jama 303: 1070-1076.

Tomasetti C, Vogelstein B. 2015. Cancer etiology. Variation in cancer risk among tissues can be explained by the number of stem cell divisions. Science 347: 78-81.

Tomlinson I, Sasieni P, Walter B. 2002. How many mutations in cancer? American Journal of Pathology 160: 4.

Travis WD, Brambilla E, Nicholson AG, Yatabe Y, Austin JH, Beasley MB, Chirieac LR, Dacic S, Duhig E, Flieder DB et al. 2015. The 2015 World Health Organization Classification of Lung Tumors: Impact of Genetic, Clinical and Radiologic Advances Since the 2004 Classification. Journal of thoracic oncology : official publication of the International Association for the Study of Lung Cancer 10: 1243-1260.

Travis WD, Colby TV, Corrin B, Shimosato Y, Brambilla E. 1999. Histological Typing of Lung and Pleural Tumours. Springer, Verlag - Berlin - Heidelberg.

Trempolec N, Dave-Coll N, Nebreda AR. 2013a. SnapShot: p38 MAPK signaling. Cell 152: 656-656 e651.

Trempolec N, Dave-Coll N, Nebreda AR. 2013b. SnapShot: p38 MAPK substrates. Cell 152: 924-924 e921.

Trimboli AJ, Fukino K, de Bruin A, Wei G, Shen L, Tanner SM, Creasap N, Rosol TJ, Robinson ML, Eng C et al. 2008. Direct evidence for epithelial-mesenchymal transitions in breast cancer. Cancer research 68: 937-945.

Tuveson DA, Jacks T. 1999. Modeling human lung cancer in mice: similarities and shortcomings. Oncogene 18: 5318-5324.

Uhlik MT, Abell AN, Johnson NL, Sun W, Cuevas BD, Lobel-Rice KE, Horne EA, Dell'Acqua ML, Johnson GL. 2003. Rac-MEKK3-MKK3 scaffolding for p38 MAPK activation during hyperosmotic shock. Nature cell biology 5: 1104-1110.

Urosevic J, Garcia-Albeniz X, Planet E, Real S, Cespedes MV, Guiu M, Fernandez E, Bellmunt A, Gawrzak S, Pavlovic M et al. 2014. Colon cancer cells colonize the lung from established liver metastases through p38 MAPK signalling and PTHLH. Nature cell biology 16: 685-694.

Valastyan S, Weinberg RA. 2011. Tumor metastasis: molecular insights and evolving paradigms. Cell 147: 275-292.

Van den Steen PE, Husson SJ, Proost P, Van Damme J, Opdenakker G. 2003. Carboxyterminal cleavage of the chemokines MIG and IP-10 by gelatinase B and neutrophil collagenase. Biochemical and biophysical research communications 310: 889-896.

Van Laethem A, Van Kelst S, Lippens S, Declercq W, Vandenabeele P, Janssens S, Vandenheede JR, Garmyn M, Agostinis P. 2004. Activation of p38 MAPK is required for Bax translocation to mitochondria, cytochrome c release and apoptosis induced by UVB irradiation in human keratinocytes. FASEB journal : official publication of the Federation of American Societies for Experimental Biology 18: 1946-1948.

Ventura JJ, Tenbaum S, Perdiguero E, Huth M, Guerra C, Barbacid M, Pasparakis M, Nebreda AR. 2007. p38alpha MAP kinase is essential in lung stem and progenitor cell proliferation and differentiation. Nature genetics 39: 750-758.

Vermeulen L, De Wilde G, Van Damme P, Vanden Berghe W, Haegeman G. 2003. Transcriptional activation of the NF-kappaB p65 subunit by mitogen- and stress-activated protein kinase-1 (MSK1). The EMBO journal 22: 1313-1324.

Vignaud JM, Marie B, Klein N, Plenat F, Pech M, Borrelly J, Martinet N, Duprez A, Martinet Y. 1994. The role of platelet-derived growth factor production by tumor-associated macrophages in tumor stroma formation in lung cancer. Cancer research 54: 5455-5463.

Visvader JE. 2011. Cells of origin in cancer. Nature 469: 314-322.

Wagner EF, Nebreda AR. 2009. Signal integration by JNK and p38 MAPK pathways in

cancer development. Nature reviews Cancer 9: 537-549.

Wakeman D, Schneider JE, Liu J, Wandu WS, Erwin CR, Guo J, Stappenbeck TS, Warner BW. 2012. Deletion of p38-alpha mitogen-activated protein kinase within the intestinal epithelium promotes colon tumorigenesis. Surgery 152: 286-293.

Wang C, Deng L, Hong M, Akkaraju GR, Inoue J, Chen ZJ. 2001. TAK1 is a ubiquitin-dependent kinase of MKK and IKK. Nature 412: 346-351.

Wang S, Yang J, Qian J, Wezeman M, Kwak LW, Yi Q. 2006a. Tumor evasion of the immune system: inhibiting p38 MAPK signaling restores the function of dendritic cells in multiple myeloma. Blood 107: 2432-2439.

Wang SE, Narasanna A, Perez-Torres M, Xiang B, Wu FY, Yang S, Carpenter G, Gazdar AF, Muthuswamy SK, Arteaga CL. 2006b. HER2 kinase domain mutation results in constitutive phosphorylation and activation of HER2 and EGFR and resistance to EGFR tyrosine kinase inhibitors. Cancer cell 10: 25-38.

Wang SN, Lee KT, Tsai CJ, Chen YJ, Yeh YT. 2012. Phosphorylated p38 and JNK MAPK proteins in hepatocellular carcinoma. European journal of clinical investigation 42: 1295-1301.

Wang W, Chen JX, Liao R, Deng Q, Zhou JJ, Huang S, Sun P. 2002. Sequential activation of the MEK-extracellular signal-regulated kinase and MKK3/6-p38 mitogen-activated protein kinase pathways mediates oncogenic ras-induced premature senescence. Molecular and cellular biology 22: 3389-3403.

Wang W, Li Q, Yamada T, Matsumoto K, Matsumoto I, Oda M, Watanabe G, Kayano Y, Nishioka Y, Sone S et al. 2009. Crosstalk to stromal fibroblasts induces resistance of lung cancer to epidermal growth factor receptor tyrosine kinase inhibitors. Clinical cancer research : an official j ournal o f t he A merican A ssociation f or Cancer Research 15: 6630-6638.

Wang Y, You M. 2001. Alternative splicing of the K-ras gene in mouse tissues and cell lines. Experimental lung research 27: 255-267.

Wang Y, Zhang Z, Kastens E, Lubet RA, You M. 2003. Mice with alterations in both p53 and Ink4a/Arf display a striking increase in lung tumor multiplicity and progression: differential chemopreventive effect of budesonide in wild-type and mutant A/J mice. Cancer research 63: 4389-4395.

Webber JL, Tooze SA. 2010. Coordinated regulation of autophagy by p38alpha MAPK through mAtg9 and p38IP. The EMBO journal 29: 27-40.

Wiggin GR, Soloaga A, Foster JM, Murray-Tait V, Cohen P, Arthur JS. 2002. MSK1 and MSK2 are required for the mitogen- and stress-induced phosphorylation of CREB and ATF1 in fibroblasts. Molecular and cellular biology 22: 2871-2881.

Wilczynska KM, Gopalan SM, Bugno M, Kasza A, Konik BS, Bryan L, Wright S,

Griswold-Prenner I, Kordula T. 2006. A novel mechanism of tissue inhibitor of metalloproteinases-1 activation by interleukin-1 in primary human astrocytes. The Journal of biological chemistry 281: 34955-34964.

Winzen R, Kracht M, Ritter B, Wilhelm A, Chen CY, Shyu AB, Muller M, Gaestel M, Resch K, Holtmann H. 1999. The p38 MAP kinase pathway signals for cytokine-induced mRNA stabilization via MAP kinase-activated protein kinase 2 and an AU-rich region-targeted mechanism. The EMBO journal 18: 4969-4980.

Wood SL, Pernemalm M, Crosbie PA, Whetton AD. 2014. The role of the tumor-microenvironment in lung cancer-metastasis and its relationship to potential therapeutic targets. Cancer treatment reviews 40: 558-566.

Wood SL, Pernemalm M, Crosbie PA, Whetton AD. 2015. Molecular histology of lung cancer: from targets to treatments. Cancer treatment reviews 41: 361-375.

Wu R, Kausar H, Johnson P, Montoya-Durango DE, Merchant M, Rane MJ. 2007. Hsp27 regulates Akt activation and polymorphonuclear leukocyte apoptosis by scaffolding MK2 to Akt signal complex. The Journal of biological chemistry 282: 21598-21608.

Wu X, Zhang W, Font-Burgada J, Palmer T, Hamil AS, Biswas SK, Poidinger M, Borcherding N, Xie Q, Ellies LG et al. 2014. Ubiquitin-conjugating enzyme Ubc13 controls breast cancer metastasis through a TAK1-p38 MAP kinase cascade. Proceedings of the National Academy of Sciences of the United States of America 111: 13870-13875.

Xia Y, Yeddula N, Leblanc M, Ke E, Zhang Y, Oldfield E, Shaw RJ, Verma IM. 2012. Reduced cell proliferation by IKK2 depletion in a mouse lung-cancer model. Nature cell biology 14: 257-265.

Xian X, Hakansson J, Stahlberg A, Lindblom P, Betsholtz C, Gerhardt H, Semb H. 2006. Pericytes limit tumor cell metastasis. The Journal of clinical investigation 116: 642-651.

Xu L, Chen S, Bergan RC. 2006. MAPKAPK2 and HSP27 are downstream effectors of p38 MAP kinase-mediated matrix metalloproteinase type 2 activation and cell invasion in human prostate cancer. Oncogene 25: 2987-2998.

Xu L, Kikuchi E, Xu C, Ebi H, Ercan D, Cheng KA, Padera R, Engelman JA, Janne PA, Shapiro GI et al. 2012a. Combined EGFR/MET or EGFR/HSP90 inhibition is effective in the treatment of lung cancers codriven by mutant EGFR containing T790M and MET. Cancer research 72: 3302-3311.

Xu X, Rock JR, Lu Y, Futtner C, Schwab B, Guinney J, Hogan BL, Onaitis MW. 2012b. Evidence for type II cells as cells of origin of K-Ras-induced distal lung adenocarcinoma. Proceedings of the National Academy of Sciences of the United States of America 109: 4910-4915.

Yagasaki Y, Sudo T, Osada H. 2004. Exip, a splicing variant of p38alpha, participates in interleukin-1 receptor proximal complex and downregulates NF-kappaB pathway. FEBS letters 575: 136-140.

Yang Q, Li W, She H, Dou J, Duong DM, Du Y, Yang SH, Seyfried NT, Fu H, Gao G et al. 2015. Stress induces p38 MAPK-mediated phosphorylation and inhibition of Drosha-dependent cell survival. Molecular cell 57: 721-734.

Yao Y, Xu Q, Kwon MJ, Matta R, Liu Y, Hong SC, Chang CH. 2006. ERK and p38 MAPK signaling pathways negatively regulate CIITA gene expression in dendritic cells and macrophages. Journal of immunology 177: 70-76.

Yoshino Y, Aoyagi M, Tamaki M, Duan L, Morimoto T, Ohno K. 2006. Activation of p38 MAPK and/or JNK contributes to increased levels of VEGF secretion in human malignant glioma cells. International journal of oncology 29: 981-987.

Yoshizuka N, Chen RM, Xu Z, Liao R, Hong L, Hu WY, Yu G, Han J, Chen L, Sun P. 2012. A novel function of p38-regulated/activated kinase in endothelial cell migration and tumor angiogenesis. Molecular and cellular biology 32: 606-618.

Yosimichi G, Nakanishi T, Nishida T, Hattori T, Takano-Yamamoto T, Takigawa M. 2001. CTGF/Hcs24 induces chondrocyte differentiation through a p38 mitogen-activated protein kinase (p38MAPK), and proliferation through a p44/42 MAPK/extracellular-signal regulated kinase (ERK). European journal of biochemistry 268: 6058-6065.

Yu H, Pardoll D, Jove R. 2009. STATs in cancer inflammation and immunity: a leading role for STAT3. Nature reviews Cancer 9: 798-809.

Zeng Y, Sankala H, Zhang X, Graves PR. 2008. Phosphorylation of Argonaute 2 at serine-387 facilitates its localization to processing bodies. The Biochemical journal 413: 429-436.

Zhang Y, Rivera Rosado LA, Moon SY, Zhang B. 2009. Silencing of D4-GDI inhibits growth and invasive behavior in MDA-MB-231 cells by activation of Rac-dependent p38 and JNK signaling. The Journal of biological chemistry 284: 12956-12965.

Zheng H, Seit-Nebi A, Han X, Aslanian A, Tat J, Liao R, Yates JR, 3rd, Sun P. 2013. A posttranslational modification cascade involving p38, Tip60, and PRAK mediates oncogene-induced senescence. Molecular cell 50: 699-710.

Zhou G, Bao ZQ, Dixon JE. 1995. Components of a new human protein kinase signal transduction pathway. The Journal of biological chemistry 270: 12665-12669.

Zochbauer-Muller S, Gazdar AF, Minna JD. 2002. Molecular pathogenesis of lung cancer. Annual review of physiology 64: 681-708.

Zondag GC, Evers EE, ten Klooster JP, Janssen L, van der Kammen RA, Collard JG. 2000. Oncogenic Ras downregulates Rac activity, which leads to increased Rho

activity and epithelial-mesenchymal transition. The Journal of cell biology 149: 775-782.

Zuluaga S, Alvarez-Barrientos A, Gutierrez-Uzquiza A, Benito M, Nebreda AR, Porras A. 2007. Negative regulation of Akt activity by p38alpha MAP kinase in cardiomyocytes involves membrane localization of PP2A through interaction with caveolin-1. Cellular signalling 19: 62-74.

# *Appendix*

# LIST OF PUBLICATIONS

Panz M, **Vitos-Faleato J**, Jendretzki A, Heinisch JJ, Paululat A, Meyer H. A novel role for the non-catalytic intracellular domain of Neprilysins in muscle physiology. Biol Cell. 2012; 104 (9):553-68. doi: 10.1111/boc.201100069.

Hallier B, Schiemann R, Cordes E, **Vitos-Faleato J**, Walter S, Heinisch JJ, Malmendal A, Paululat A, Meyer H. Drosophila neprilysins control insulin signaling and food intake via cleavage of regulatory peptides. Elife. 2016; 6; 5. doi: 10.7554/eLife.19430.

Warr N, Carre GA, Siggers P, **Vitos Faleato J**, Brixey R, Pope M, Bogani D, Childers M, Wells S, Scudamore CL, Tedesco M, Barrantes IB, Nebreda AR, Trainor PA, Greenfield A. Gadd45$\gamma$ and Map3k4 interactions regulate mouse testis determination via p38 MAPK-mediated control of Sry expression. Dev Cell. 2012; 23 (5): 1020-31. doi: 10.1016/j.devcel.2012.09.016.

**Vitos-Faleato J**, Drösten M, Villanueva A, Barbacid M, Nebreda AR. p38$\alpha$ promotes progression of lung adenocarcinoma. [In preparation].